

"A STUDY OF THE INTERACTION OF FLAMES AND SURFACES"

A thesis
submitted for the
Degree of Doctor of Philosophy
in the Faculty of Science,
University of London

by

Gyan Prakash TEWARI
M.Sc.(London), D.I.C.

Department of Chemical Engineering and Chemical Technology,
Imperial College,
London, S.W.7.

October, 1967.

ABSTRACT

The Egerton-Powling burner has been suitably modified and adapted for studying flames quenched by cold surfaces. The necessary instrumentation for measuring gas flows and their initial temperatures has been set up and successful efforts have been made to obtain flames which are reproducible and perfectly steady for long periods. Schlieren photography and particle track techniques have been tried for establishing the location of the flame front and for burning velocity measurements.

The region of interaction of a cooled metallic heat sink with a premixed lean flat ethylene/air flame has been investigated. The detailed distribution of burning velocity has been measured, by means of a refinement of the particle track method. Two dimensional distributions of temperature and composition in this region have been obtained from thermocouples and microprobe sampling, followed by gas-chromatographic analysis. The burning velocity-heat loss relation has been found to depend on the orientation of the flame front to the heat sink. Heat release rates deduced by substituting temperature and flow data into conservation equations revealed some unexpected features close to the heat sink; in particular the zone of heat release becomes narrower and the maximum rate

of heat release does not decrease appreciably towards the heat sink, in spite of a considerable reduction in temperature. These features have been interpreted in terms of the composition pattern, which suggests that the narrowing is due to quenching of the second stage of the reaction, while the reaction rate effect is caused by diffusion of hydrogen atoms to the surface, which acts as a sink for them. It has been shown that a reaction such as $H + O_2 \xrightarrow{\text{Surface}} HO_2$ would account for all the features observed; conclusions are drawn regarding the status of quenching theory and the role of flame-surface interactions in flame structure studies.

ACKNOWLEDGEMENTS

The author wishes to express his gratitude to Professor F. J. Weinberg for suggesting the problem and for helpful guidance throughout this work.

Thanks are also due to:

Professor A. G. Gaydon, F.R.S., for his advice on the subject of the reaction mechanism and kinetics.

Mr. E. S. Brett and Mr. A. Jones, for help in constructing the apparatus.

Miss Pat Taylor, for help in the preparation of this thesis.

The author also wishes to express his thanks to the Imperial College for a Bursary in support of this research.

LIST OF CONTENTS

	<u>Page No.</u>
CHAPTER 1.	
1. INTRODUCTION	9
1.1 Direct measurement of quenching distance	11
1.1.1. The burner method	12
1.1.2. The tube method	13
1.1.3. The flanged electrode method	14
1.2 Burner stabilized flames	15
1.3 Stability diagrams at low pressures	21
1.4 Theories of flame quenching	21
1.5 Conclusions	35
2. STATEMENT OF THE PROBLEM	37
CHAPTER 2 - PERIPHERAL HEAT SINK	42
2.1 Considerations for the choice of burner system	42
2.2 Burner systems	45
2.3 Measurement of initial temperature	46
2.3.1. Calibration	48
2.4 Flow system	50
2.5 Flame stabilization	56
2.6 Preliminary investigation	57
2.7 Schlieren system	60
2.8 Determination of burning velocity profiles	64

	<u>Page No.</u>
CHAPTER 3 - THE AXIAL HEAT SINK	82
3.1 Burner-heat sink system	82
3.2 Location of the flame front	89
3.3 Schlieren system	91
3.4 Particle track method for locating schlieren surface	95
3.5 Application of the technique	98
3.6 Results	103
 CHAPTER 4 - THE HEAT LOSS PATTERN	 107
4.2 The burning velocities of cooled flames	108
4.3 Definition of temperature	113
4.4 Methods of temperature measurement	115
4.4.1. Optical methods	115
4.4.2. Particle track technique	118
4.4.3. Thermocouple method	118
4.5 Comparison of methods	121
4.6 Thermocouples	123
4.7 Thermocouple holder	124
4.8 Thermocouple traverses	127
4.9 Method of measurement	129
4.10 Calculation of the true temperature of flame gases	131

	<u>Page No.</u>
4.11 Temperature profiles	132
4.12 The heat loss distribution	133
4.13 Conclusions	137
CHAPTER 5 - THE HEAT RELEASE PATTERN	140
5.1 Heat continuity equation	141
5.2 Determination of gradients of temperature and velocity	143
5.3 Calculation of thermodynamic and transport properties of flame gases	145
5.4 Rate of heat release	146
5.5 Discussion	148
CHAPTER 6 - THE COMPOSITION PATTERN	152
6.2 External effects	152
6.2.1. Aerodynamic effects	153
6.2.2. Thermal effects	156
6.2.3. Composition changes	156
6.3 Internal effects	157
6.4-6.4.1. Choice of the probe	158
6.4.2. Sampling	159
6.5 Outline of gas chromatography system	161
6.6 Choice of columns	162

	<u>Page No.</u>
6.7 Determination of water	163
6.8 Preparation of standard mixture	169
6.9 Analysis of the samples	170
6.10 Results	173
CHAPTER 7 - CHEMICAL EFFECTS	174
7.2 Concentration of C_2H_4	176
7.3 Concentration of oxides of carbon	178
7.4 Distribution of elements	179
7.5 Discussion	185
CHAPTER 8 - CONCLUSIONS AND RECOMMENDATIONS FOR FUTURE WORK	187
APPENDIX (A)	189
APPENDIX (B)	192
APPENDIX (C)	196
REFERENCES	199

CHAPTER 1.

1. INTRODUCTION

The phenomenon of flame quenching by solid surfaces was observed and studied already by Sir Humphrey Davy in 1816. This pioneering work was mainly concerned with the development of flame arresters which could eliminate the risk of explosion in mines - frequently caused by the miners' lamps. Although the safety lamp, thus developed, out-lived its utility with the advent of electric lighting, the study of flame quenching acquired greater importance. Not only were better and more efficient flame arresters needed in other fields, but they had to be studied in connection with the use of electrical apparatus in coal mines also. Thus, for example, Stratham and Wheeler (1930) studied several types of flame arresting devices, Egerton, Everett and Moore (1953) evaluated the efficiency of sintered-metal flame arresters and Palmer et.al. (1957, 1963) concentrated their efforts on wire gauzes and perforated sheets and blocks. In spite of the enormous amount of work done (see e.g. Palmer, 1956) several factors important for the design of flame arresters are not understood very well (see e.g. Potter, 1960).

The process of flame quenching is of tremendous engineering importance even where the hazard is not concerned

with initiating explosions. For instance, the automobile industry is keenly interested in reducing the quantity of hydrocarbons escaping unburned in the exhaust. That flame quenching is responsible for such components of the exhaust from internal combustion engines has been demonstrated by the work of Daniell (1956) and Mawla and Mirsky (1965). It has been shown experimentally that

(i) there always exists a "dead space" in contact with cylinder walls when a flame front propagates inside,

(ii) there are some reactions always going on in this "dead space" and

(iii) the quenching effect of the wall extends beyond this visible region.

This aspect of quenching has now acquired an added dimension by pending legislation on air pollution. It has thus become important to know what chemical species are produced due to flame quenching in internal combustion engines. The physico-chemical processes involved have to be clearly understood because they seem to become more significant in high altitude (turbojet) combustion systems where they relate to "re-lighting" .

On a laboratory scale, flame quenching appears to be relevant to flame stabilization (see section 1.2) and the general behaviour of flames near cold walls (see section 1.1).

In addition to the interaction of flame with solid surfaces, flame quenching can be brought about by other methods (e.g. quenching by gas phase suspensions of finely divided solids, or the addition of inhibitors). However in the present study attention has been confined to quenching by solid surfaces only.

Flame quenching has usually been studied in terms of the minimum channel size that will allow a given flame to propagate. The cross-section of such a channel may be circular or slot-shaped. In the case of the tubular channel, its minimum diameter below which a flame fails to propagate has been called the "quenching diameter", D_0 . In the case of a slot-like channel the minimum separation between parallel walls under such limiting conditions is usually referred to as the "quenching distance", D_{11} . The two quenching dimensions are related (Berlad and Potter, 1955) by the equation

$$D_0 = \sqrt{2.67} D_{11}$$

1.1 Direct Measurement of Quenching Distance

The definition of quenching diameter (or distance) suggests some direct methods of its measurement. They can be broadly divided into three types:

- (1) The burner method
- (2) The tube method
- (3) The flanged electrode method.

In addition to these, other methods based on the stability of flames have been frequently employed. They are dealt with in the subsequent sections.

1.1.1. The Burner Method:

This is historically the first (Holm, 1932 and 1933) and the most widely used method for the determination of quenching diameters. A combustible mixture was led through a needle valve into a cylindrical chamber. The top of this chamber could be closed either by a thin plate punctured by a small hole or by a plug carrying a short metal or glass tube. The mixture was ignited at the exit of the hole or the tube and its rate of flow was gradually reduced. Depending upon the size of the exit, this resulted either in the flame flashing back and igniting the mixture in the chamber or extinguishing abruptly, without producing such ignition. Holm chose to take the minimum hole diameter allowing passage of the flame as the quenching diameter.

The method has been adapted by Friedman (1949), and von Elbe and Lewis (1949) for obtaining the quenching distance and by Friedman and Johnston (1950) and Berlad (1954) for studying its variation with pressure. It has also been modified (e.g. Anagnostou and Potter, 1959) for use with short pulses of combustible mixture flow.

1.1.2. The Tube Method:

This method (see for example, Garner and Pugh, 1939) involves propagation of a flame front in quiescent mixtures and is therefore usually employed for investigating pressure dependence of quenching diameter. The apparatus essentially consists of a flame tube and spark ignition source. The ignition section of the flame tube is smoothly sealed at one end and connected to a propagation tube and to a plenum chamber at the other end, which can also be left open to the atmosphere, if desired. The combustible mixture is ignited by a spark and the flame can either propagate through the tube or be quenched at its entrance. Using the same mixture strength, the experiment is repeated at different pressures and the limiting pressure at which the flame fails to propagate in the tube is determined. The tube diameter is then the quenching diameter at this pressure. As in the previous methods, modifications (e.g. Belles and co-worker, 1954 and Simon and Belles, 1953) have been made for measuring quenching distances.

The need for doing successive runs at different diameters is avoided with a modification introduced by Miler and co-worker (1958). In this a conical or wedge shaped propagation tube is used in place of the straight sided one. The flame in such a tube will fail to propagate beyond a section where its

diameter just falls short of the quenching diameter. A photograph of this propagating flame directly yields the required result.

1.1.3. The Flanged Electrode Method:

This method has been developed mainly by Lewis and Von Elbe (1949, 1961) and has been an outcome of their efforts at finding the minimum energy required to ignite a combustible mixture by an electric spark. Two types of electrode were used: electrodes tipped with small spheres and electrodes flanged with glass plates. In the latter case it was found that at electrode separations larger than a critical value, the minimum spark ignition energy remained constant. At the critical spacing, the minimum spark ignition energy exhibited an abrupt and discontinuous rise. It was proposed that under this condition, the flanges tend to quench the flame and a very large additional amount of energy would be needed to enable it to propagate clear of the channel. In this way, the critical electrode spacing was taken as the quenching distance D_{11} . In practice, a spark source of constant energy was used and the flanged electrode separation systematically varied; the quenching distance being taken as the mean of the minimum spacing which allowed ignition and the maximum spacing which prevented it. The method is specially suited for the study of unstable substances such as ozone and other fuels

which can be obtained in small quantities only.

1.2. Burner Stabilized Flames:

The phenomenon of flame quenching plays a dominant role in the stability of flames on burners. It has been shown by Lewis and Von Elbe (1961) that the stability of Bunsen-type flames is mainly governed by the conditions existing at the rim of the burner. An outline of flame stability criteria is given below.

Consider a combustible mixture streaming out of a cylindrical tube with a free stream velocity, u . On its ignition, a flame can usually be stabilized at a certain distance from the burner rim. The local orientation of the stable flame front with respect to the approach stream is then given by

$$S = u \sin \theta \quad (1)$$

where S is the velocity with which the flame front propagates upstream in a direction perpendicular to itself (the "burning velocity"). Equation (1) will be applicable locally to small segments of the flame front. Thus it can be shown that in the case of a parabolic distribution of the approach stream velocity, u , the local gradients of the segments are given by

$$\frac{dh}{dr} = \pm \sqrt{4 \left(\frac{\bar{u}}{S}\right)^2 \left(1 - \frac{r^2}{a^2}\right)^2 - 1} \quad (1.1)$$

where h and r are the cylindrical coordinates respectively measured along and at right angles to the axis; a is the radius of the cylinder and u is given by

$$u = 2 \bar{u} \left(1 - \frac{r^2}{a^2} \right) \quad (1.2)$$

where \bar{u} is the mean velocity.

At the wall, $u \rightarrow 0$ as $r \rightarrow a$, and the local gradient of the flame front becomes imaginary, indicating flashback, as can be seen from eqn. (1.1) if S is constant. However, in the proximity of the wall, the heat transfer from the gases to the solid surface tends to increase and S therefore falls. At the wall itself, which acts as a massive sink for heat and free radicals from the flame, the burning velocity of the mixture is zero. Hence as $r \rightarrow a$, S also approaches zero. The stability of the flame front is therefore governed by the relative rate of decrease of free stream velocity and of burning velocity in the vicinity of the wall. The nature of the variation of burning velocity near a solid wall is shown schematically in Fig. 1. Over small distances the gradients of velocity can be taken to be linear as shown by the broken lines. If the stream velocity u near the wall is greater than the local burning velocity (as for case 1) the flame front will be stable against flash-back although it may eventually blow off. On the contrary, if u

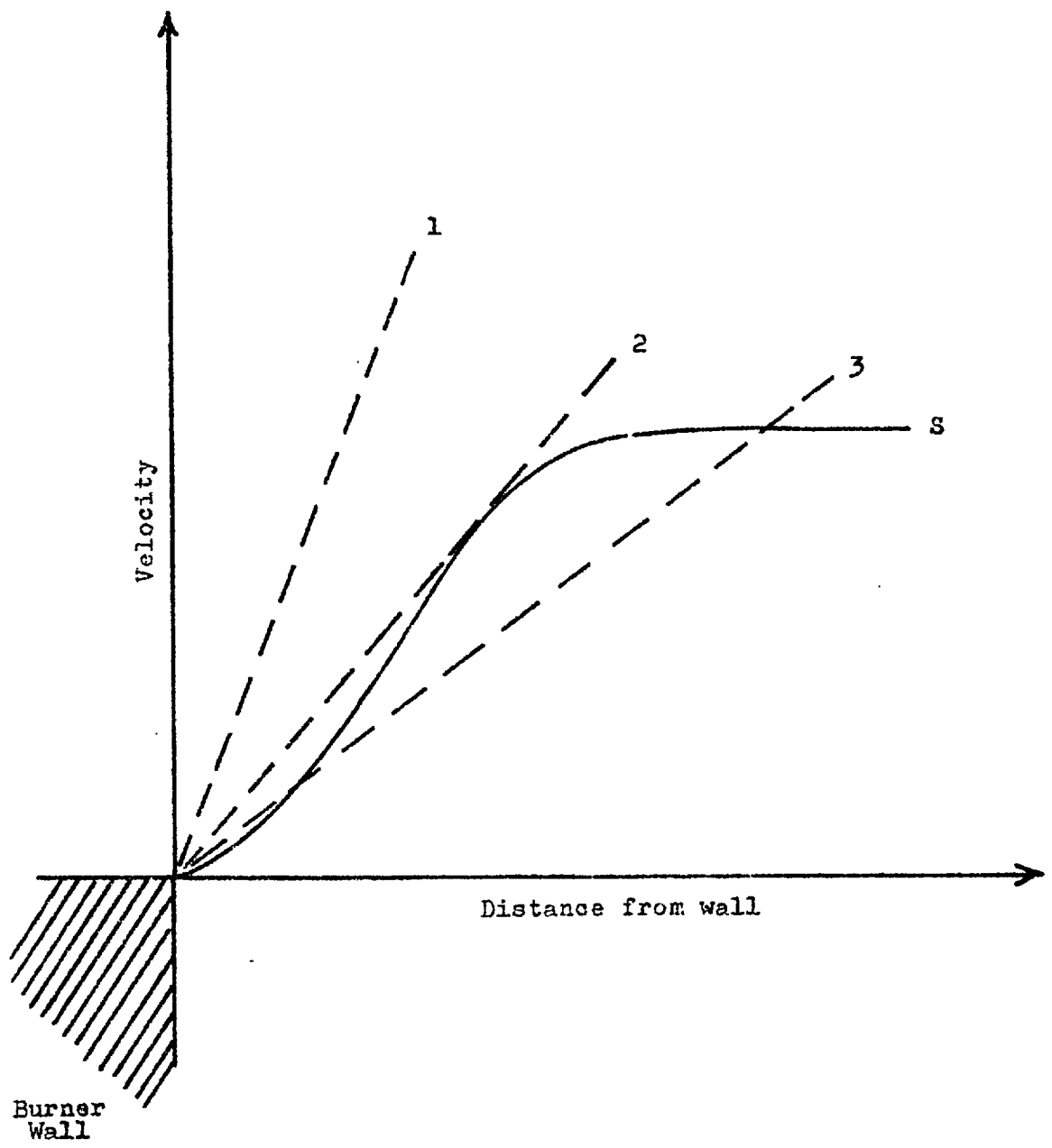


FIGURE 1.

is less than the local burning velocity at any distance from the wall (as for case 3) the flame front will move upstream with resultant flashback unless steps are taken to counteract this. The slowest flow for which flash back will just not occur is that at which the line and curve touch each other (as for case 3). If V_f is the volume flow rate of the mixture, at flash back it is related to the critical velocity gradients for flash back (g_f) by

$$g_f = \frac{4}{\pi} \frac{V_f}{a^3} \quad (1.3)$$

In an experimental study, Lewis and von Elbe (1943) plotted critical flows for flash back as a function of mixture composition in cylindrical tubes of various diameters. The points at zero flow were taken as the quenching diameters for the corresponding mixture composition. Further it was also shown that the velocity gradient at the flash back conditions (eqn. 1.3) remains constant for various flow rates and larger tube diameters.

It has been shown (e.g. Lewis and von Elbe, 1943; Wohl, Kapp and Gazley, 1949) that blow-off is also governed by a critical velocity gradient, g_b . The condition of stable burning is thus

$$g_f < g < g_b \quad \text{or}$$

$$\frac{\pi a^3}{4} g_f < v < \frac{\pi a^3}{4} g_b$$

As will be seen, the entire mechanism of stabilization of flames on burners, is closely related to the subject of interaction of flames with solid surfaces.

The critical velocity gradient provides a measure of the distance up to which the quenching effect of a solid surface can extend. If the variation of S with distance were linear, this depth of penetration of quenching, d_p , would be

$$d_p = \frac{S}{g_f} \quad (1.4)$$

d_p is also the distance from the wall at which the gas velocity at flash back becomes equal to the adiabatic burning velocity. At distances less than d_p , the burning velocity of the mixture is less than its adiabatic value owing to the presence of the heat sink. The penetration distance d_p has been used to correlate with values of quenching distances found experimentally. Thus in the case of two parallel walls, d_p was expected (von Elbe and Mentser, 1945) to be half their separation bringing about quenching of a flame; in the case of cylindrical tubes it has been compared with the radius which would just prevent the flame from flashing back. In Fig. 1.1 these three distances have been compared. Curve 3 represents the values of $2d_p$ and is seen to be of the right order of

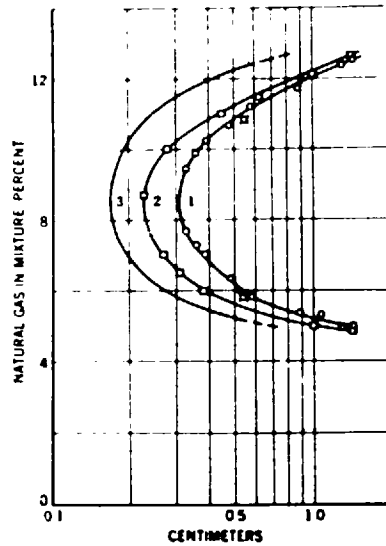


FIGURE 1.1 - Depth of penetration of the quenching of the burner wall for natural gas-air mixtures. Curve 1, quenching diameter d_o of cylindrical tubes; Curve 2, quenching distance d_{11} between plane-parallel plates; Curve 3, depth of penetration, d_p calculated from critical velocity gradients for flash-back.

magnitude, but not as large as the quenching distance between parallel plates. An interesting observation emerging out of such studies (e.g. Blank, et al, 1949) is that the penetration distance has been found to be less for richer mixtures as compared to lean mixtures having the same burning velocity.

1.3 Stability Diagrams at Low Pressures.

The measurement of quenching diameter can also be discussed in connection with the work done on low pressure flames by Gaydon and Wolfhard (1953). The method is based on the stability regions for a flame on a given low pressure burner. For a certain geometry and gas flow, a stable flame will have two pressure limits of stability, the blow-off point and the point at which the flame strikes back. As the gas flow is reduced the flash-back and blow-off limits become closer. Thus by changing the gas flow the whole stability region can be explored. A diagram as shown in Fig. 1.2 is obtained for the stability region of a flame. At the junction point of the stability diagram as shown in the figure, the burner diameter is the quenching diameter at that pressure.

1.4 Theories of Flame Quenching.

(i) The experimental studies of flame quenching have led to many attempts at explaining the observations theoretically. An early theory was postulated by Friedman (1949). It is

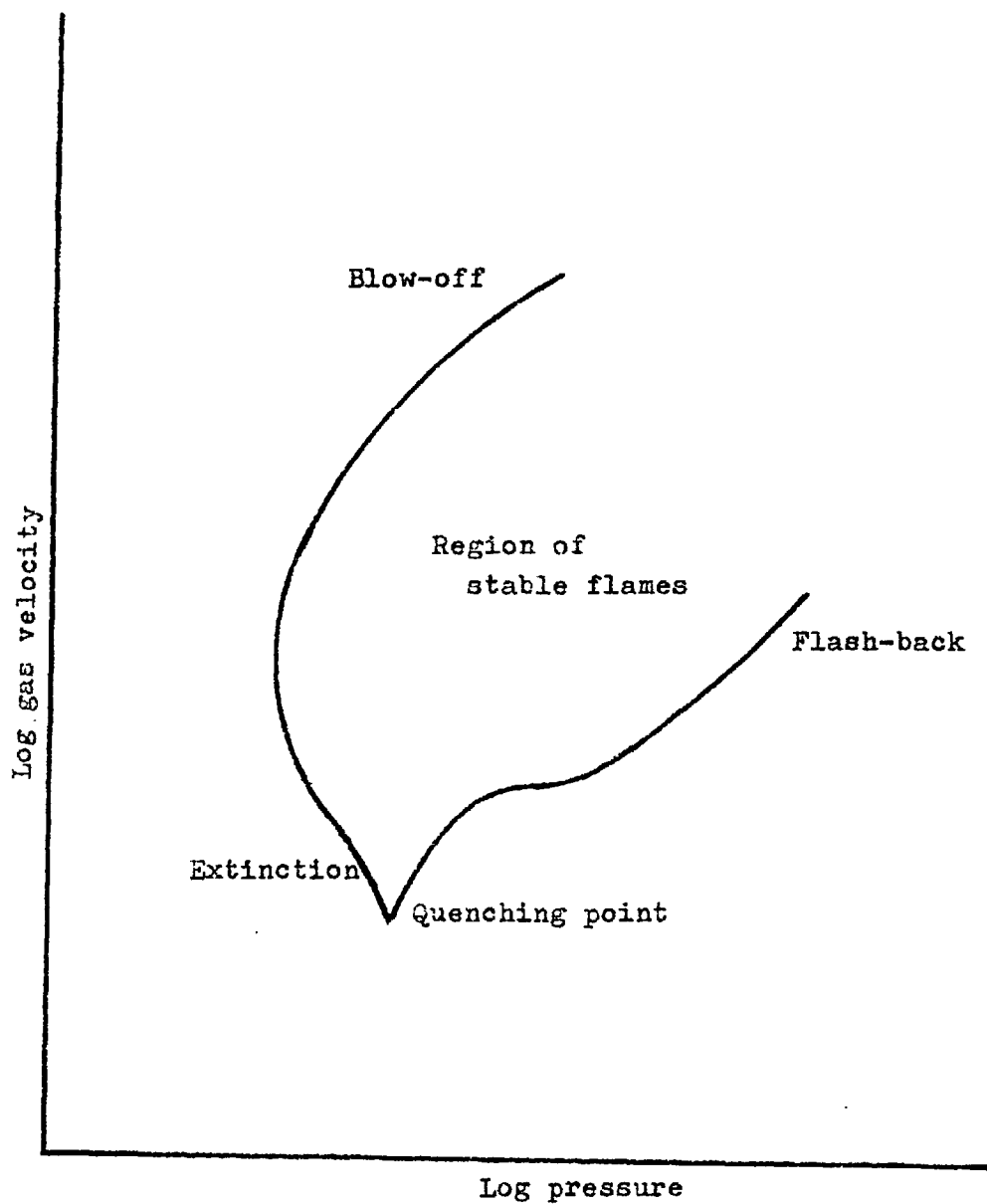


FIGURE 1.2 - DETERMINATION OF PRESSURE AT WHICH THE BURNER DIAMETER IS THE QUENCHING DIAMETER.

essentially a thermal theory which supposes that a flame is quenched when the rate of heat transfer to a wall becomes equal to the rate of heat generation by the flame. Thus an equation for quenching distance (in a rectangular opening between two plates) was deduced and it was expressed as

$$D = \frac{\alpha}{S_u f} \left(\frac{T_f - T_i}{T_i - T_u} \right)^{1/2} \quad (1.5)$$

where α is the thermal diffusivity of the unburnt gas at temperature T_u , T_i its "ignition temperature", T_f the flame temperature and f a dimensionless constant related to the geometry of the tube or slot. The relative importance of diffusion and heat conduction was also discussed but it was concluded that thermal conductivity is the controlling factor in laminar flame quenching.

If it is assumed that T_i is a constant factor of T_f , the theory yields a confirmation of the experimental results of Putnam and Jensen (1949) who observed that the quenching Peclet numbers $\left(\frac{D S_u}{\alpha} \right)$ were approximately constant for a number of hydrocarbon flames.

The most serious objection to Friedman's theory is that it assumes that the flame loses heat to the walls solely by conduction. No account has been taken of the diffusion of atoms and free radicals, which is contrary to many theories of

flame propagation including that of Tanford and Pease (1947) Simon, et al (1952), basing their assumptions on the postulates of Tanford and Pease, put forth their diffusional theory of flame quenching. They assumed that the proximity of a wall brings about a destruction of active particle chain carriers diffusing from the flame front towards its surface. When the number of events initiated by these species while diffusing to the walls becomes equal to or greater than the number of events required to maintain a flame, the flame is quenched. Thus they expressed the quenching distance as

$$D = \left[\frac{G A P}{N_f \sum_i \frac{p_i k_i}{D_i}} \right]^{1/2} \quad (1.6)$$

where P is the pressure, N_f the number of fuel molecules per c.c., p_i the partial pressure and D_i the diffusion coefficient of the i^{th} active species, k_i the rate constant of the reaction of the i^{th} species with fuel, G , a geometrical constant and A an empirical constant which represents the fraction of molecules which must react for flame propagation. The values of k_i determined from burning velocities combined with the experimentally observed quenching distances give a value of A very close to the lean limit fuel mole fraction. This theory successfully predicts the variation of quenching distance with tube geometry and pressure. Based on the diffusion model described above, Belles and

Berlad (1956) have developed a theory of flame quenching in which some of the restrictions of the preceding theory have been removed. Chain branching and chain breaking in the gas phase as well as incomplete destruction of active particles at the walls have been taken into account. After correlating some of the available data on propane/air flames successfully, it was concluded that the basic assumptions of Simon et al were of the right order for the quenching of propane-oxygen-nitrogen flames. (A thermal analogue of Simon's theory has also been put forth by Potter and Berlad (1956). Although it is useful for correlation and simple predictions of quenching parameters, it does not constitute any fundamental advance over the preceding theories).

A different approach in terms of the kinetic properties of the combustible mixture has been proposed by Weinberg (1955). The important concept of this theory is that the fractional increase in rate of a particular reaction with temperature depends so strongly on the activation energy, that chain branching is likely to be more important as a source of active centres than diffusion from the final equilibrium state. It is supported by the fact that fractional reaction rates of two reactions one of 40 k.cal/mole activation energy and the other of 4 k.cal/mole at 1000°K is in the ratio of 6×10^7 times, the latter being greater than the former, which had previously

been considered as relevant to the overall reaction in flame propagation theory. This suggests that during the temperature rise in the pre-ignition zone of^a/flame front the production of radicals by a low-activation energy chain branching reaction may render negligible not only the transport of active species by diffusion but also their production by thermal dissociation. Weinberg applied these concepts to ignition temperature and ignition lags and then extended them to predict the flammability limits and burning velocity. Although this theory is not directly applicable to quenching of flames by solid surfaces it provides a very good insight into the process by which chain branching and chain breaking can bring about quenching of flames in the proximity of a heat sink. This theory neglects diffusion and thus provides a counterpart to another treatment based on competition between chain branching and chain breaking - that of van Tiggelen (1946, 1949) - which is a pure diffusion theory.

(ii) The earliest flame propagation theory providing some insight into the mechanism of flame quenching was advanced as early as 1930 by Daniell. He obtained solutions of the energy balance equations for flames in the presence of heat losses. Two cases of flame propagation were considered. In one, the flame and burnt gases were supposed to lose heat continuously. In the other, heat was supposed to be lost only

from the flame zone. In both these treatments, two solutions of the energy equation were obtained if the heat losses were small. One of these was shown to represent a physically unstable state. It was found, however, that if the heat loss exceeded a critical value, no solutions to the energy balance equations existed. For the maximum heat loss the calculated burning velocity had a non-zero value - half of that without heat loss. The manner in which the heat loss itself increases with decreasing diameter of the tube was estimated. Thus Daniell postulated a minimum diameter below which a flame could not propagate in a tube - a concept put forth before any experimental values of quenching diameters were available.

Von Elbe and Lewis (1949) solved energy conservation equations for a two-dimensional flame propagating in a tube. Taking into account the heat loss to the tube walls, they calculated the temperature distribution in the combustion wave and the accompanying changes in burning velocity. The calculated maximum temperatures at various distances from the wall were found to lie on a parabola with its apex along the axis. Two such parabolic distributions of temperature were found for large tubes. With decreasing tube diameter, the two curves, one of which is found to be physically untenable, approach each other till they merge at a critical tube diameter. For diameters less than this critical value, identified with the

quenching distance, no solutions to the energy balance equations were found. In order to calculate the quenching distance from this theory both the minimum ignition energy and burning velocity must be known. The quenching Peclet numbers thus calculated for stoichiometric methane-air and methane-oxygen flames were found to agree fairly well with the results of Putnam and Jensen (1949) and Cullen (1953). As expected from the theory, the speed of flames propagating in tubes of diameters slightly greater than the quenching diameter, were found (e.g. Singer and von Elbe, 1957) to be equal to the adiabatic burning velocity.

According to Mayer (1957), the mechanism of flame quenching can be outlined as follows: the rate of heat generation in a flame, being dependent on reaction kinetics, can be expressed with an exponential law of the Arrhenius type. But the rate of heat loss due to conduction to the walls will depend upon the excess of peak flame temperature over that of its surroundings. Hence for a flame propagating with heat losses to solid walls, as the peak flame temperature decreases, the rate of heat generation diminishes more rapidly than the rate of heat lost to the walls. Therefore, energy balance requirements limit the level down to which the peak flame temperature can fall without extinction.

The rate of heat loss from a flame, consistent with a steady state balance of energy has been expressed as

$$q = \rho_u C_p (T_f^a - T_f) B \exp\left(\frac{-E}{2RT_f}\right) \quad (1.7)$$

where ρ_u is the density, C_p is the specific heat of the gas, T_f^a is the adiabatic flame temperature, T_f is the flame temperature, B is an empirical constant and E is the apparent activation energy. On the other hand, the heat loss rate due to convective heat transfer from the flame to the walls has been postulated to be

$$q_{\text{conv.}} = 4F^2 \left(\frac{\bar{\alpha} \bar{k}}{D^2 S_u}\right) (T_f - T_u) \quad (1.8)$$

where F is a "flame configuration factor," \bar{k} is the average thermal conductivity, and T_u is the tube wall temperature.

For different peak temperatures a simultaneous solution of the two equations gives the conditions for a stable flame in contact with a solid wall. For large diameters, two such solutions are possible, one corresponding to slow, and the other to a fast flame. As the tube diameter diminishes the two solutions approach a limiting value beyond which no stable flame propagation can be expected. This limiting diameter is the quenching diameter and can be expressed as a function of the adiabatic burning velocity, thermal diffusivity, adiabatic flame temperature and flame activation energy. The quenching

Peclet numbers thus calculated are in satisfactory agreement with experimental values.

In setting the energy conservation equation, none of the above thermal theories consider the enthalpy transport by diffusion. A significant advance was made by Spalding⁽¹⁹⁵⁷⁾ by taking this into account. Using a one-dimensional model and neglecting diffusion to the wall Spalding considers a single step reaction of A with B and one-dimensional flame with heat loss to surroundings for deriving two differential equations (dimensionless) by taking

$$D_A \rho = D_B \rho = \frac{k}{C_p} \quad (1.9)$$

These were

$$\frac{d^2 \tau}{dz^2} = - \frac{\lambda}{z^2} \left[\phi(\alpha, \tau) - k \psi(\tau) \right] \quad (1.10)$$

$$\frac{d^2 \alpha}{dz^2} = \frac{\lambda}{z^2} \phi(\alpha, \tau) \quad (1.11)$$

where

D = Diffusion coefficient of components of reactants.

ρ = Density of gas mixture

k = Thermal conductivity

C = Specific heat

$\tau = \frac{T - T_u}{T_f - T_u}$ Dimensionless temperature or reactedness

$$z = \exp \frac{CGx}{k} \quad \text{distorted space variable}$$

$$\alpha = \frac{m_A}{m_{A_u}}$$

$$\lambda = \frac{HR_A^* k_f}{(T_f - T_u)(CG)^2} \quad \text{Eigenvalue}$$

$$\phi = \frac{k R_A}{k_f R_A^*} \quad \text{dimensionless reaction rate}$$

$$\psi = \frac{kL}{k_f L^*} \quad \text{heat loss rate}$$

$$k = \frac{L^*}{R_A^* H} \quad \text{heat loss parameter}$$

T_f = the adiabatic combustion temperature

T_u = the temperature of the unburnt mixture

R_A^* = the value of R_A when $T = T_f$ and $m_A = m_{A_u}$

m = mass component per unit mass of mixture

k_u = the thermal conductivity of the unburnt gas

L^* = the value of L at $T = T_f$

H = heat of reaction

Subscripts u and f denote unburnt gas condition and adiabatic burnt gas condition.

Taking the boundary conditions as

$$z = 0, \quad \alpha = 1, \quad \tau = 0$$

$$z = 1, \quad \alpha = 0, \quad \frac{d\alpha}{dz} = 0 \quad \tau = \tau_1 \quad \frac{d\tau}{dz} = \left(\frac{\partial \tau}{\partial z}\right)_1$$

solutions of the equation were obtained for two cases (i) no heat losses to the surroundings and (ii) with heat losses. The former case reduced to some of the unquenched flame theories put forward prior to this theory and an analytical solution for calculation of flame speed was presented. In the second case, when heat losses were taken into account, the profiles of temperature and concentration as given by equations (1.10) and (1.11) were not identical and both equations had to be solved. The reaction rate was assumed to vary as n^{th} power of temperature ($\phi = \alpha \tau^n$) and the heat loss rate to vary to the m^{th} power of temperature ($\psi = \tau^m$). Finally an approximate analytical solution was obtained. Usually the value of 'n' lies between 6 and 15 and that of 'm' between 1 and 5, depending upon whether the heat transfer is predominantly by conduction or radiation.

In common with previous theories, two burning velocities were found for each combustible mixture when heat loss was present. The slower flame was shown to be unstable. With increasing heat loss the two burning velocities approached each

other till they merged into one at the point of critical heat loss rate. Beyond this the flame ceased to exist. The theory was extended to quenching of flames by cold walls. The quenching Peclet number (60) thus derived was found to agree with experimental results.

A non-adiabatic flame theory taking into account heat losses by both conduction and radiation has been proposed by Berlad and Yang (1960). They considered a flame propagating in an infinitely long tube. The heat released by chemical reaction and heat losses were approximated as functions of average temperature and concentration at each cross-section of the tube. Heat losses on the downstream side of the flame were considered irrelevant. Following Spalding's notation, equations for energy and for each of the reactants were formulated. Using the same boundary conditions as in the adiabatic theory, approximate solutions were obtained for two values of Lewis number - zero and unity - $(\frac{D_A \rho C}{k}, \frac{D_B \rho C}{k})$. These were expressed in the form of a general equation having three major terms corresponding to heat release and losses.

It was found that heat losses by conduction were mainly responsible for flame quenching. Such losses increase as the tube diameter is decreased, becoming dominant (almost 99%) at its minimum value, beyond which flame propagation becomes impossible. The values of quenching diameters for stoichiometric

propane-oxygen nitrogen flames were found to agree well with experimental results.

A theoretical analysis of the structure and burning velocity of a laminar one-dimensional flame near a heat sink has been presented by Chen and Toong (1960). The rate of heat loss from within the flame and the hot boundary was described by arbitrary functions. The reaction kinetics were assumed to be of the first order Arrhenius type and the reaction rate was taken to be zero at the cold boundary. The theory presents two main results.

(i) The adiabatic burning velocity was found to decrease very rapidly as the adiabatic flame temperature dropped to its limiting value corresponding to zero value of the initial mixture temperature. It was expressed in the form

$$S_u \sim \exp\left(-\frac{T_f^a}{T_f}\right)$$

where T_f^a is the adiabatic flame temperature and T_f the temperature of the burnt gases.

(ii) The burning velocity was found to be strongly temperature dependent when the fraction of total heat loss rate per unit flow area was a function of the fraction reacted. Further, the flame thickness was shown to be decreasing as the burning velocity diminished. When the heat sink was chosen at the hot boundary parallel to the gas flow no steady-

state burning velocity could be found below some lower limit for the temperature of the combustion products.

In addition to the preceding theories dealing with the fundamental aspects of flame quenching, the work of von Karman and Millan (1953) and Wohl (1953) is relevant to laminar flames near a cold wall. These are based on the behaviour of a "dead space" between flame and the wall, this being defined as the distance between the wall and a point in the flame front corresponding to ignition temperature. It was shown by von Karman that the ratio of the dead space to the flame thickness remained approximately constant. From this, it was concluded that thermal conduction is the fundamental process which determines the behaviour of the flame near the wall. The findings of Wohl were similar, and it was shown that the distance from the wall at which a flame can be maintained is a function of the amount of heat transferred to the wall; that is, should the heat transfer increase, a greater distance would be necessary to reduce the heat transfer and maintain the flame, otherwise the flame would be extinguished. These concepts may be important in engineering applications of combustion.

1.5 Conclusions.

It would appear from the above discussion that the situation is far from fully understood. A large number of

theories have been proposed and experimental results cited in their favour. Gerstein and Potter (1958) have compared some of these theories and have found an order of magnitude agreement between experiment and theories of Potter and Berlad, and Mayer and Spalding. On the other hand there are experimental data which appear to support other theories. Although two pieces of experimental evidence (e.g., Simon, 1954,) appear to favour diffusion theories (rather than thermal ones) it seems more probable that both thermal conduction and diffusion of free-radicals and molecules, play an important role in flame quenching. Even if either of the two processes may appear predominant under different circumstances and satisfactorily explain a certain range of experimental observations, they cannot be correct in any comprehensive sense. Theories based on comprehensive equations may be mathematically correct but can be solved only on insertion of fictitious, temperature-explicit kinetics. What they show, in fact, is that if a flame reaction existed which could be described in this manner, then its quenching would follow the laws established. No attempt has been made to obtain a solution in terms of the detailed kinetics of the many reactions involved - using rate laws in the form given, e.g. by Fristrom and Westenberg (1965), taking into account not only heat losses but also the diffusion of individual active species and their interaction with a solid surface. One of the

conclusions of this work is that the latter is important and that the corresponding theoretical problem is an exceedingly difficult one.

2. STATEMENT OF THE PROBLEM

It is thus apparent that in flame quenching, heat transfer to solid walls, heat release rates both in the proximity of the walls and away from them, diffusion of species in their vicinity and the production of reaction intermediates, all may be relevant to its mechanism. Previous experimental work has only succeeded in establishing that all these parameters must be known if any comprehensive and meaningful results are to be obtained. This implies the need for a simultaneous determination of the physical and chemical structure of the flame in the vicinity of a solid surface and away from it.

Experimental studies on unperturbed pre-mixed flames have been greatly facilitated by the development of the flat-flame burner. Near limit hydrocarbon-air mixtures have been used to stabilize nearly one-dimensional flames on this burner. These flames, together with /appropriate techniques for their investigation, provide a powerful tool for quantitative studies of a wide variety of problems. These include burning velocity determinations, mechanism and reaction kinetics, determination of structure and heat release rates, infra-red absorption studies of reaction

intermediates and investigations of inhibition of pre-mixed flames. Most of the analytical experimental studies are essentially based upon a determination of burning velocity and temperature distribution. The variation of these quantities with temperature and composition and the detection and measurement of concentrations of stable flame species have also been used in such flames.

The thermal structure of flames has been studied by a large number of methods including the use of thermocouples, α -particles and sound waves. Probably the most powerful tool for such studies is the use of optical methods (Weinberg, 1963) grouped under the general headings of schlieren, shadow, deflection mapping and interferometric studies. These provide an instantaneous record of the thermal field without introducing any solid body in the flame. These methods have, however, a disadvantage that they tend to become insensitive at the higher temperatures and are limited by diffraction at any solid boundaries in the optical system. The use of thermocouple probes and particle track techniques can yield reliable records of temperature distribution in flames provided certain precautions are taken. Thus very fine thermocouple wires coated with silicon dioxide have been successfully used for this purpose (e.g. Friedman, 1953; Kaskan, 1956). Nevertheless, conduction down the leads has

to be minimised and corrections have to be made for the radiation cooling of the hot junction.

The particle track method measures local velocities, but can be used with the law of conservation of mass for the determination of local densities and hence temperatures along any stream line. This method suffers, however, from certain limitations (see e.g., Fristrom and Westenberg, 1965) which have to be borne in mind when reliable results are required. Most of these concern the type and size of the tracer particles and can usually be taken care of.

As regards the measurement of burning velocity, of all the methods available (e.g. Linnett, 1953), the particle track technique is the most accurate. Here the velocity is determined normal to a specific flame surface, usually the schlieren surface, the position of which can either be calculated (Weinberg, 1956) for a one dimensional flame, or experimentally determined (Weinberg, 1963).

The velocity and temperature distributions are sufficient to determine the physical structure of a pre-mixed flame and the distribution of an overall chemical reaction rate based on the heat release rate. But the chemical and ionic structure of such flames have also been studied. The techniques for this are summarized in Fristrom and Westenberg⁽¹⁹⁶⁵⁾ and their use provide additional specific data of the course of the reaction from

which kinetic constants can be deduced. Two experimental techniques have been used prominently,

- (i) direct spectroscopic analysis and
- (ii) sample withdrawal using a fine quartz probe.

The sampling method is more universal but there are a number of problems connected with this method :

(a) since distance rather than time is the important variable, the limitation to resolution due to probe size is a problem,

(b) the question as to what effect the introduction of a probe has on the flame must be answered,

(c) the problem of interpretation of the sample in terms of the transient species sampled becomes important. This technique is limited to flame temperatures below the softening point of probe material and only species which are stable to sampling are ultimately analysed. The limitations and justification of the techniques have been discussed in some detail by Fristrom and Westenberg (1965), with the conclusion that the results are reasonable and self consistent.

Since several of these experimental techniques are already well established it seemed promising to investigate if they could be adapted for a study of pre-mixed flames propagating near a wall. However, before this could be done experimentally, it was necessary to suitably modify the flat-flame

burner so as to incorporate a heat sink near the flame, without affecting its amenability to optical, particle track and probe sampling techniques.

The following pages describe such attempts and the consequent use of the afore-mentioned experimental techniques for the elucidation of the physical phenomena responsible for flame quenching near solid boundaries.

CHAPTER 2.PERIPHERAL HEAT SINK2.1 Considerations for the choice of burner system.

A suitable burner is the most important part of any apparatus for flame structure studies. In the present investigation the choice was dictated firstly by the nature of interaction between a solid wall and a flame front, and secondly by methods intended to be used for its study. The presence of a wall in the proximity of a flame modifies not only the inflow of gases but also the heat balance as compared with a freely propagating flame front. Thus the wall absorbs heat from the reaction zone and the burning velocity therefore undergoes a change in its vicinity and the flame front re-orientes itself accordingly. Even in the simplest case of a flat flame front such an interaction causes the flame fringe to acquire a curvature near the wall. In other systems the changes can be more complicated. To study such an interaction the flame front must therefore be accessible to experimental probes both mechanical and optical, in order that the state of the gas at each point over a distance in which burning velocity is affected by surface proximity can be easily determined.

Among the techniques available for determining the

thermal structure, as well as changes in geometry, the family of the optical methods (Weinberg, 1963) seemed to be the most promising. Interferometry has been employed even for studying structures of flames of complex geometries, but the analysis and interpretation of the interferogram is simplified in the case of a one dimensional flame. In view of the ease, versatility and non-interfering nature of the optical methods it seemed worthwhile to choose a burner system which, in addition to the above considerations, would be amenable to such optical studies, but, at the same time, could be modified to suit any other methods necessary to elucidate the detailed structure of the flame front in the vicinity of a wall.

The flat flame burner described by Powling (1949), and Egerton and Thabet (1952) seemed to provide an ideal basis for the proposed system. This burner has since been modified by Burgoyne and Weinberg (1954) to suit optical studies of flame structure. With these modifications an approximately uni-dimensional flame can be stabilized (against the incoming reactant stream) away from any solid boundaries of the burner system. The flame is stabilized only near the lower limit of inflammability and thus yields^a/relatively thick reaction zone at atmospheric pressure. The tolerances on spatial resolution are correspondingly less critical. Moreover the excess of one

reactant (usually air) makes all the physical properties much more dependent on temperature than on composition. In such slow burning mixtures (burning velocity \approx 4 to 10 cms/sec) it seems unlikely that the error introduced in temperature measurements due to thermodynamic disequilibrium among the various degrees of freedom will be appreciable. In fact, Levy and Weinberg (1959)¹ using lean ethylene flames found that such errors are negligible as compared to other errors in temperature measurements. Using ethylene as a fuel has the additional advantages that

(i) complete combustion of the fuel takes place across the flame front without any change in overall mole number,

(ii) the chemical kinetics has previously been analysed in a similar system.

These advantages are not indispensable, but they do simplify the necessary corrections in the measured properties of the gaseous mixture and provide a suitable datum. They will be discussed in the appropriate parts of the thesis.

In order to exploit these initial advantages of using a flat-flame burner, the optimum geometry and location of the heat sink had to be determined by some preliminary experiments. It seemed desirable, at first, that for using optical techniques for temperature measurements the flame front near the heat sink should be planar and normal to the latter. The solution to this was thought to lie in varying the angle of approach of

the flame by varying the flows locally in the vicinity of the heat sink. In this way it was proposed that the shape and position of the flame could be adjusted somewhat to make it perpendicular to the surface of the heat sink.

2.2. Burner systems.

The burner was made of a Pyrex glass tube of about 7 cms. diameter and 25 cms. length with both ends ground flat and normal to the axis of the tube. One end was sealed with a rubber bung carrying two tubes: one for the gas inlet and the other for the thermocouple leads. At the other end, a matrix made by spirally winding an adjacent plane and a corrugated strip (2.25 cm. wide and 0.05 cm. thick) of cupro-nickel was inserted with its upper face flush with the end of the glass tube. The matrix is a crucial part of the flat flame burner as it divides the burner outlet into a large number of fine passages of equal dimensions, parallel to the burner axis. The space between the matrix and the rubber bung was packed with glass beads of 6 mm. diameter. The column of glass balls randomises the gas flow while the matrix at the top rectifies the flow. This combination therefore gives a flat velocity profile on the downstream side of the matrix when the reactants are admitted through the inlet tube in the rubber bung. The burner was held by three screws inside a brass cylinder

carrying a flange which could be moved up and down by a rack and pinion arrangement. On this flange rested a cylindrical Pyrex chimney whose top was covered by an asbestos sheet having evenly distributed holes across its thickness. This sheet was 0.65 cm. thick and the holes (3 mm. in diameter) were drilled at a separation of 1 cm, forming a grid-like pattern.

The Pyrex chimney was of 15 cm. diameter and 22 cm, height and gave adequate protection to the flame from draughts and also helped in stabilizing the flame over the burner port. Since the chimney was transparent it was possible to inspect the flame and carry out any measurements for the flame drifts by a cathetometer. The position of the floating flame could be adjusted to a small extent by varying the height of the chimney above the burner post. This small shift of the flame did not affect the flow in the reactant gas stream.

2.3. Measurement of Initial Temperature.

It has been found that once the flame is stabilised on such burners, the matrix is heated to temperatures well above room temperature. It has been shown (Weinberg, 1953) that the local temperature of the downstream face of the matrix is irresolvably close to that of the gases as they leave it. This property of the system has made the measurement of the initial temperature of the reactants much easier; it is merely necessary to measure the temperature distribution across

the downstream surface of the matrix with the help of thermocouples. One of the two dissimilar conductors of the thermocouple used was the matrix itself and the other was a nichrome wire. In previous studies (Weinberg, 1953, Levy, 1958) the e.m.f. generated by such a thermocouple was found reproducible and of suitable magnitude for measurement by a sensitive millivoltmeter. As the e.m.f. generated by the thermocouple is independent of the method of making the junction - so long as good electrical contact is maintained - one is free to choose either soldering, welding or just twisting the two different materials together. In the present case, equal lengths of nichrome wire (20 S.W.G.), after being lead through the fine passages of the matrix, were spot welded on its downstream surface. This wire was especially obtained for thermocouple work and was covered with a glass fibre sheathing capable of withstanding temperatures up to 500°C without breakdown in its insulation. The hot junctions were formed by momentarily striking an arc between the wires and the matrix. In order to ensure a good electrical contact, the spot welding was done in an inert atmosphere with a pointed carbon electrode. A D.C. potential difference of 230 volts applied between the carbon electrode and matrix through a 100 ohm resistance gave the best results. In all, seven such hot junctions were positioned in a spiral distribution over the

matrix surface, thereby making possible temperature measurements at radii increasing in steps of 5 millimeters from the centre. A junction made from a strip of the matrix material and nichrome wire served as the cold junction. The metal strip of the cold junction was lead through the base of the burner and connected to the matrix. The free ends of the nichrome wires were connected to a switch board, the thermocouple circuit being completed as shown in the Fig. 2.1 . The connections were checked with the reference junction in ice and the matrix in the burner at room temperature when identical deflections were obtained with each thermocouple.

2.3.1. Calibration: Since the thermocouple formed by the matrix material and the nichrome wire is not a standard one it had to be calibrated against an accurate mercury thermometer having a range from 0 - 100^oC and graduated to a tenth of a degree. In order to avoid the exposed stem corrections at higher temperatures, the thermometer was completely immersed in water contained in a bath. A thermocouple identical to those fused on the surface of the matrix was separately made. To obtain the calibration curves this thermocouple was used as a hot junction in series with the above reference junction. The bulb of the thermometer and the hot junction of the thermocouple were kept very near each other so that no temperature difference could exist between them. In order to

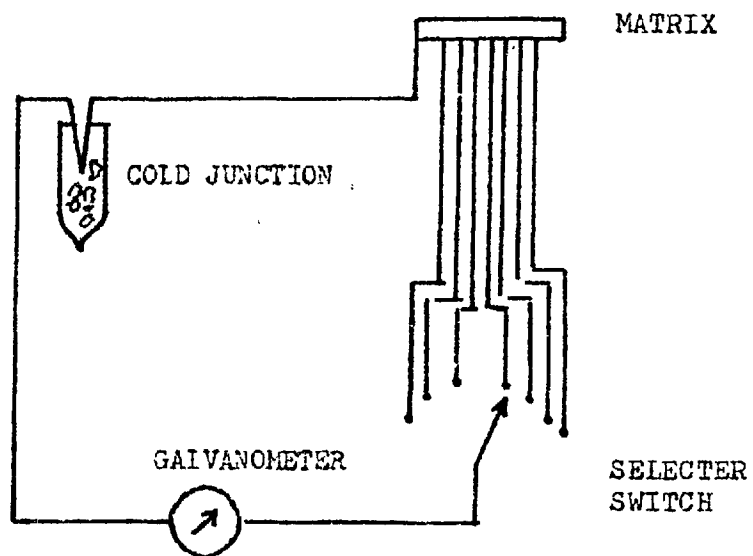


FIGURE 2.1 - CIRCUIT FOR THERMOCOUPLES

minimize temperature gradients, the water bath was constantly agitated by means of a stirrer driven by an electric motor. For measuring the e.m.f. generated, a sensitive moving coil galvanometer was inserted in series with the thermocouple. This was a Pye galvanometer functioning as a microvoltmeter. The temperature of the bath was raised very near to the boiling point of water and the sensitivity of the galvanometer was adjusted to give a maximum deflection at this temperature. Starting from 90°C , the deflections of the galvanometer were noted during the fall of the bath temperature at intervals of 5°C , read by the mercury in the glass thermometer. The calibration was repeated to check reproducibility and a calibration curve was plotted. This curve was used to determine the initial temperature and its distribution on the surface of the matrix.

2.4. Flow system.

The flow system is shown schematically in Fig. 2.2 . Air was pumped by a high speed rotary pump and passed through dust and oil filters, and a large capacity reservoir which served to damp any pulsations or irregularities in the flow. The pressure inside the reservoir was kept at nearly 30 lb/sq. in. From this reservoir, the air was led through a control throttle to three drying towers filled with silica gel. Interposed between the drying towers and the air flowmeter (rotameter) was a high precision "Zambra Negretti"

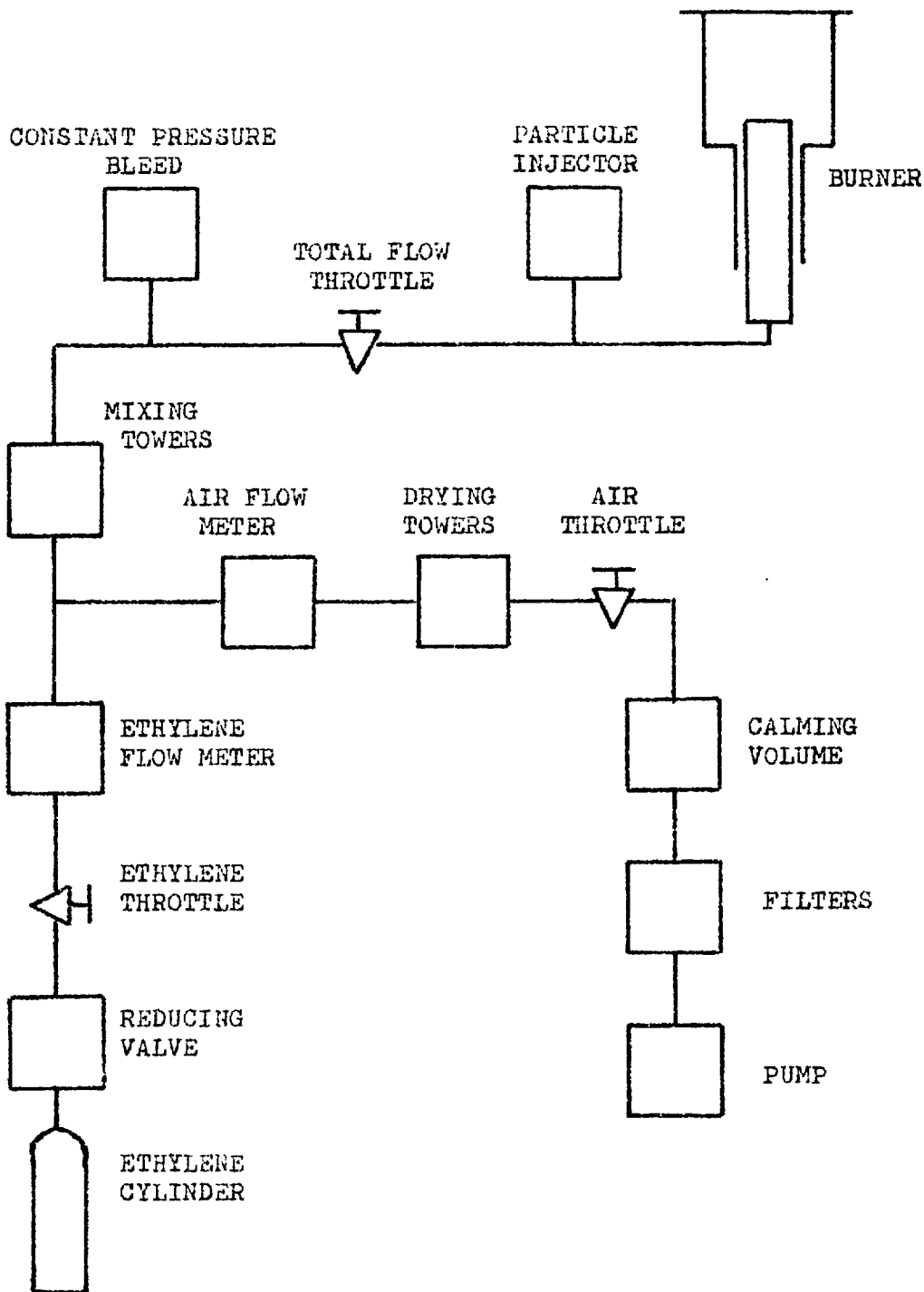


FIGURE 2.2 - FLOW DIAGRAM

throttle valve and a pressure gauge connected in parallel to the flow line. Thus the backing pressure on the inlet valve for the air flow-meter was accurately controlled and kept constant at 20 lb/sq.in. throughout the investigation. In order to deliver air at a constant line pressure, indicated by a mercury manometer in parallel with the rotameter, a needle valve was introduced in series with the flow line on the downstream side of the manometer.

Ethylene was supplied by a cylinder fitted with a reducing valve. Due to the small volumes required, the ethylene flow was metered through a capillary flowmeter shown in Fig. 2.3 . The liquid used in the manometer registering pressure difference across the capillary tube was di-butyl-phthalate (Sp.Gr. 1.046). This was preferred to water because it has negligible vapour pressure at room temperature and thus dry gases could not pick up vapour impurities. By using a system similar to that used in the air flow-line, different flow rates of ethylene could be delivered at a constant line pressure.

From their respective flowmeters, the air and ethylene flows were lead to a T-junction and its common outlet was connected to three mixing towers in order to thoroughly mix the gases. The towers were filled with glass balls of 6 mm. diameter. Adequate mixing of air and ethylene is very

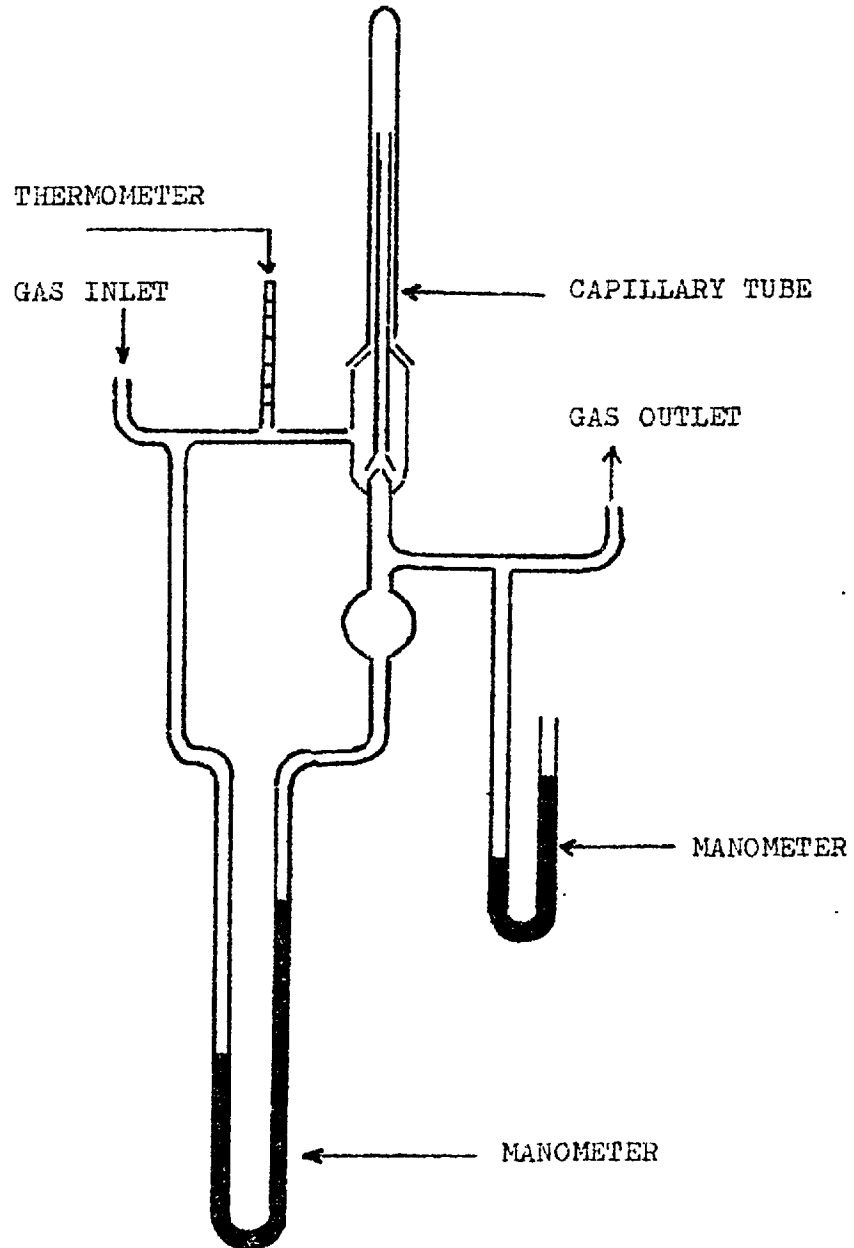


FIGURE 2.3 - CAPILLARY FLOWMETER FOR MEASURING
ETHYLENE FLOW.

important, for a steady flame could be obtained only after passing the mixture through an adequate length of column filled with glass beads. Any length short of the requisite may leave the mixture inhomogeneous and feed the burner with a mixture whose strength may slightly vary with time about its mean value. Levy (1958) experienced some difficulty in stabilizing his flame presumably due to inadequate mixing of the reactants.

In flat flame burners, since the flame velocity balances the uniform approach stream velocity of the mixture, it is evident that the shape of the flame can vary with its temperature distribution. The effect of initial temperature rise of the gas mixture on the flame position can be controlled within reasonable limits by varying the total flow rate of the mixture through the burner. It was therefore decided to introduce some device which would permit variation in total flow rate without adjustment of the mixture composition. This was accomplished by introducing a rotameter immediately upstream of the burner (which is in effect a variable orifice with a constant pressure drop). This works as a constant pressure bleed which also measures the bleed flow. Thus any excess flow which passed through mixing towers and was not required through the burner could be let off to the atmosphere through the rotameter at a constant pressure drop.

The spatial stability and the structure of a flame is affected by any change in pressure, temperature or composition of the initial mixture. If it is desired to restrict the flame front movement to a small fraction of its thickness, it is necessary to regulate these variables and the flow parameters in particular with comparable accuracy. This was accomplished by using precision needle valves at the inlet and outlet ends of the flowmeters. The pressure drop across the input valves was always kept sufficiently high so that the gas velocity would equal the speed of sound at the throat. With such an arrangement, the flow becomes a function of the orifice area and upstream pressure and is independent of variations in downstream pressure. Day-to-day variations in pressure can also change the flows by several per cent. This was overcome by keeping the total line pressure constant, this being achieved by throttling the flow at each setting to a given sum of line plus the atmospheric pressure. Composition constancy was thought to be very important in the present study. As the stabilized flame was of a weak mixture strength (2.72 % C_2H_4) in the region where burning velocity is highly composition-dependent, it was important to minimize changes in initial mixture composition. The ethylene and air flowmeters were therefore calibrated separately by comparison with standard bubblemeters and the mixture strength calculated from the

calibration curves thus obtained. A full account of the calibrations of flowmeters is given in Appendix A. Since the laboratory temperature remained reasonably constant and any flow induced temperature variation in the line becomes a unique function of flow velocity which is automatically incorporated in the calibration, no further steps to control temperature were considered necessary.

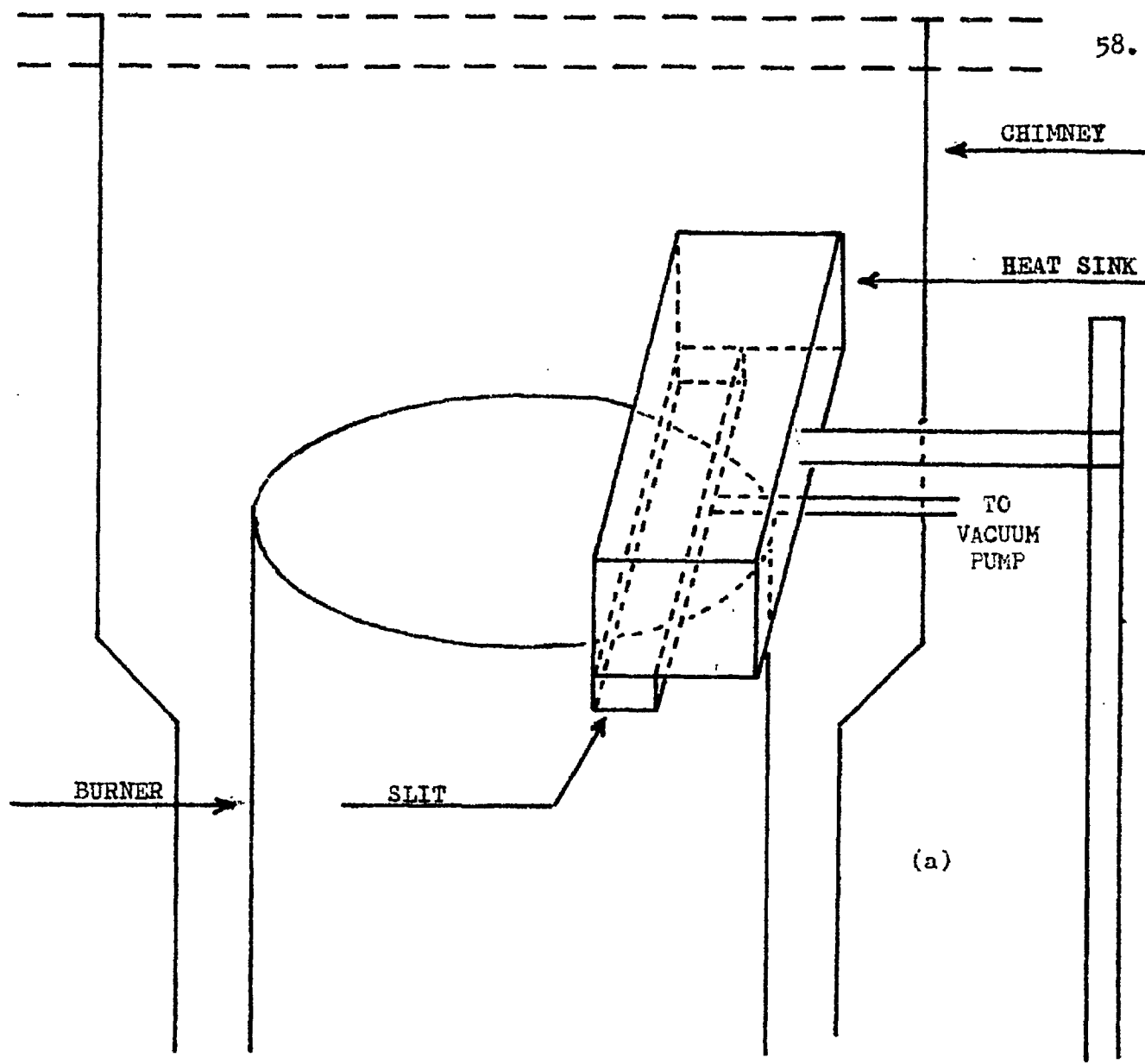
2.5. Flame Stabilization.

At this stage it was thought desirable to test how stable a flame could be obtained with the existing flow system. The attempt involved continuously metering air and fuel, mixing them thoroughly, igniting the mixture above the burner port and observing the resulting flame front with the aid of a cathetometer. At the outset, the day's barometric pressure was recorded and the necessary pressure heads for the two flowmeters were calculated so as to reproduce the condition under which they were calibrated. After turning on the gas flows, the pressure on both the flow meters was set at values calculated to give flows which produced the preselected mixture strength (near the lean limit) and whose sum was the greatest value of the total flow which would be required. By controlling the total flow through the burner the mixture was easily ignited at a particular flow rate where the burning velocity of the mixture slightly exceeded the flow velocity. Under this condition

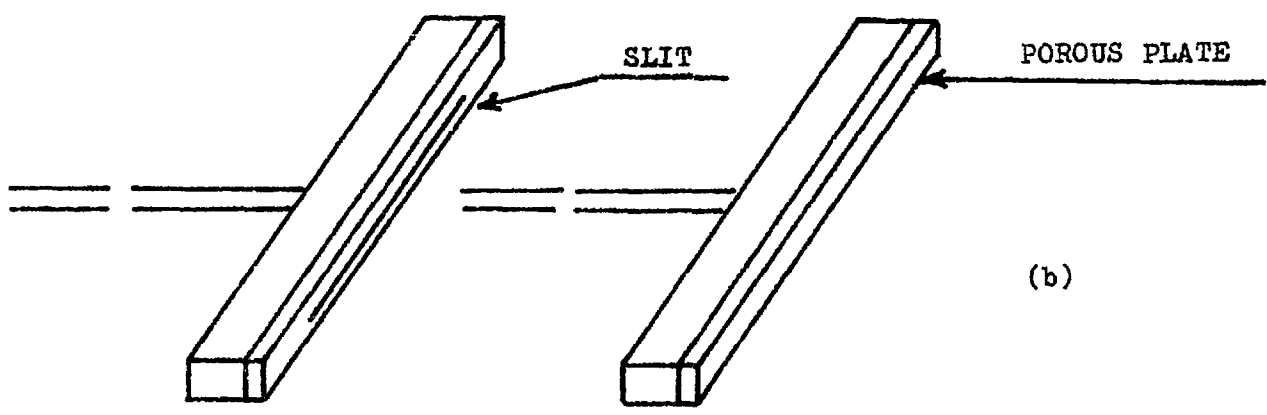
the flame would sit on the matrix. On slowly increasing the flow rate, the flame tended to lift off the matrix, the process starting along its periphery. By suitably adjusting the flow rate and sometimes gradually changing the concentrations of the fuel a floating flat flame could be stabilized above the burner. Before the thermal conditions approached equilibrium, the temperature of the matrix surface tended to rise causing the flame to approach the matrix surface. During this transition period the flame was adjusted back to its original position by suitably altering the flow. However, once thermal conditions reached equilibrium (which normally took approximately 45 minutes) the flame was found to be stationary. A careful observation was made by a cathetometer and it was found that over a period of one hour no change in the flame position could be detected. After the flame became stationary a number of readings of the thermocouple fused on the surface of the matrix were taken at intervals of 15 minutes. This confirmed that the temperature distribution on the matrix surface had also reached equilibrium values.

2.6 Preliminary Investigation.

A brass block (2.5 cm x 2.5 cm. x 7.5 cm) was used as a heat sink in the preliminary investigation. This was clamped in position on a heavy stand, Fig. 2.4a, using a brass rod inserted through a hole in the chimney and soldered



(a)



(b)

FIGURE 2.4 - BURNER AND THE RECTANGULAR HEAT SINK

on to the back surface of the block. In the presence of this heat sink, a stable flame was quenched at its periphery and was found to turn towards the downstream side in its proximity. Attempts were therefore made to bring this part of the flame front back to its original orientation in a direction normal to the heat sink, by reducing the mainstream velocity in its proximity. To this end a slit to which suction could be applied was placed across and under the heat sink. The sketch of the slit system is given in Fig. 2.4b. The suction was applied first by a filter pump and then by a more powerful vacuum pump. This was connected to the slit via a reservoir at the other end of which a throttle valve was fitted. Though there were no fluctuations in time, the pressure drop across the slit was not uniform; the induced gas velocity being undesirably greater in the middle, opposite to where the outlet hole was situated. This was attributed to too large a width of the slit. Accordingly the slit was replaced by a porous metal plate. The pressure drop across the porous plate was found uniform and on controlling the suction, the flame could be made to change its position. In the beginning it was expected that, by this device the flame could be made exactly perpendicular to the face of the sink, but on actually attempting to bring this about, the flame always manifested a turned edge near the sink. The alternative of increasing the local burning velocity near the heat sink was

then tried. This could be done by introducing additional fuel near the heat sink. It was therefore introduced through the same porous ^{metal plate} / connected to a second ethylene cylinder fitted with a reducing valve. Injection of controlled amounts of additional fuel did bring the edge of the flame down to its original position in the immediate vicinity of the heat sink, but the flame front still remained upturned only a little distance away from it. On increasing the rate of fuel supply the flame flashed back on the porous metal plate. Thus it proved too difficult to match the flow and burning velocity profiles everywhere so as to retain a flat flame.

2.7 Schlieren System.

In order to confirm these visual observations by some more permanent and analysable record it was considered desirable to use schlieren photography. In addition to visualization such photographs were expected to give a rough idea of temperature distribution near the heat sink.

The cylindrical Pyrex glass chimney used so far was thought to be of too poor an optical quality for this work. It therefore became necessary to design a cylindrical chimney, of good optical quality, capable of withstanding high temperatures and retaining its quality at these temperatures. Thin mica sheets had previously been used for optical work on flat flames (Burgoyne and Weinberg, 1954 and Levy and Weinberg,

1959²). After a little care in their selection, such sheets were found to be adequate for the optical requirements of a schlieren system. The final version of the chimney is shown in Fig. 2.5. This was made from a brass tube by cutting windows separated by three ribs 120° apart. These were glazed with thin mica sheets held by circlips against the top and bottom rings of the tube. The diameter of this chimney was kept the same as that of the previous one, in order that it could be easily replaced on the flange of the burner housing.

The schlieren system (Fig. 2.6) was set up by using two 6 cms. aperture doublet lenses. A high pressure mercury arc was used as the light source. The light was condensed on a pin hole placed at the focus of the first doublet, the second acting as the schlieren lens. The flame was located in between these two lenses. A knife-edge capable of rotation in the vertical plane was mounted at the focus of the schlieren lens. A camera was mounted beyond the knife edge and focused on the part of the flame under study. All the accessories were mounted on an optical bench for accuracy and ease of adjustment. The changes in the position of the edge under various conditions described above were studied and some preliminary photographs of the flame were obtained. An inspection of these photographs confirmed the visual observations made earlier and gave a rough indication of temperature

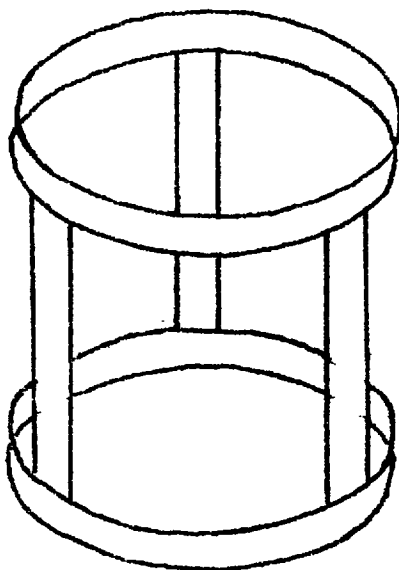


FIGURE 2.5 - FRAMEWORK FOR MICA CHIMNEY

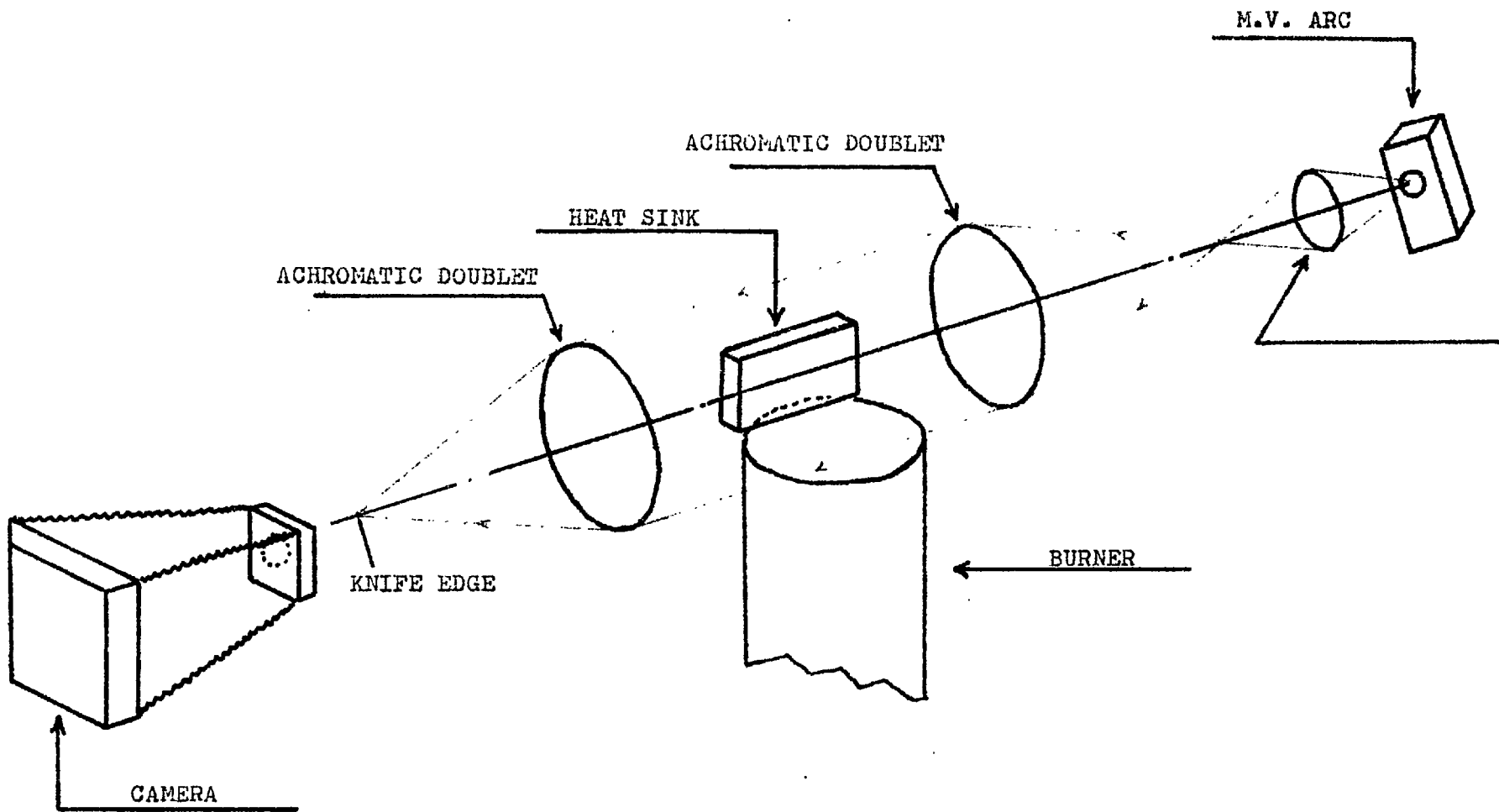


FIGURE 2.6 - SCHLIEREN SYSTEM

distribution near the heat sink.

During these preliminary investigations an undesirable feature of the flame shape was an edge distortion at the two extremities of the heat sink. At these edges the flame did not remain flat, i.e. along the face of the heat sink the intersection of the flame with its plane was not linear. Various methods were tried in an attempt to reduce this to a minimum. These included varying the flows, adjusting the chimney height and masking the segment of the matrix in the up stream region under the heat sink. Eventually the defect was remedied by a combination of all these variations, the precise arrangement being a matter of trial and error.

2.8 Determination of Burning Velocity Profiles.

(i) Method: The most direct method of measuring burning velocity on burner stabilized flames, as mentioned previously, is by the use of quantitative flow visualization with suspended microscopic dust particles. These are illuminated by an intense light beam interrupted at a known frequency and their broken tracks photographed at an angle to the direction of illumination. The method has been applied to flames by a number of workers. It is simple and accurate and aims at deducing the component of flow velocity perpendicular to the flame front from these particle track photographs. The angle between the direction of the particle track in the

cold reactants and flame front at the point where the track passes through it is measured and the local burning velocity is calculated by the following expression

$$S_u = V_u \sin \theta_u$$

where S_u is the burning velocity, V_u is the flow velocity vector and θ_u is the angle between it and the flame front; the suffix 'u' denotes the initial state.

(ii) Application: Before proceeding with the measurement of burning velocities two modifications were made in the burner system. The solid heat sink described above had the disadvantage that its surface facing the flame front could not be maintained at a uniform temperature. It was therefore replaced by a water-cooled heat sink of identical dimensions (Fig. 2.7). The cooling was accomplished by circulating water from a thermostatically controlled bath via a centrifugal pump. To avoid condensation of moisture on its surface nearly boiling water was circulated through the heat sink.

The second modification was to make provision for introducing the tracer particles into the gas stream. These were of bentonite, a finely divided colloidal clay (density, 2.7 gms/cc.). They were extremely small in dimension. A determination of their particle size by a projection microscope

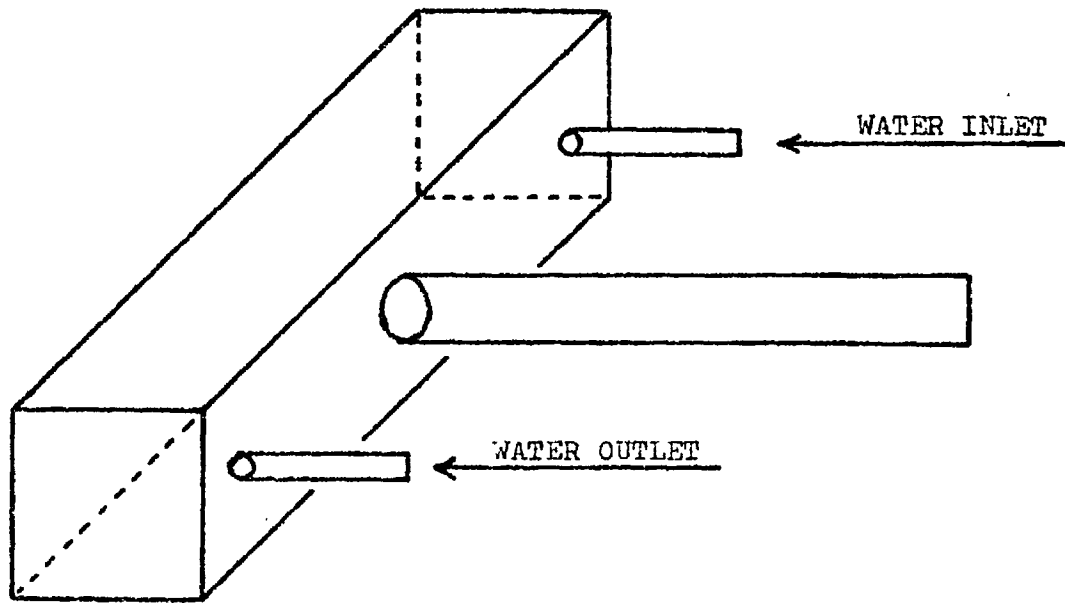


FIGURE 2.7 - HEAT SINK WITH COOLING DEVICE.

showed that the mean diameter of the particles was 4 microns and deviations from this mean value were small both in frequency and magnitude. To this end, the flow line was broken just before it entered the burner and a T-tube inserted. A test tube containing the bentonite particles was connected to the vertical leg of the T-tube. This device ensured that the supply of particles contained in the test tube could not leak into the gas stream unless the tube was tapped. On gently tapping the test tube a burst of particles would be entrained in the gas stream and carried to the flame zone.

(iii) Optical system: As the dimension of these particles is very small they are recorded by scattered rather than reflected light - a method which requires a highly intense source. The source is focused on the area to be photographed so that maximum illumination per unit area is obtained. In the present work, a high pressure mercury vapour lamp run on A.C. mains was used as the light source. Providing sufficient intensity of illumination in the test zone was largely a matter of arranging for sufficient convergence of the beam whilst maintaining an appreciable working area. Adequate results were obtained by using a condenser lens of 7.50 cm. aperture working at $f/1$. The system used is shown in Fig. 2.8. A magnified image of the arc was thus thrown on the face of the heat sink.

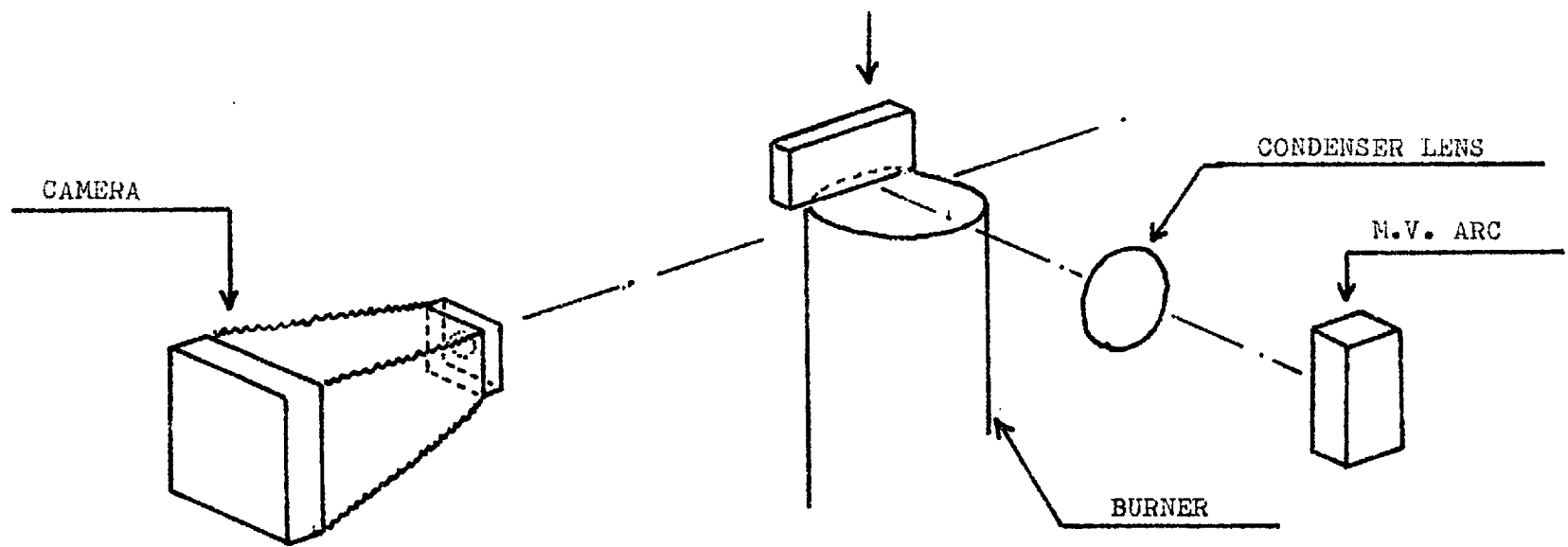


FIGURE 2.8

Since particle track studies require high resolution, some thought was given to the photographic arrangement which would yield the most efficient results. In order to study the particle tracks in a diametral plane of the flame, a large aperture lens of good quality was used for light gathering power and sharp definition of the plane of focus. A plate camera with a Kodak 17.8 cm. f/3.5 lens was used as the objective. It was placed at right angles to the illuminating beam and focused on the test space to give an image at a magnification of 1.5 x. The depth of field could thus be considerably reduced (\sim 2 mm.) with the result that the particles on either side of the relevant region were thrown out of focus. This produced clear and distinct particle tracks from a region confined to within a zone of 2 mm. around the diametral plane.

It was soon observed that tracks of particles very near the heat sink were masked by the light reflected from the face of the heat sink. To minimise these reflections the face of the heat sink was painted with matt black. The inside of the chimney was also painted black except at two places to allow for the illumination and photography of the particles. This greatly increased the contrast of the particle tracks on the photographic plate.

Having set up the optical system attempts were made to

record particles in the presence of a flame (2.72% C_2H_4 in air).

The photographs were taken after the flame and the matrix temperature had reached a steady state. An exposure of 1/5th sec. on HP3 plates developed in Ilford contrast FF developer was found to give the best results. The particle tracks were recorded over the entire region between the matrix and the flame. The interval between the streaks corresponded to twice the mains frequency, i.e. 0.01 sec. Having recorded the particle tracks for a freely propagating flame near the heat sink, the whole procedure was repeated for a flame modified by suction, where the front became nearly normal to the heat sink. The photographs obtained in the above two cases are shown in Fig. 2.9 and 2.10 respectively.

(iv) Measurement of Burning Velocity: Three best negatives were selected for each case and enlargements were produced on large sheets (40 x 50 cms) of Kodak document paper. To avoid any error due to photographic build up all the enlargements were printed and developed under standard conditions. To inter-relate and compare the burning velocity data it was necessary to establish a co-ordinate system on these enlargements. The edge of the heat sink and the surface of the burner port were taken to represent the ordinate and abscissae respectively.

Velocity in the flame front, if it is strictly one-

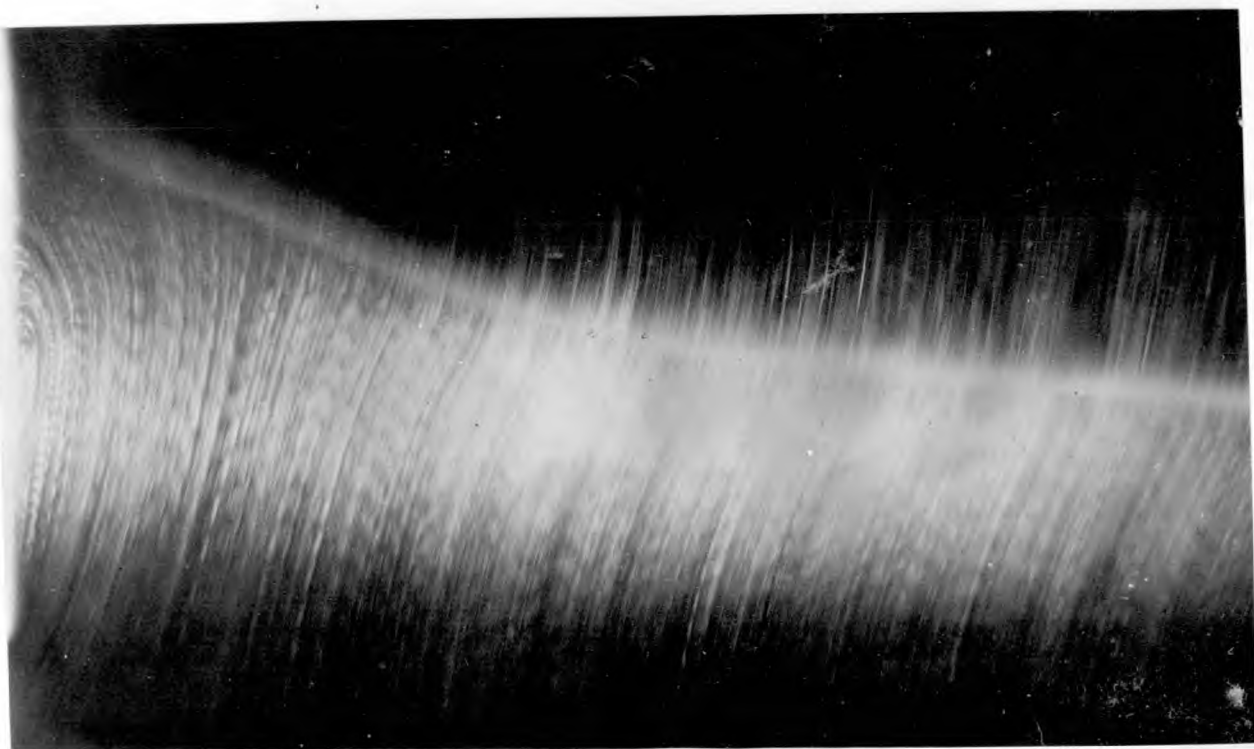


FIGURE 2.9 - Particle track photograph with
rectangular heat sink. (Unperturbed flow)

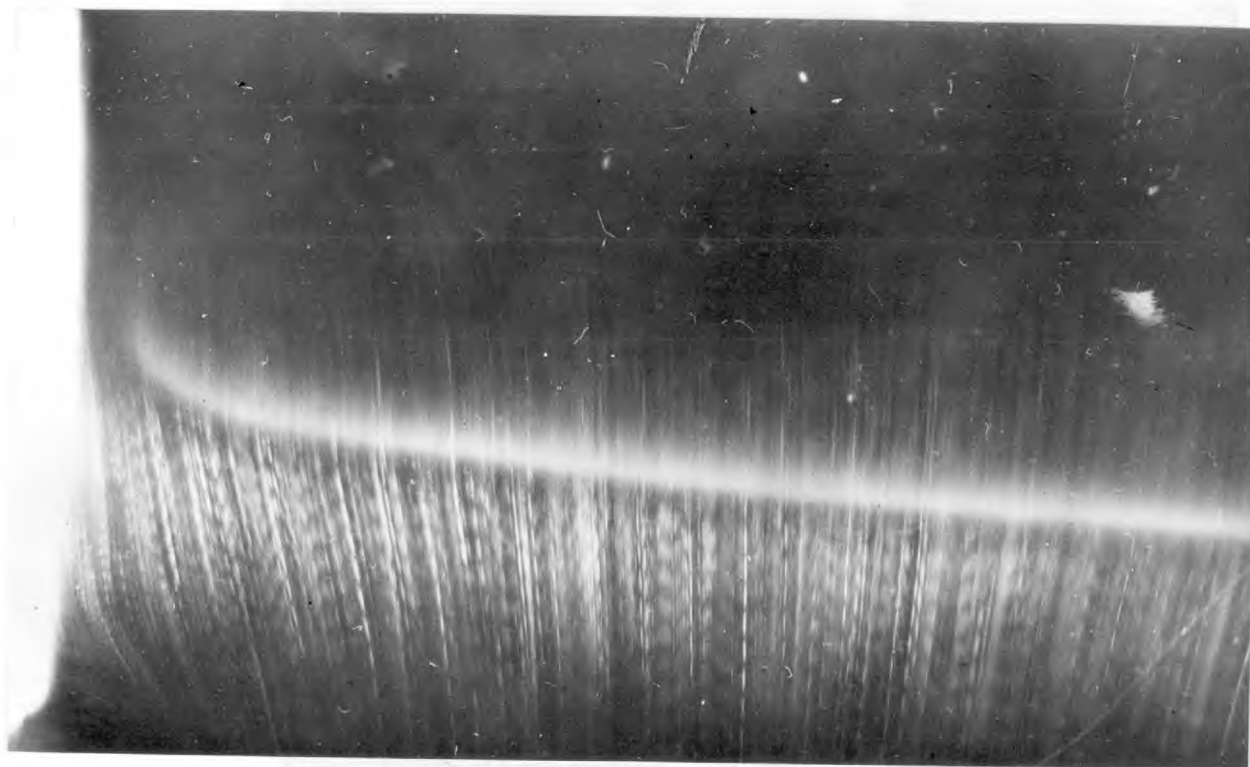


FIGURE 2.10 - Particle track photograph with
rectangular heat sink. (Induced flow)

dimensional is described by a profile which obeys the conservation equation

$$M (= \rho_u S_u) = \rho S = \text{constant}$$

where S is the unidimensional velocity at any point, ρ is the density of the gas, M is the mass burning rate and u denotes the initial state. An inspection of the equation shows that the flow velocity in a flame varies from zone to zone and tends to become equal to burning velocity towards the cold boundary. In a non-unidimensional flame directional flow distortion must also be taken into account.

The mass conservation equation then becomes

$$\rho_u v_u A_u = \text{constant} = \rho v A$$

where A is the cross-sectional area of an elemental stream tube. This is related to the one-dimensional equation by

$$v \sin \theta = S$$

where θ is the local angle between the flow line and the perpendicular to the flame. In particular, the burning velocity

$$S_u = v_u \sin \theta_u$$

as stated previously. Throughout this work it was never assumed that the flame is one-dimensional, but θ did not vary

greatly along each streamline. Nevertheless to obtain local flame orientation the reference surface for the purpose of measuring the burning velocity should be at a low temperature. Thus the reference state was taken 3 mm. below the luminous zone where the gas stream temperature is around the isotherm corresponding to the schlieren image of the flame. Several perpendiculars were drawn to the luminous zone and each was marked at a distance of 3 mm. from the lower edge of the luminous zone and the reference surface was constructed by joining these points. Subsequently the angle of incidence of the particle tracks at this surface was determined and finally from the knowledge of the distance between successive streaks and magnification of the photographs, the burning velocities were calculated at different distances from the heat sink.

In flat flame burners the mechanism of flame stabilisation is always accompanied by the transfer of a small amount of heat to the matrix. Much of this heat is given up by the matrix to the reactants flowing through it - it has been mentioned that as the flame is stabilized the matrix heats up to temperatures around 100°C . This temperature rise depends upon the design of burner, and on the types of flame burnt. The mechanism of heat transfer has been investigated in the past (Levy and Weinberg, 1959)² and it has been shown that heat is supplied to the matrix by various mechanisms, from the hot products, for example by

radiation from the chimney housing and by a vortex which occurs at the edge of the flame.

As mentioned earlier, the reactants passing through the matrix very nearly attain its temperature. This initial temperature rise (T^0 K) affects the burning velocity in two ways,

(i) by its effect upon the mechanism of propagation, and (ii) by simple expansion according to the gas laws. Usually, the values of burning velocity have been corrected for the effect on propagation in terms of an equivalent composition change and for the expansion by reduction to S.T.P. conditions using the perfect gas law. Thus as regards the latter,

$$(\text{Burning velocity})_{\text{S.T.P.}} = \frac{273.2}{T_0} \times (\text{Burning velocity})_{T_0}$$

Ideally correction to standard pressure from ambient pressure should also be included in the above equation but since the discrepancy involved does not usually exceed half a per cent, it can be neglected. The distribution of burning velocity with distance from the heat sink in the presence and absence of flows induced by suction through the sink are given in Fig.

2.11 It will be seen that the two profiles of burning velocity agree within experimental error except just beyond the region of zero burning velocity where the profile for the freely stabilized flame is found to exhibit a maximum.

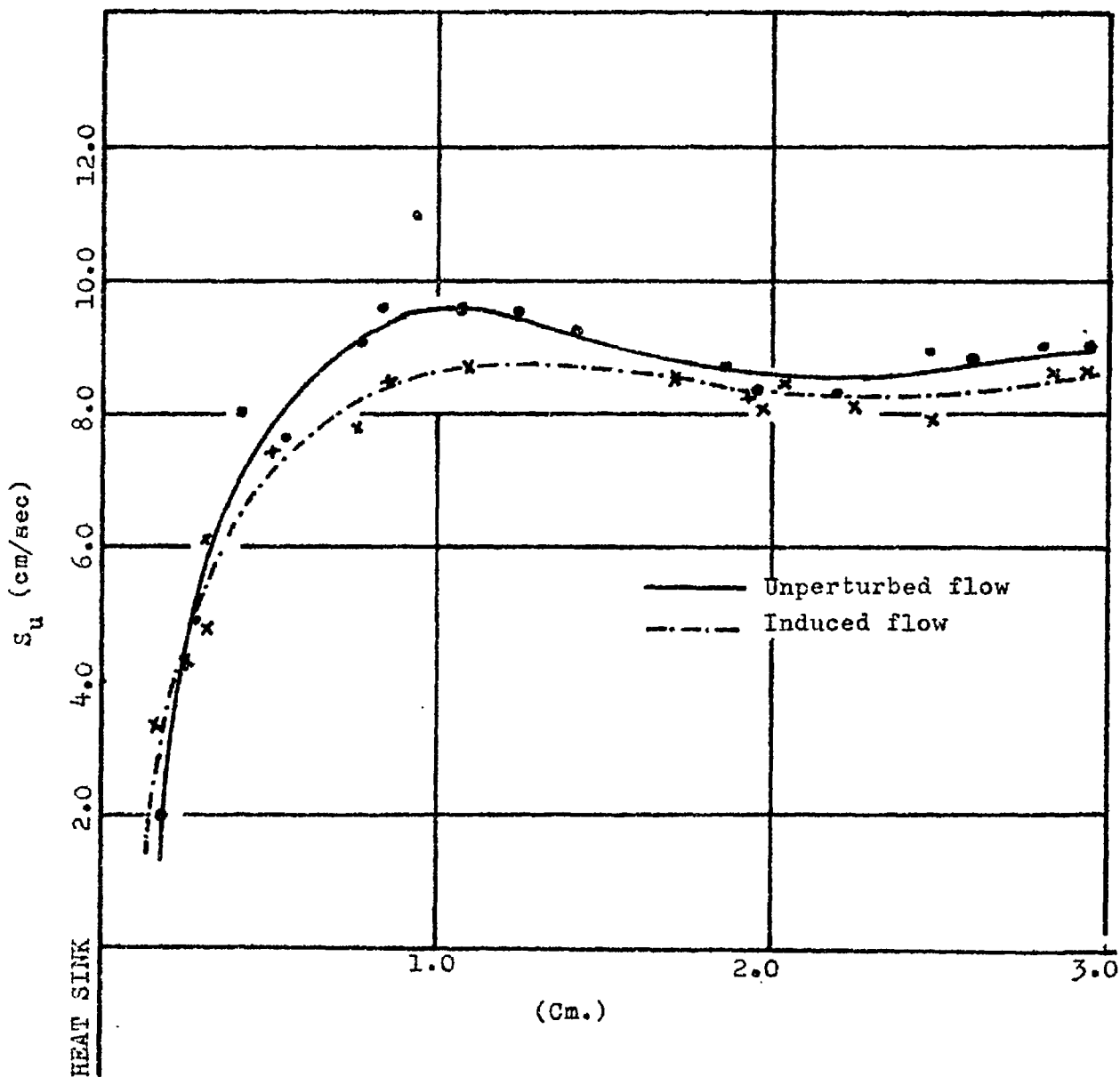


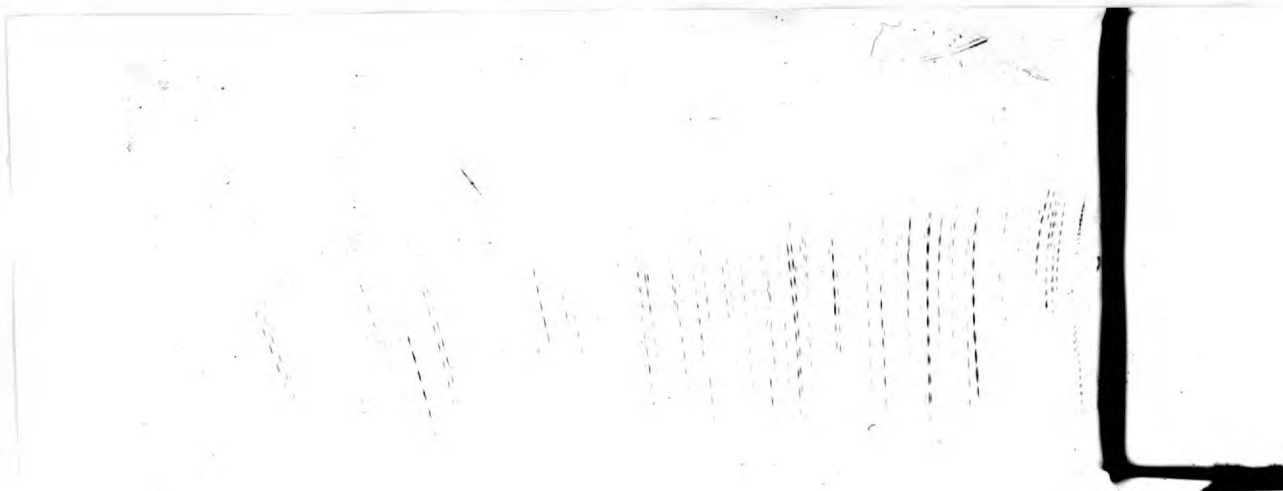
FIGURE 2.11 - VARIATION OF BURNING VELOCITY WITH DISTANCE FROM THE HEAT SINK (PERIPHERAL)

To investigate the causes of this anomaly it was necessary to obtain the burning velocity profiles of flame fronts varying in shape and stabilized in different flow regimes. This was done by successively increasing the volume rate of flow of the reactants, keeping the mixture strength the same each time. Three such flow regimes were investigated and the results are shown in Fig. 2.12. In addition to the particle tracks, they also show the orientations of the flame front with respect to the heat sink under these conditions. Burning velocities are shown in Fig. 2.13. It is observed that three profiles agree within experimental error in the region where the quenching effects become prominent. The same is also found true for the profiles far removed from the heat sink. In between, however, the burning velocities are again found to be considerably different in the three cases and show a gradual fall with the reduction of induced flows, the maximum velocities occurring in the case of a freely propagating flame.

At the time it was thought inconceivable that a burning velocity higher than that of the free flame could exist. This is far less obvious at the conclusion of the work, but at the time it led to a serious investigation for any possible causes of this abnormal observation. The choice of the flame zone for obtaining the burning velocities was scrutinized first.



(a)



(b)



(c)

FIGURE 2.12 - Photographs showing the particle tracks and the orientation of flame fronts with respect to heat sink (Axial). (a) Unperturbed flow; (b) and (c) induced flows.

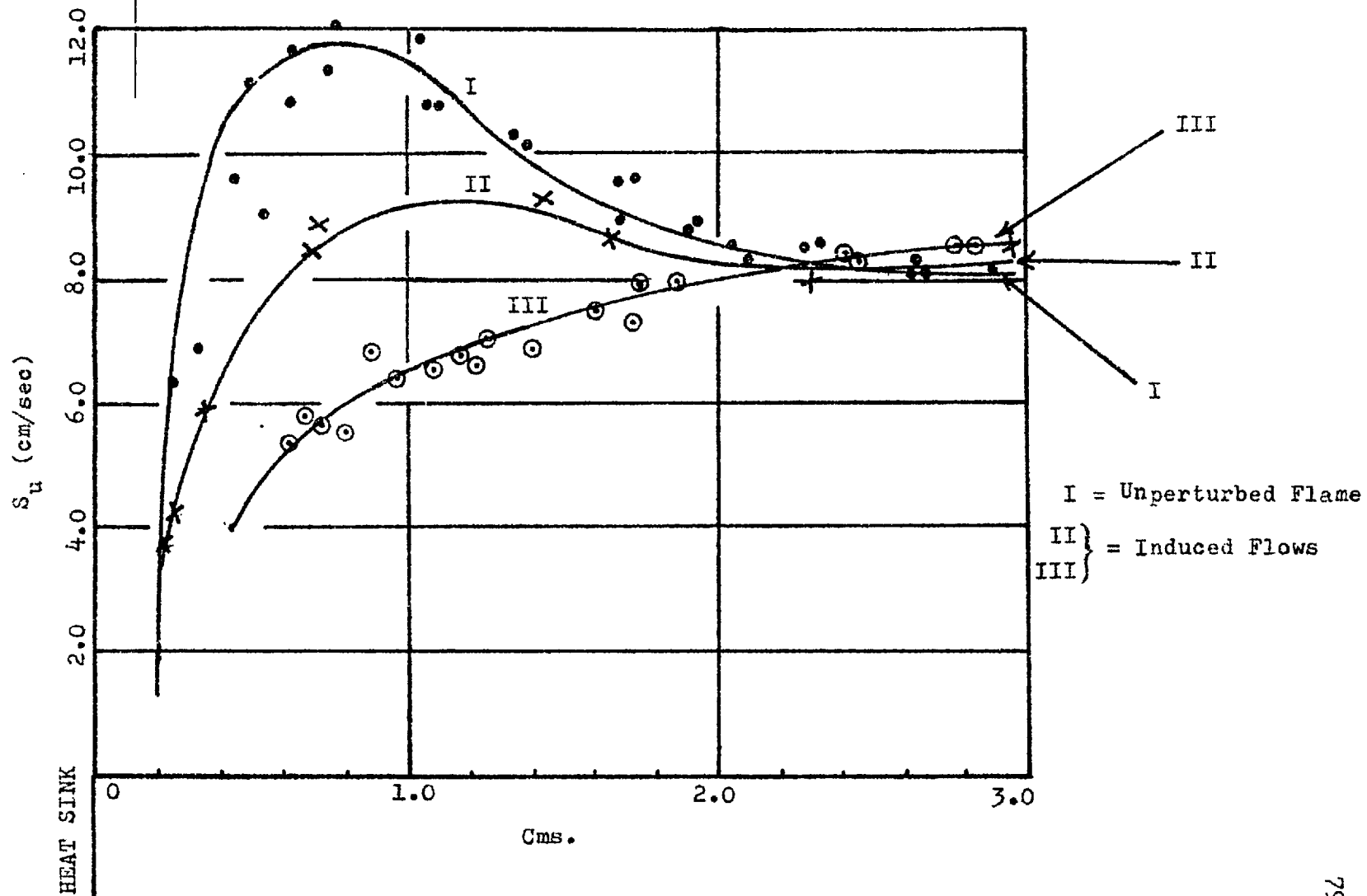


FIGURE 2.13 - VARIATION OF BURNING VELOCITY WITH DISTANCE FROM HEAT SINK (PERIPHERAL)

Accordingly burning velocity profiles defined on the basis of two different zones, located at a distance of one millimeter on either side of the previous one were determined. For the two cases of induced flows, these profiles remained practically unchanged and only for the case of a freely propagating flame was a small difference noticed. In this case the observed maximum in the profile appeared less pronounced as the reference zone was shifted towards the luminous zone.

The entire concept of these measurements was then re-examined. It is based on the supposition that the system is two-dimensional, i.e., that all sections by planes perpendicular to the heat sink surface are identical. It is only if the intersection of this surface with the isothermal planes in the flame indeed gave straight lines over appreciable distances, that the appearance of burning velocities greater than that in the unperturbed flame seemed inconceivable. The occurrence of localized turbulence was ruled out by the small Reynolds numbers involved. However on viewing the flames in a direction perpendicular to the heat sink it was observed that at least some of them varied in their orientation with respect to the approaching reactants. Proceeding along the intersection between sink and flame and starting with an almost horizontal surface such flames had fronts which gradually became curved and concave towards the reactants only a small

distance away from the edge. Their curvature too did not seem inappreciable in comparison with the local flame thickness. Such curvature would be expected to produce a local increase in burning velocity, but since the shape of the relevant sections cannot be reliably ascertained without using a transparent heat sink attempts at a theoretical analysis of the effect seemed unprofitable. Moreover recently Fristrom (1965) has cast doubt on the hitherto accepted views regarding the dependence of burning velocities on curvature. It was, therefore decided not to pursue the matter further and instead a heat sink geometry was sought by which the system might become symmetrical about the burner axis so that information concerning the flame shape can be evaluated from a single radial section. Further studies on such a system and its construction is described in the next chapter.

CHAPTER 3.THE AXIAL HEAT SINK3.1 Burner-heat sink system.

An obvious way of obtaining a system in which all sections would be identical was to make it symmetrical about the axis. All the basic features of the previous burner were, therefore, retained and a hollow cylindrical heat sink was incorporated along its axis. This was constructed of two identical brass tubes 1.2 cm. in diameter joined coaxially at a sealed interface, Fig. 3.1a. A new matrix was completely wound on one of these tubes with an appreciable length of the tube protruding from the upstream face of the matrix. This end of the tube was connected to rubber tubing which was led out of the base of the pyrex glass burner. Five thermocouples, identical to those described before were again spot-welded in a spiral distribution on the down-stream face of this matrix. The burner was reassembled by packing it with glass beads and sealing the other end by a rubber bung with suitable channels for thermocouple wires, gas inlet and the rubber tube mentioned above.

The other tube, which served as the heat sink, was screwed on top of that in the matrix, a circular slit of variable width forming at the interface between the two. In

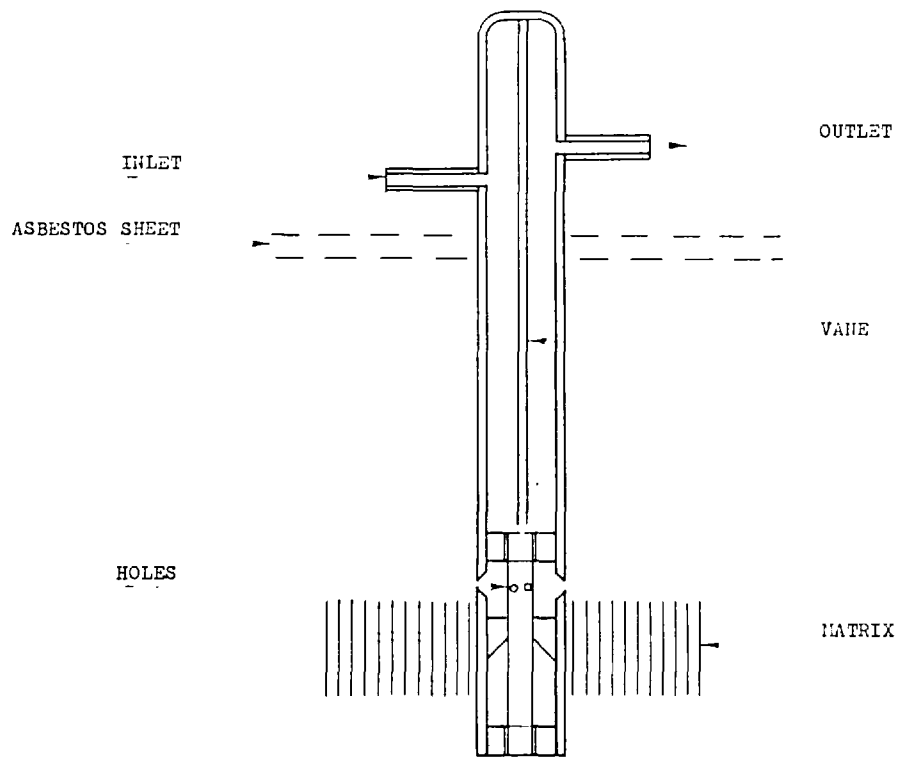


FIGURE 3•1(a) - THE HEAT SINK

the plane of this interface were located four holes which could be connected to either a suction pump or an auxiliary ethylene cylinder via the lower part of the heat sink carrying the rubber tube.

In order to maintain the heat sink at a constant temperature, two side connections were provided at its upper extremity for circulating water from a constant temperature bath. A vane in the middle of the upper tube helped to improve the circulation of water inside the heat sink. This tube was passed through a positioning hole in the asbestos sheet topping the mica chimney in such a way that the inlet and outlet tubes for circulating water were always outside the enclosed space, Fig. 3.1 b.

When attempts were made to stabilize a steady-state flame in the presence of the new heat sink, fresh complications arose. A mixture much richer than that used before was easily ignited resulting in a flame sitting on the surface of the matrix. The volume flow of ethylene was then gradually adjusted to give the exact mixture composition which had been previously studied. As the mixture of the desired strength approached the flame, it tended to lift off the matrix surface starting from the centre, and soon blew out in the central regions. This blowing off of the flame persisted in spite of adjustment to the chimney height, variation of the total flow

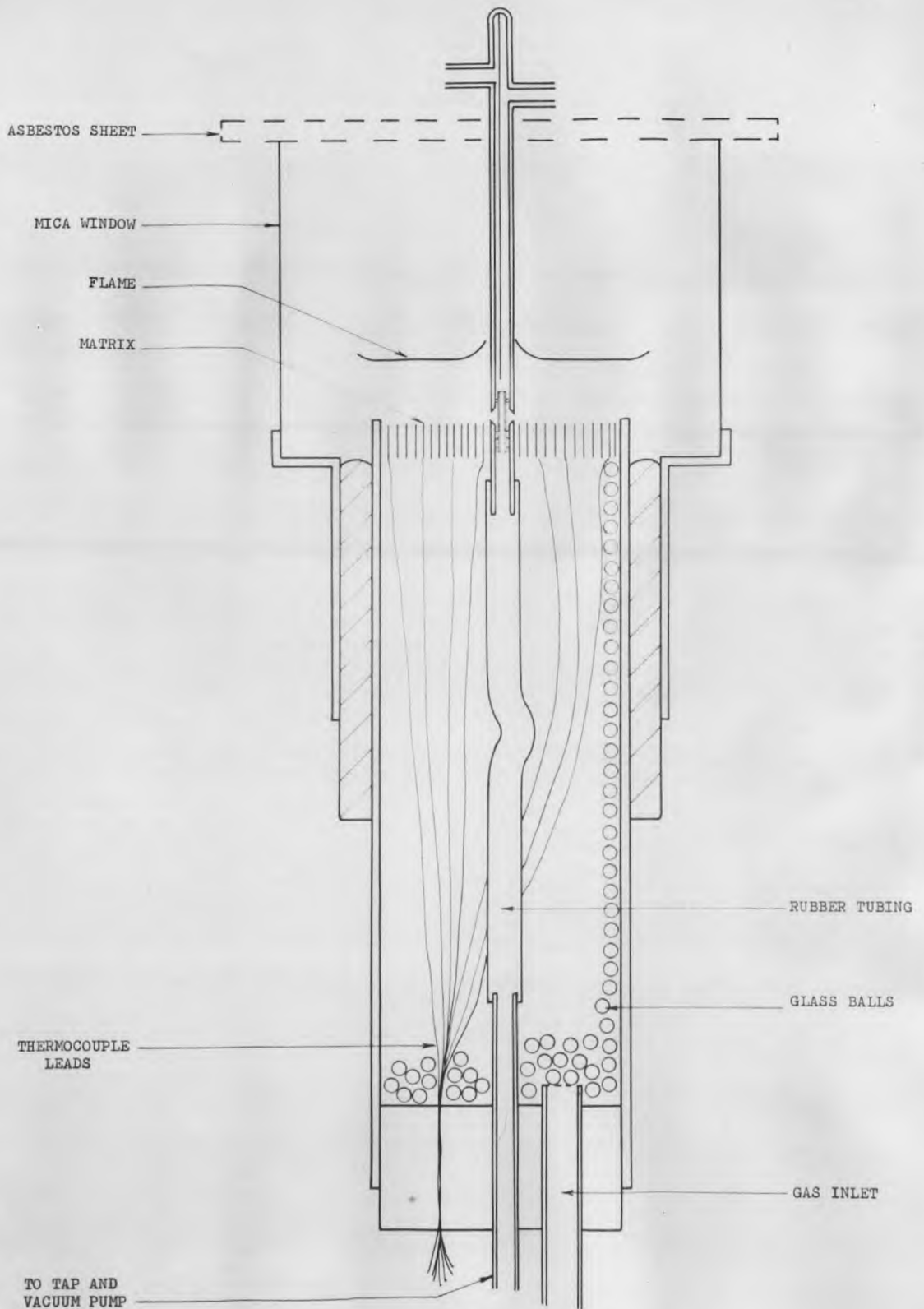


FIGURE 3-1 (b) - BURNER AND THE AXIAL HEAT SINK ASSEMBLY

rate of the reactants and even the use of slightly richer mixtures. In the case of richer mixtures the flame burnt only along the periphery of the burner port and had the appearance of the mouth of a bell.

An explanation of this behaviour of the flame may be thought of in terms of the mechanism of flame quenching. The distance from the wall at which a flame can be maintained is a function of the amount of heat transferred to the wall, the heat transfer itself depending upon the area of the flame front exposed to the heat sink. In the system discussed, therefore, the quenching of the flame in the immediate vicinity of the heat sink left a cylindrical annulus around it, through which reactants at a temperature much lower than the surrounding luminous zone can flow past unburnt. This unburnt stream of reactants becomes the new, and larger, heat sink and also results in more cooling of the matrix near the axis. Thus the region over which the flame is quenched can rapidly start spreading from the centre. It was thought that if this explanation is correct a reduction in the amount of heat transferred to the wall, as by taking a sink of a smaller diameter, and thus reducing the area of flame exposed to it, may permit a steady state with local quenching to be established.

Another heat sink of identical design but only of 0.6 cms. diameter was therefore tried. This modification was

immediately successful because with the new set-up a flame of the same composition as used in the first series could be easily stabilized. A photograph of this flame with the new heat sink is shown in Fig. 3.2. Although the system was perfectly symmetrical and there was no irregular pattern in the shape of the flame front, it again tended to turn upwards in the quenching region and had an open cusp around the heat sink.

This system, therefore, seemed satisfactory for undertaking a quantitative analysis of flame quenching. Before proceeding with this, it was thought desirable to standardise the conditions, so that reproducible flames could be produced in spite of day-to-day changes in ambient conditions. The procedure adopted was as follows:

A stable flame of the desired mixture strength was obtained. Its position was carefully noted over a period of forty five minutes and once the steady state was reached, this was read off on a cathetometer. The temperature distribution along the matrix of the burner was also noted at the same time. The setting of the cathetometer was kept unaltered until all the information on that mixture strength was obtained. Each time the flame was stabilized subsequently, its steady state position was made to coincide with the cathetometer crosswire. This could be done by slightly adjusting the height of the chimney. But it was important to know if the displacement of

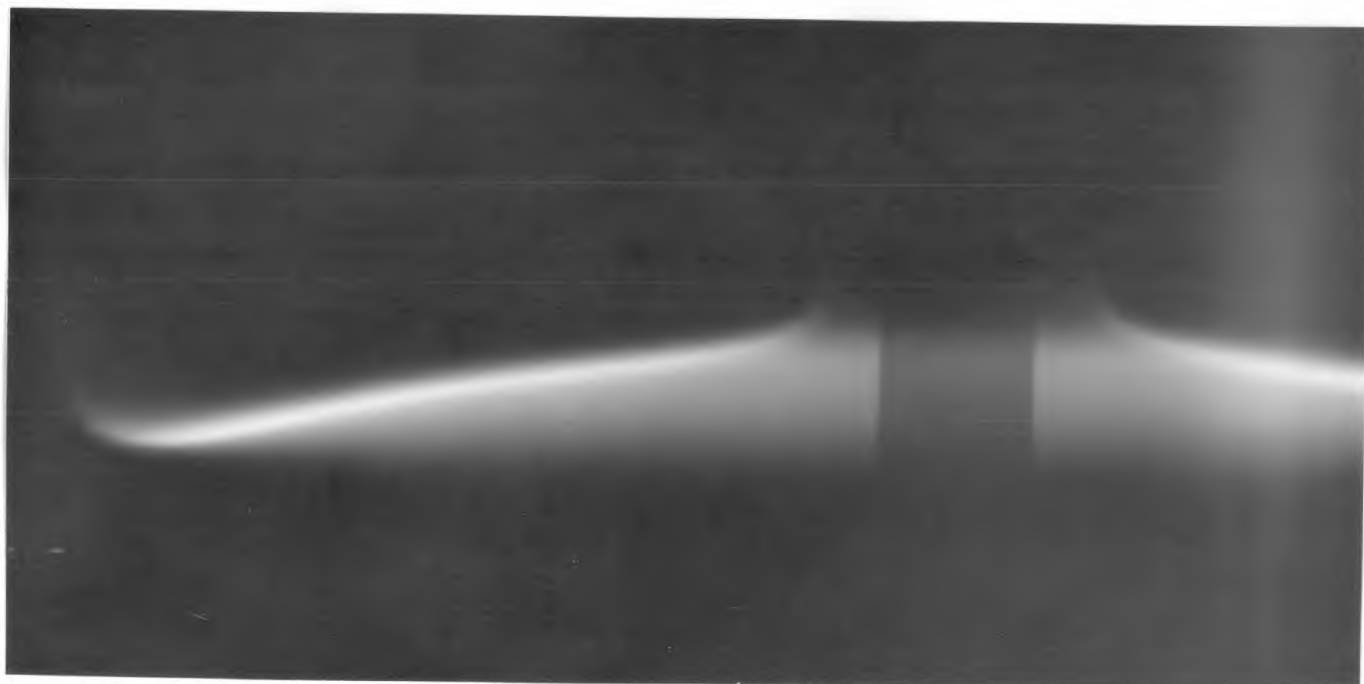


FIGURE 3.2 - Photograph of the cylindrical
heat sink and the flame.

the chimney had any effect on the shape of the flame - both in the presence and absence of flows inducted by suction at the slit. A series of photographs were accordingly taken while adjusting the chimney height, in steps, over a distance of about 4 mm. An examination of these photographs revealed that the shape of the flames remained unaltered; only their position with respect to the matrix underwent a slight change. Thus it was possible to make the flame of a particular mixture strength occupy the same position day after day. These flames were strictly reproducible because not only were their locations exactly the same but also the temperature distribution over the matrix in the steady state was found to be always the same. All the quantitative work reported here has been done on flames reproduced in this manner.

3.2 Location of the flame front.

For the purpose of burning velocity measurements the choice of a suitable and reproducible reference surface is very important, as previously mentioned. In the early work this was arbitrarily taken at a known distance from the luminous zone, but with the new system the luminosity of the flame became indiscernible in the proximity of the symmetrical heat sink and could not be recorded on the photographic plate. Moreover, since, according to thermal theories, the flame thickness is approximately inversely proportional to the local burning velocity,

the validity of locating the flame front photographically in the vicinity of the heat sink was thought rather doubtful. In order to obtain a more accurate and reliable reference surface recourse was made to the schlieren image of the flame front.

It has been shown (Weinberg, 1955, 1956) that in the case of laminar pre-mixed flames of the type under study the schlieren image of the flame coincides with an isothermal surface whose temperature T_s is given by

$$T_s = T_u \frac{a + 2}{a + 1} \quad (3.1)$$

where T_u is the initial temperature of the reactants and a is the exponent of the temperature correlating the variation of thermal diffusivity k/C with temperature over the relevant range, i.e.

$$\frac{k}{C} = \frac{k_u}{C_u} \left(\frac{T}{T_u} \right)^a \quad (3.2)$$

For a mixture which is predominantly air, 'a' can be taken to be unity. This value gives the location of the schlieren surface at a temperature $T_s = 1.5 T_u$. Thus if the initial temperature of the reactants is say 18°C , it will coincide with 163°C isotherm. This temperature is low enough for no appreciable reaction and for little flow distortion to take place.

This schlieren record of the flame is in fact a focused image of the zones where the transilluminating beam of light undergoes maximum deflection which in turn takes place in the regions of maximum refractive index gradient. It is, therefore, very easy to locate and was accordingly considered for fixing the reference surface for burning velocity measurements.

3.3 Schlieren system

A very large number of optical systems have been described in publications (e.g. Weinberg, 1963). However, the choice of a particular system depends upon the requirements of the problem under study. Generally the size and quality of the optical components are decided by the sensitivity and field of view required. In the present investigation the desired field of view was approximately 4 cm. square and a sensitivity corresponding to deflection of 1 mm. of the flame front was considered sufficient. Although a system fulfilling these requirements could be achieved by ordinary single lenses of 50 cms. focal length working at $f/8$, a parallel beam system seemed preferable because of the large flat flame involved. This was set up using two schlieren mirrors of 8 ft. focal length working at $f/10$.

In addition to its suitability for quantitative measurements such a system has many advantages (Weinberg, 1963).

Thus the transluminating beam is parallel and passes through the test zone only once, the position of the test object within the beam is an independent variable thereby enabling a change of conjugates for the projection system, while keeping the approach angle of the beam constant across the test space; this versatility was an added attraction. The layout of the system is shown in Fig. 3.3. Light from a high pressure mercury vapour lamp was focused on a pin hole of 1 mm. diameter located at the focus of the first mirror. After traversing the working space the reflected beam was again brought to a focus by the second mirror on a schlieren stop. In order to minimise optical aberrations of the system, the schlieren stop and the pinhole were placed symmetrically about the parallel beam. The second mirror was also made to project the image of the flame at a unit magnification onto a ground glass screen placed near the first mirror. To obtain a well defined image of the flame different types of schlieren stops were tried. These included small opaque discs, small apertures and edges of razor blades. Of all these an opaque disc gave the best picture. Three photographs, one in the absence and two in the presence of flows induced by suction through the slit are shown in Fig. 3.4. It will be seen that in all three cases well defined schlieren surfaces, especially near the heat sink could not be obtained.

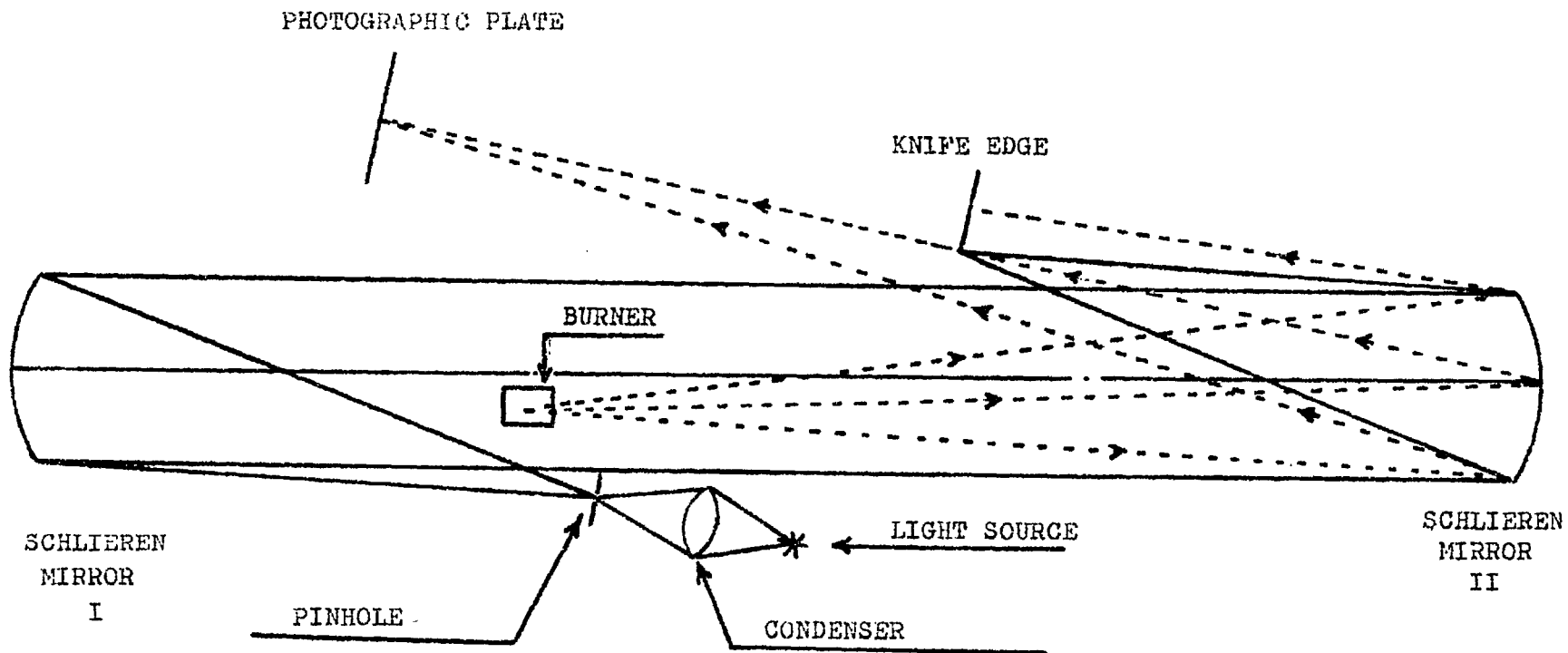
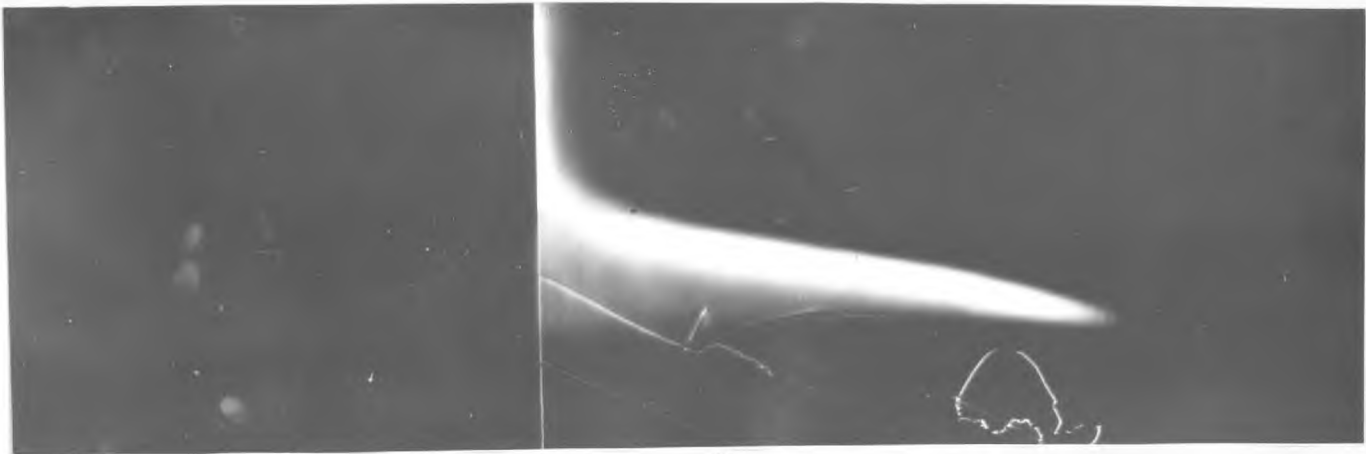
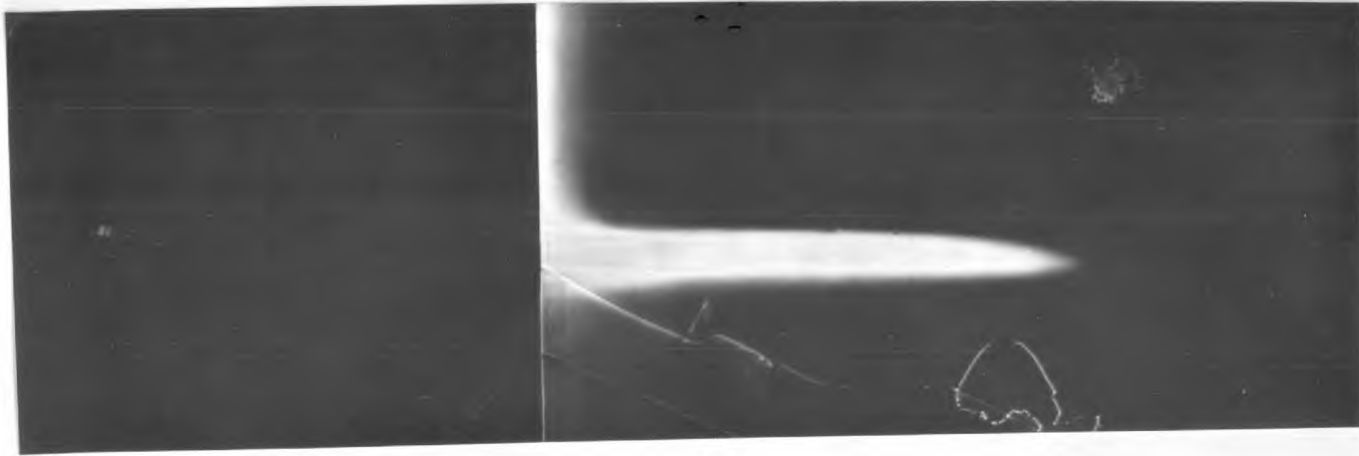


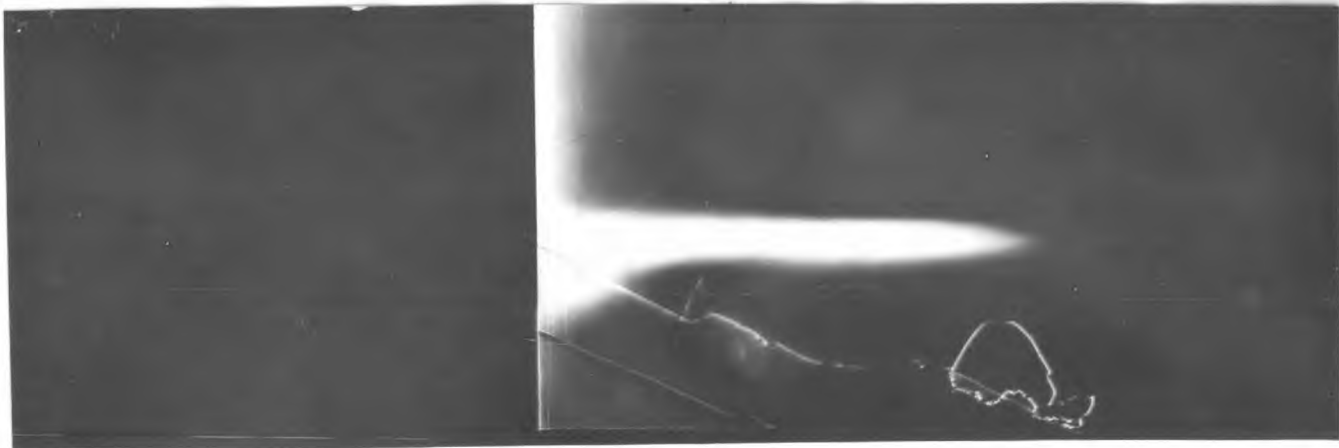
FIGURE 3.3 - SCHLIEREN SYSTEM WITH MIRRORS.



(a)



(b)



(c)

FIGURE 3.4 - Schlieren Photographs of the Flame.

(a) Unperturbed; (b) and (c) Induced Flows

This was thought to be due to the short optical path tangential to the cusp, in combination with the effects of quenching near the heat sink, giving rise to local temperature gradients which are not steep enough to give rise to an appreciable deflection of the traversing light beam. Normally, this would be dealt with by increasing sensitivity, but this would make worse the already noticeable masking caused by the tangential portions of the flat flame with their large optical path gradients on either side of the zone of interest. The shape of the flame front - an inverted saucer having an open cusp - near the heat sink appears to make schlieren methods particularly unsuitable.

3.4 Particle track method for locating schlieren surface.

The alternative method of using the particle tracks themselves for locating the zone of the schlieren image was next explored. Like the optical techniques used for flame analysis, this method also employs the flame gases as a gas thermometer. Since its mention by Smith (1937) it has been used quantitatively (e.g., Lewis and von Elbe, 1943; Anderson and Fein, 1949; Fristrom, et al., 1953 and 1954; Levy and Weinberg, 1959)² for measuring burning velocities as well as temperature distribution in premixed flames. Using this technique an overall accuracy of 2% has been claimed. The particle track photographs give not only the local gas velocities in a flame

system, but also the stream tubes defined by any adjacent tracks. The aerodynamic variables which determine these stream tubes are the local velocity and density of the gaseous mixture. The geometry of the stream tubes is thus uniquely dictated by these physical properties of the gas. It can be shown that mass rate of flow of gases within each stream-tube remains invariant and is given by the continuity equation

$$\rho v A = \text{const.} \quad (3.3)$$

where ρ and v are respectively the local density and velocity of the gaseous mixture and A is the local cross-sectional area of the stream tube measured in a direction normal to the adjacent stream-lines defining it. If the mass rate of flow is known, as from the initial settings, this relationship yields the local density of the gaseous mixture at the point where the stream velocity and stream tube area A is found from the particle track photographs. The distribution of local densities can then be converted into temperature by way of the perfect gas law

$$P V = n R T \quad (3.4)$$

where the symbols have their usual meanings. Equations (3.3) and (3.4) on combination give

$$T \propto (M, v, A) \quad (3.5)$$

where M is the local molecular weight of the gaseous mixture. Equation (3.5) may also be written as

$$\frac{T}{T_u} = \frac{M}{M_u} \cdot \frac{v}{v_u} \cdot \frac{A}{A_u} \quad (3.6)$$

A plot of the distance travelled by gases along each stream tube and the corresponding temperature calculated from equation (3.6) can therefore give their complete thermal history.

For a determination of reliable temperature profiles in a flame, a knowledge of the local molecular weight of the gaseous mixture may become necessary when the change in mole number is appreciable. In the present study, however, the method was intended to be used merely for tracing an isothermal surface corresponding to the schlieren image of the flame which has been seen to occur at temperatures of the order of only 200°C . It was therefore, been assumed that this surface defines the regions up to which no appreciable chemical reactions take place. Moreover the mixture under study was mostly air. It was, therefore, justified to treat the molecular weight of the gaseous mixture as remaining unchanged for this purpose. Thus equation (3.5) gives

$$T \propto (v, A) \quad (3.7)$$

The local area A of the stream tube can be evaluated from the geometry of the particle tracks. The present system

was symmetrical about the axis of the heat sink as shown in Fig. 3.1 and 3.2. If therefore r is the mean local distance of the stream tube from the axis and p is the perpendicular distance between the stream lines selected, A is given by the relation

$$A = 2 \pi r \cdot p \quad (3.8)$$

Equations (3.7) and (3.8) therefore give

$$T \propto (r, p, v) \quad (3.9)$$

The quantities needed for plotting any isothermal surfaces subject to limitations discussed above, are therefore r , p , and v , all of which can be determined from particle track photographs. In the special case of ^a/schlieren image, the isothermal surface will be the locus of all the points reached along consecutive stream tubes, at which the function $f(r, p, v)$ defined by equation (3.9) attains one and a half times its initial value.

3.5 Application of the technique.

In order to obtain meaningful results from such measurements, it is important to analyse the assumptions in the theory outlined above and see how far they are satisfied in practice. The most important of these is the supposition that the particles suspended in the gas stream do actually follow the stream lines. All flame systems are characterised

by very steep temperature gradients. In the presence of these, the gaseous mixture undergoes accelerations which are of the order of $10^4 g$ in stoichiometric hydrocarbon-air flames and exceed $10 g$. even for flames stabilizable on the flat flame burner. The tracer particles may not automatically be expected to keep in step with the gases under such thermal accelerations. Any lag in velocity of the particles depends on their size and the thermal gradients involved. For a four micron particle, as used in this investigation, Fristrom, et al (1954) have calculated that for a premixed propane air flame, this acceleration lag amounts to less than two per cent at its maximum. The only steady state lag - that due to gravity - can be calculated from Stokes law and is usually insignificant for the bentonite particles employed here.

Closely associated with the acceleration lags discussed above is the "thermo-mechanical lag". It has been found (Waldmann, 1961) that in the presence of non-uniform thermal gradients, the dust particles suspended in a gas experience a mechanical force which tends to push the particles away from the hotter regions. This effect again depends upon the magnitude of the thermal gradients and the size of the particles and can again be shown to be negligible in the present study. In fact, Fristrom (1965) has calculated the effect of the two effects discussed so far and has suggested the optimum size of

tracer particles to keep these errors small - Fig. 3.5.

It will be observed that conditions obtaining in the present study are well within the calculated limits. The effects of Brownian movement are of an order of magnitude less than the above lags.

Another important consideration in tracer studies is the effect of the particles themselves on the thermal gradients present in the flame. These particles have a finite heat capacity and if introduced in copious bursts, may extract an appreciable amount of heat from the system and possibly decrease the burning velocity sought to be measured. In extreme cases the flame may even be extinguished, specially if the tracer particles are of larger sizes. But the errors can be reduced to almost insignificance by controlling the size and number of particles suspended in the gas stream.

It would thus appear that the particle track photographs can be safely used for velocity measurement and for locating the position of the schlieren image of the flame front. The following attempts were made further to improve the accuracy of measurements. These were mainly directed at the optical system used for tracer studies.

With a high pressure mercury lamp run on A.C. mains the bentonite particles were illuminated at twice the mains frequency

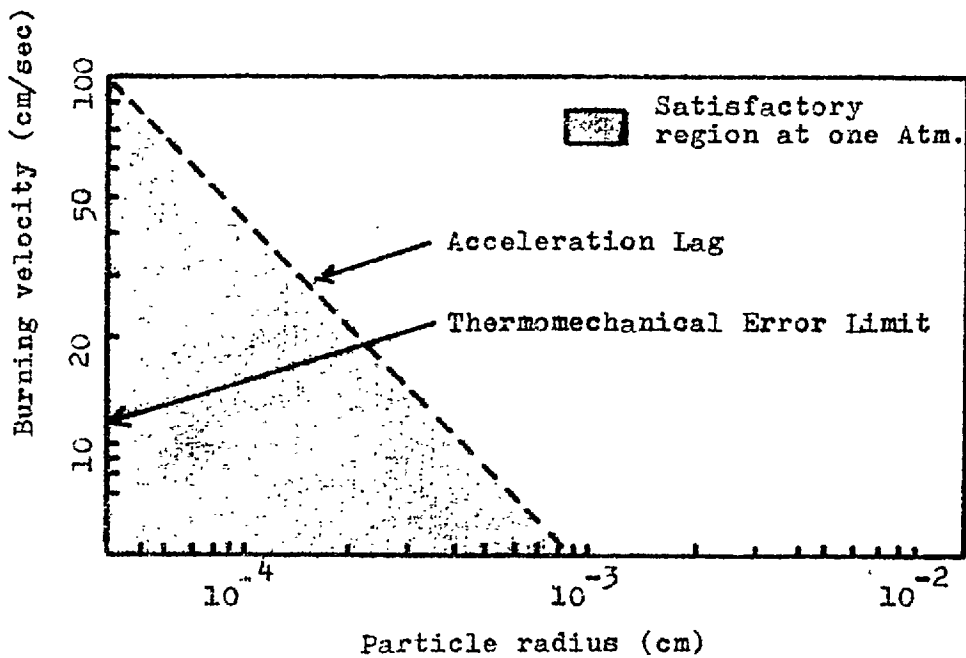


FIGURE 3.5 - REGION OF QUANTITATIVE APPLICABILITY
OF PARTICLE TRACK STUDIES

Thus each track on the photographs determines the distance travelled by the particle in 10 m.sec. At a stream velocity of 10 cms/sec, during this time the particle would be expected to travel a distance of one millimeter in the temperature field of the flame. The assumption of a constant stream velocity over one millimeter within the flame's structure, however, could lead to erroneous results. The error could be serious in the vicinity of the schlieren surface where the temperature gradients are near their maximum value. It was therefore decided to illuminate the particles at a higher frequency by running the mercury lamp on D.C. and interrupting the beam of light with the help of a chopper disc having equal numbers of open and closed slits. The chopper disc was rotated by a 110 volt induction motor. But to obtain a greater chopping frequency this was overrun by using a variac. It was observed with the help of a stroboscope that its speed could be maintained constant for two to three minutes. With this arrangement the particles could be illuminated 550 times a second. This frequency was chosen because it was desired to have the tracks only 2 to 3 mm. long when the photographs were enlarged about 20 times for the purposes of measurement. In this way, the corresponding length of track in the radial plane under study could be made as small as 0.02 cm. and thus "local" velocities could be determined.

Equation (3.9) derived above will hold only for a section through the axis, in the case of radial symmetry. Thus, ideally, only one diametral plane of the system should be illuminated and photographed. Although this theoretical requirement cannot be met by practical systems, the optical set-up used for particle track photography (see chap. 2) had only a 2 mm. depth of field. This set up along with the precautions taken during actual measurement of particle tracks, was considered adequate for the application of equation (3.9) and the determination of the schlieren surface by particle track photographs.

3.6 Results.

Particle track photographs were taken for two cases - for a flame with and without suction through the slot in the heat sink (Fig. 3.6 a & b) - having the same mixture strength as before. These were printed at a magnification of 18.3 x on Kodak document paper. The schlieren surface was constructed for each of the two cases, as outlined in section 3.4. Tracks for measurement were chosen solely on the basis of their sharpness of focus and availability of adjacent tracks from which the required measurements could be obtained. Heavier tracks formed by large particles were discarded.

For finding the initial value of the function $f(r,p,v)$,

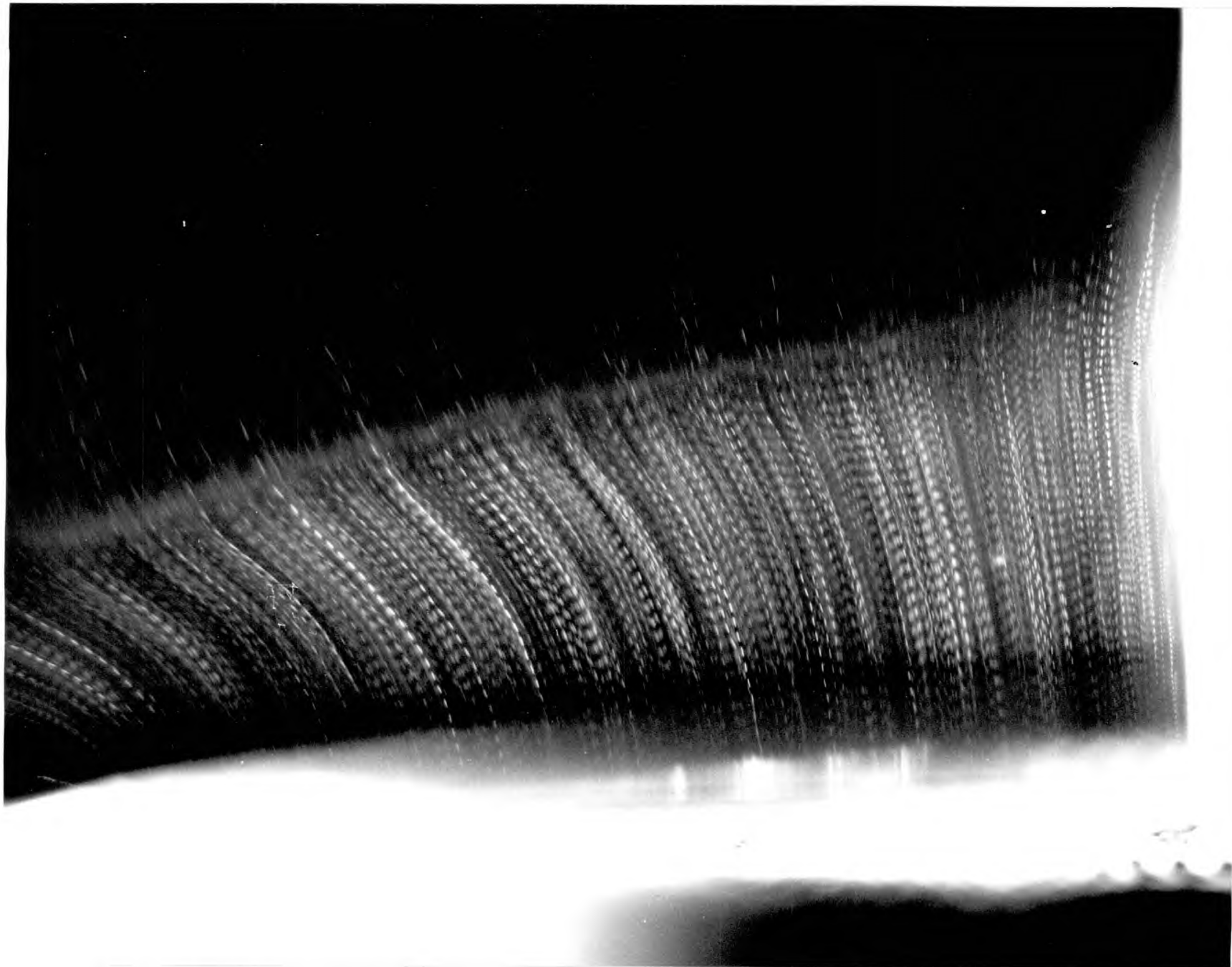


FIGURE 3.6a - PARTICLE TRACK PHOTOGRAPH WITH THE AXIAL HEAT SINK (WITHOUT SUCTION)

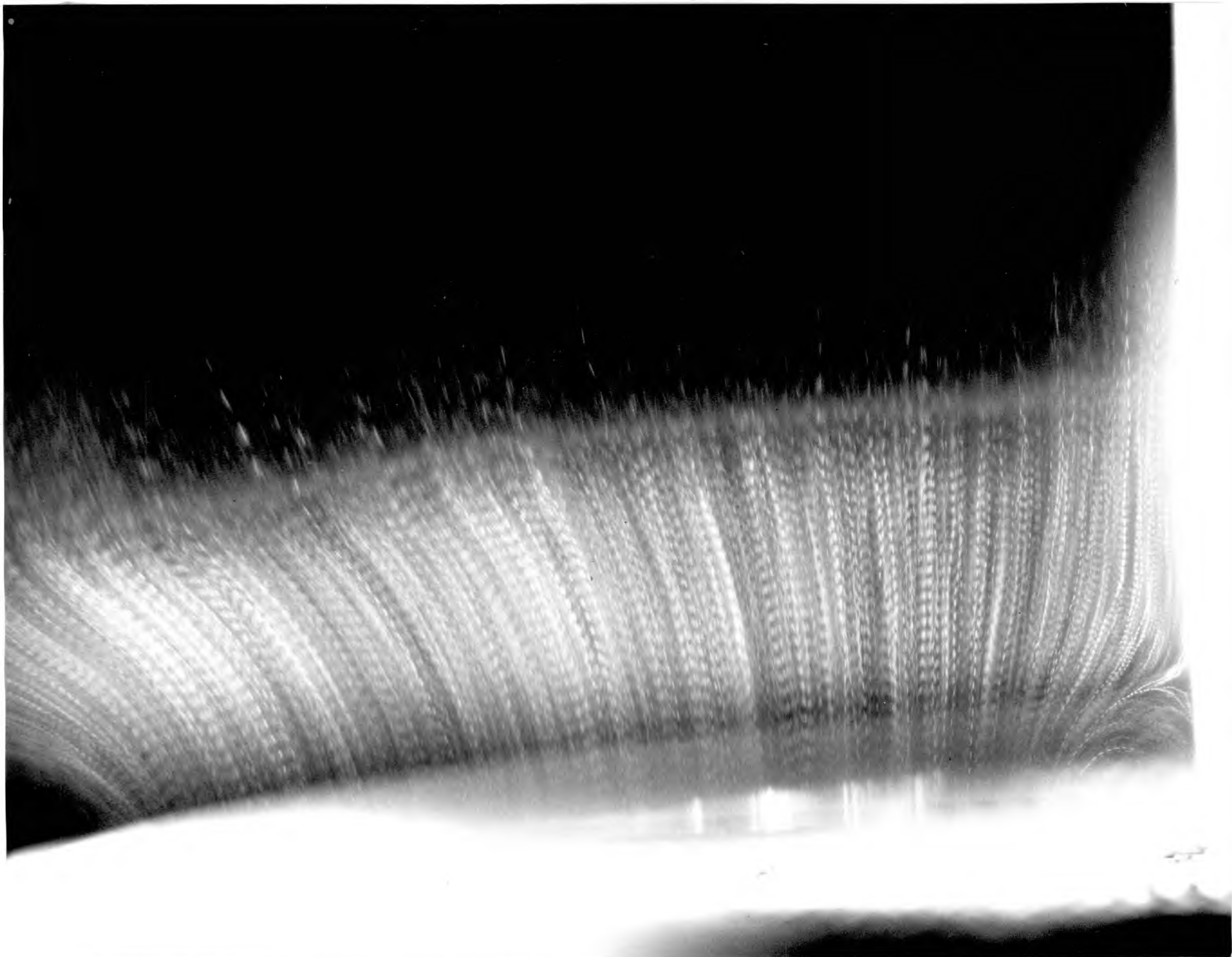


FIGURE 3.6b - PARTICLE TRACK PHOTOGRAPH WITH THE AXIAL HEAT SINK (WITH SUCTION)

a reference line was drawn on the prints just above the matrix image and as follows, the value of r , p , and v , determined from the particle tracks in its locality.

Two adjacent stream-lines were selected on the prints and the perpendicular distance between them was measured. The value of r was taken as the mean of the distance of each stream-line from the axis of symmetry. The local stream velocity was again taken as the mean of the gas velocities along the two stream lines. Thus the initial value of $f(r, p, v)$ was calculated for a large number of stream tubes in the vicinity and away from the heat sink. The process was repeated at different distances from the reference line. A graph was then plotted of the value of $f(r, p, v)$ against the curvilinear co-ordinate measured along the direction of the mean of the stream tube under study. The schlieren surface could then be constructed as the locus of all the points along successive stream tubes at which $f(r, p, v)$ attained a value of 1.5 times that at the reference line. The burning velocities (in each case) were then determined at these surfaces as explained in section 2.8. These were corrected to yield the values at S.T.P. The results thus obtained are shown in Fig. 3.7. The initial mixture was identical in two cases (2.72 % C_2H_4) but curve 2 shows results with a flow velocity distribution, and hence geometry, modified by the suction near

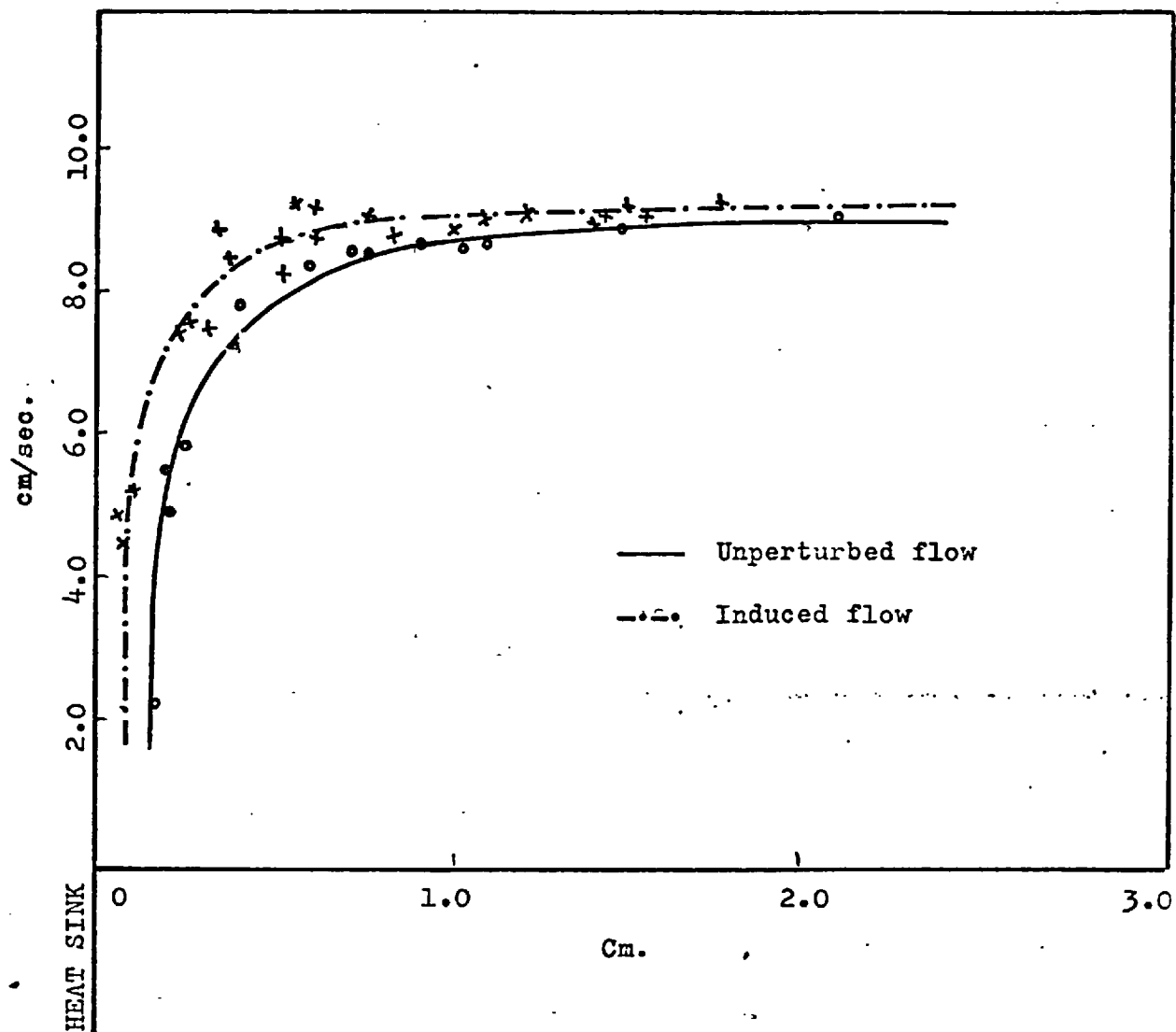


FIGURE 3.7 - VARIATION OF BURNING VELOCITY WITH DISTANCE FROM HEAT SINK (AXIAL)

the heat sink. These graphs show quenching distances, or more precisely the distances over which the proximity of a heat sink affects burning velocity, of about the expected magnitude. The dependence on flame shape is not unexpected at this stage, since heat loss is likely to depend not only on the distance of the flame from the heat sink, but also on the orientation of the isotherms to it.

CHAPTER 4.THE HEAT LOSS PATTERN

4.1. The next step in this investigation was an attempt to correlate the distribution of burning velocity with the distribution of heat loss as a function of distance from the heat sink. This seemed particularly desirable in view of the finding that burning velocity is not a unique function of this distance - even for one mixture strength - since the distributions are different (Fig.3.7) for different orientations of the flame to the surface of the heat sink.

To this end it was necessary to measure the distribution of temperature in the vicinity of the heat sink, for use in conjunction with the velocity distributions. Much of this chapter is therefore concerned with such temperature measurements. It starts, however, with a review of previous work on the dependence of burning velocity on heat loss. It must be clearly understood that none of this previous work was as analytical as the present in that none attempted to relate heat loss from each stream tube with a local burning velocity. The effects studied so far always extended - or were deemed to extend - to the flame as a whole. Nonetheless, it would have been incorrect to omit such a survey altogether and this chapter seemed the most appropriate place to summarize current concepts regarding the dependence of burning velocity on heat loss.

4.2 The burning velocities of cooled flames

One point which most of the theories of flame quenching have in common is that flames from which heat is abstracted have two burning velocities. Most of the theories infer that one of these is physically unstable but it appears from Spalding's treatment of the problem that the so-called unstable velocity may, under certain conditions, be realised in practice. The major step in this direction was the development of Botha and Spalding's porous plate burner (1954). The burning velocities of a large number of combustible mixtures were determined on such a burner. A flame was stabilized on a porous disc which was water cooled. In the steady state the burning velocity must match the flow velocity. Under this condition, the quantity of heat carried away by the water cooling the disc was determined. The effect of heat transfer on burning velocities was then found by plotting a graph of the flow velocities against heat transfer to the porous disc. On extrapolating this graph to the condition when the heat transfer was zero, the adiabatic burning velocity of the combustible mixtures could be determined and the results were found to agree with other experimental observations.

Botha (1956) in a subsequent work reported that the heat delivered to the plug per unit volume of fuel ^(Q) first showed an increase and then fell off as the flow velocity of the

combustible gases was reduced. Thus over a small range, it appeared that the mixture had two burning velocities as predicted by Spalding's theory. Spalding and Yumlu (1959) sought to confirm these results by repeating the work with several fuels. In order to increase the downstream heat loss, these workers introduced a cooled porous plug above the burner also. Apart from confirming Botha's observations, Spalding and Yumlu found that there exists a maximum value of Q for a gas mixture at which the two burning velocities coincide and this was called the critical burning velocity. But the observations have been criticised by Kaskan (1960) on the basis that the values of Q cited (Spalding and Yumlu, 1959) were too small to account for the difference between the adiabatic flame temperature and the observed temperature for the same flame. Notwithstanding Kaskan's observations, the fact remains that the Q of Spalding and Yumlu does not seem to be a well-defined quantity; perhaps it did not take into consideration the unknown conditions near the edge, the unknown fraction of heat radiated by post-flame gases and the heat losses from the burner itself. In fact, considerable doubts on such measurements have been cast by the observations of Kydd and Foss (1964, a and b). Using a much bigger porous disc burner, for which the edge effects were claimed to be insignificant as compared to those in Spalding and Yumlu's work, Kydd and Foss

found that even a slight variation of conditions near the edge could significantly alter the observed values of Q .

Moreover no appreciable change in the value of Q could be detected when the flow rate of the combustible/^{mixture} was varied.

The main findings of Spalding and Yumlu have however been reaffirmed by the recent work of Yumlu (1966), on a version of the burner improved over that used in the former work.

Certain discrepancies have nevertheless been reported but they have been explained in terms of the inefficiency of the heat extracting properties of the earlier burner and also entrainment of air in the flame from the surroundings.

While the observations of Kaskan and Kydd and Foss may not amount to a contradiction of Spalding and Yumlu's work, the fact remains that measurements such as those reported in all such studies could not be made reliable enough to constitute any evidence for or against the theory. A better method appears to be a determination of the rate of heat loss in a system where it will be independent of the mechanism of the stabilization of the flame by the solid surface.

The approach in the present investigation has been directed towards an in situ determination of the rate of heat loss by the flame in the vicinity of solid surface and its variation with position. Along an adiabatic stream line, the temperature profile of a premixed flat flame has been found to

be of the form shown in Fig. 4.1. Starting from the unburnt gas temperature T_u , the temperature rises slowly and exponentially at first, until reaction sets in. The rate of rise continues less steeply till all the reactions are completed at a certain distance from the matrix. The temperature, thereafter, remains stationary because no further heat release or appreciable heat loss takes place. Since hot gases do not radiate any appreciable quantities of heat, the temperature at $z = z_1$ should ideally be the adiabatic flame temperature T_f^a . If, however, a heat sink is present in the vicinity of the flame, the temperature will start falling off due to heat transferred to the sink and the final flame temperature will no longer be T_f^a , but considerably less, as has been shown by the dotted curve in Fig. 4.1. Thus, if the maximum temperature occurring along a stream line is known, the heat loss, Q , may be calculated from the deficit of the final enthalpy, as compared with that in the absence of heat losses. It can thus be expressed as

$$Q = \int_{T_f}^{T_f^a} C_p dT \quad (4.1)$$

where T_f = maximum temperature attained along any stream-line
 C_p = specific heat of combustion products.

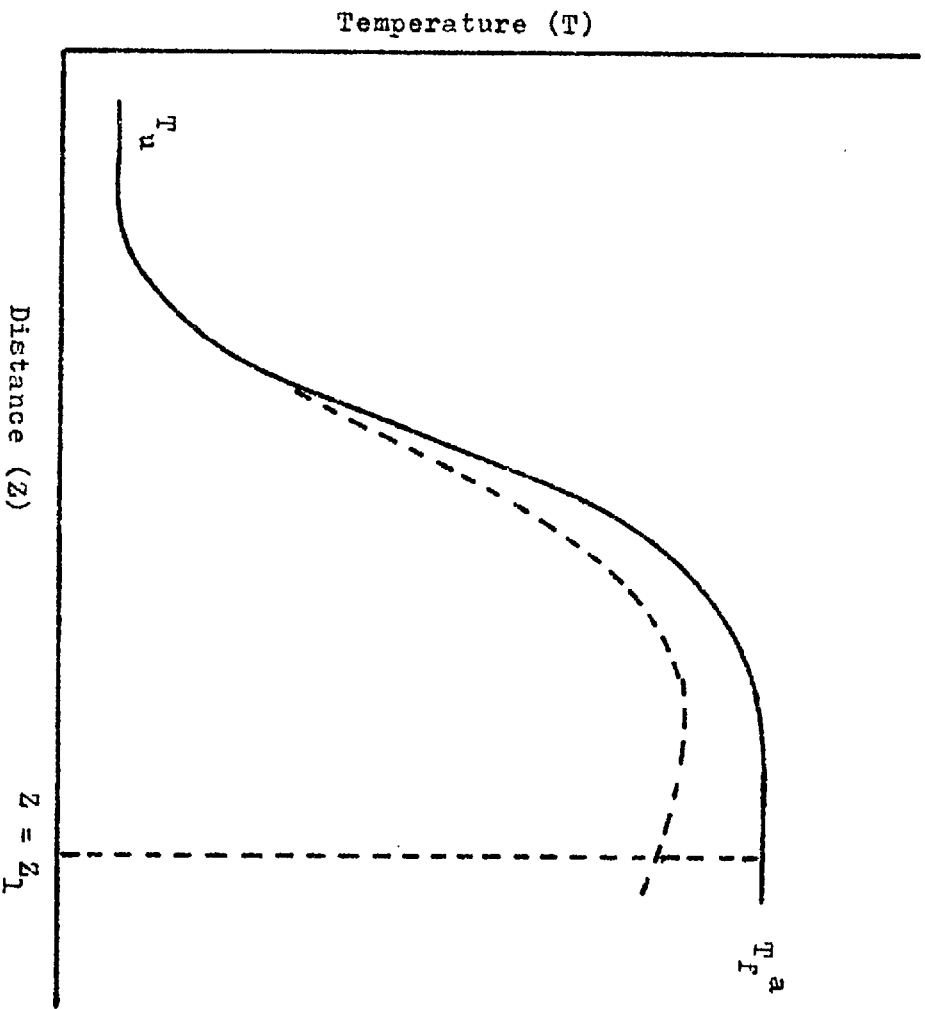


FIGURE 4.1

The heat loss thus evaluated might be due to conduction to the heat sink, the loss of energetic chemical species by diffusion to it, radiation or several of these processes taking place simultaneously. Whatever be the mechanism, its magnitude will be indicated by the temperatures along the stream tubes when determined simultaneously with velocities, in situ. These records can be matched by a suitable frame of reference and the heat loss rate determined using the above equation.

4.3 Definition of temperature.

The temperature mentioned in section 4.2 is the thermodynamic equilibrium gas temperature corresponding to a Boltzman distribution of velocities. For a gas in equilibrium, energy is equally divided amongst the various degrees of freedom - translational, vibrational and rotational. A single temperature, T , can then be assigned to each of these such that the total energy per molecule is $3/2 kT$, k being the Boltzman constant. Although the flame propagates in a steady manner, the flame gases themselves are subjected to extreme gradients of physical properties. Thus accelerations as high as 10^4 g have been reported and even in comparatively slow flames stabilized on a flat flame burner, the flame gases may experience a rate of rise of temperature as high as 2×10^5 deg/sec (Levy, 1958). Because of the rapidity of the reactions involved, the vibration degree of freedom may

not get sufficient time to attain thermal equilibrium with translational and rotational ones. The situation will be further complicated if the temperature is high enough to cause dissociation. Under non-equilibrium conditions the various degree of freedom can no longer be assigned the same "temperature, T". Instead, the state of the gas will be determined by a set of "temperatures", one for each degree of freedom. Such systems have been encountered as in CO-O₂ flames (e.g., Silverman, 1952) and the problem has been discussed by Gaydon (1948).

In laminar flames, however, the temperature of most concern is the translational temperature, because this is the temperature used in the equation of state and in the calculation of transport processes. Attainment of local translational equilibrium (see, e.g., Fristrom and Westenberg, 1965.) is a very fast process requiring only a few collisions. At each "point" therefore an effective translational temperature will exist. If the distance between such "points" at which the properties of the flame gases are measured are large as compared to their mean free path ($\sim 10^{-5}$ cms.), the assumption of local translational equilibrium will be valid.

A detailed point-to-point calculation of possible lags in equilibrium throughout the structure of pre-mixed flames of strengths similar to those used in the present study has been

reported by Levy and Weinberg (1959, 1). It was found that for pre-mixed flames which can be stabilized on a flat flame burner (burning velocities 4 to 10 cms/sec), the uncertainty of temperature due to dis-equilibrium between the various degrees of freedom is insignificant as compared to errors incurred in the experimental determination of temperature. Following Levy and Weinberg, it is an excellent approximation for the purpose of the present study, that the "temperatures" of all degrees of freedom are equal and a simple temperature profile is sufficient to describe the energy content of the flame gases.

4.4 Methods of temperature measurement.

A large number of methods (see e.g., Gaydon and Wolfhard, 1954) have been used for temperature measurements in combustion systems. However, only a few of these techniques possess sufficient reliability and spatial resolutions to be of use in pre-mixed flames. A short account of these is given below.

4.4.1. Optical methods

In flames, the local variations in temperature can be measured in terms of the associated refractive index changes. For a perfect gas it can be shown that $\delta \times T = \text{const.}$, where $\delta = n - 1$, n being the refractive index of the gas at temperature $T^{\circ}\text{K}$. If the local value of δ is experimentally

determined, the gas temperature can be calculated from the above equation with reference to a known state.

The effect of temperature and hence refractive index gradients in a test space is to distort the transilluminating wavefront of light. If this distorted wavefront is compared with the original undistorted one, the local changes in the beam introduced by the test space can be determined. Two methods of such comparison have been used for quantitative measurements. One of these measuring the distortions of the wavefronts in terms of the local slopes of the emergent wavefront is known as deflection mapping method, while the other, which records distortions as phase differences is based on interferometric records.

(i) Deflection mapping method

If the transilluminating wavefront is plane, i.e. is a parallel beam of light and is made to pass through the test zone, the emergent rays will have a radius of curvature R given by the following equation

$$\frac{1}{R} = \left(\frac{1}{n} \text{grad } n \right) \sin \phi \quad (4.2)$$

where ϕ is the angle between the direction of the incident light and the refractive index gradient in question.

On account of this curvature the emergent rays will be deflected from the original directions by an angle θ , depending upon

their lengths of path X through the test zone. Since θ is small, equation (4.2) can be expressed as

$$\tan \theta \cong \theta \int_0^X \left(\frac{1}{n} \text{ grad. } n\right) \sin \phi \, dx \quad (4.3)$$

Knowing the geometry of the test space and the angle θ , the local gradient of refractive index can be determined. A further integration with reference to a known state can then yield the distribution of refractive index and hence of temperature across the test space.

In practice a number of inclined slits or half-wave steps are interposed in the path of the transilluminating beam. The shadows or images of these slits will be distorted if a refractive index gradient is introduced in the path of light. On comparing the distorted and undistorted images of the grid, the values of θ at different places can be determined.

The inclined slit method has been developed and successfully used for studying the structure of pre-mixed flames (see e.g., Burgoyne and Weinberg, 1954 ; Levy and Weinberg, 1959 1, and 2).

(ii) Interferometry:

In certain systems where the refractive index gradients are not steep enough to cause accurately measurable deflections

of the light beam, the complementary technique of interferometry can be usefully employed. In this case the change of phase rather than ray deflections provides a measure of the refractive index field. These changes of phase are seen as an interference pattern when the distorted wavefront is superimposed upon a reference wavefront. The pattern and distributions of fringes will again depend upon the distribution of lengths of the optical path which the transilluminating wavefront encounters in the test space. If the geometry of the test space and conditions in the reference space are known, the interferogram can be interpreted to yield the local refractive index value. A full account of the technique has been given by Weinberg (1963).

4.4.2 Particle track technique

Another method employing the flame gases themselves as a thermometer is the particle track technique. Originally developed for the determination of burning velocities it has also been employed for the determination of temperature distribution in flames. This has already been discussed in Chapter 3.

4.4.3. Thermocouple method.

Perhaps the most direct method of determination of temperature distribution in a flame is that using thermocouples. The e.m.f. developed when the hot junction of two dissimilar metals is introduced in the flame is measured with the help of

a potentiometer and can then be converted into temperature of the thermocouple. For flame studies the two metals are generally Pt and Pt + 13% Rh, OR Ir and Ir + 40% Rh. The method is however, not so straight forward as it appears at first sight. Even in the simple case of a thermocouple junction in a hot air stream, the observed temperature is never quite the same as the true temperature of the gas because the radiation and conduction losses of the metal far exceed those of the gas. The difference can be calculated by writing the heat balance equation (MacAdams, 1954) between flame gases and the thermocouple junction. The most significant factors in this equation are:

- (i) heat transfer to the wire by convection
- (ii) heat lost by the wire by radiation ($\Delta T_{\text{rad.}}$)

The other factors in the heat balance equation are either negligible or can be made negligible in laboratory scale experiments (for example, thermal conduction along the leads can be minimized by stretching the couple along an isotherm) If the actual temperature of the gas is higher by a certain amount ΔT , it can be shown that

$$h \Delta T_{\text{rad}} A = \epsilon \sigma (T_w^4 - T_o^4) A \quad (4.4)$$

where

- h = heat transfer coefficient
 ϵ = emissivity of the wire
 σ = Stefan's constant
 A = area over which heat transfer takes place.
 T_0 = temperature ($^{\circ}\text{K}$) of the surface which the thermocouple sees.

The above applies strictly only for an inert gas. In flames catalysis, recombination on the surface and other chemical effects also enter. These are usually minimized by coating the thermocouple with an inert substance.

The values of emissivity given by Kaskan for a coated (with silica) and uncoated (Pt-Pt/Rh) thermocouple are respectively, 0.22 and 0.16. The heat transfer coefficient can be obtained from a knowledge of the Nusselt number Nu and Reynold's number, Re . Thus:

$$h = \frac{k}{D} Nu = \frac{k}{D} f(Re) \quad (4.5)$$

the function $f(Re)$ for obtaining the corresponding Nusselt's number is given for example by McAdams (1954). Thus, knowing the wire diameter, thermal conductivity of the flame gases and the Reynold's number of flow, h can be calculated. Combining equations (4.4) and (4.5)

$$\Delta T = \frac{\epsilon \sigma (T_w^4 - T_o^4) D}{k f(Re)} \quad (4.6)$$

In order to obtain the true gas temperature, the correction ΔT and hence the expression on the R.H.S. of the equation must be known.

The first attempt to measure temperature distributions in flames by thermocouples was made by Klaukens and Wolfhard (1948), who made thermocouple traverses in low pressure acetylene flames. This work can however be taken as only an illustration of the possibility because the corrections applied at certain locations amounted to as much as 1500°K. The technique has been considerably refined by Friedman (1953) and Kaskan (1957) who measured the temperature of flame gases both by coated and uncoated thermocouples. A comparative study of the two sets of temperatures revealed that a thermocouple coated with a thin layer of quartz or silica could be expected to cut down the catalytic effects by a very significant amount. The reproducibility of their results was good and the corrections applied at temperature around 1500°K amounted to only 40°K. It appears that the method is a sensitive one and accurate measurement (within $\pm 1^\circ\text{C}$) can be obtained by using suitable Pt-Pt/Rh wires.

4.5. Comparison of methods.

It is difficult to compare the relative merits of these

methods since they depend so much on the system studied. Thus it follows from the discussion following schlieren photography (p. 90) that optical methods are not suitable for the region quenched by an axial heat sink (although this was not apparent at the outset of this investigation).

The particle track method gives only limited precision and spatial resolution for temperature distribution measurements. Moreover temperature profiles derived by this method exhibit some peculiar shapes (e.g., Anderson and Fein, 1949; and Fristrom, et. al., 1953, 1954) which are not found in those derived by other methods. This has been attributed to inertial effects (in the fast flames to which it applies).

A direct comparison of thermocouple and inclined slit methods has been carried out by Dixon-Lewis and Isles (1962). The agreement found is good. The optical methods are capable of reasonable precision and spatial resolution. They have the advantage of not disturbing the flame and provide instantaneous measurement of temperature profile. The sensitivity of the methods drops with rising temperature, but there is no absolute upper limit of temperature. The accuracy of optical methods is, to a large extent, governed by the precision with which the conditions at the boundary between the hot test space and surrounding colder regions can be determined. Since the changes in phase or ray direction along any direction are averaged over

the entire path length, these methods are most useful in an approximately one-dimensional system and analysis of three-dimensional fields is therefore difficult. This in fact summarises the main reasons why they could not be used in the relevant region here.

The objections mentioned above do not apply to thermocouple measurements of temperature. Moreover the method is capable of high precision and spatial resolution, provided suitable corrections are made for the errors mentioned in section 4.4.3., and precautions are taken to avoid aerodynamic wake effects and to eliminate catalytic recombination on the thermocouple surface. This method was therefore thought most suitable for the determination of elevated temperatures in the present study.

4.6 Thermocouples.

Thermocouples were made from .0025 cm. diameter platinum and platinum + 13 % rhodium wires. They were welded to give an approximately cylindrical junction of diameter 0.0036 cm., by passing a controlled amount of electric current through the wires. The thermocouple was then coated with silica by passing it through a hot flame to which hexa-methyl-di-siloxane had been added. A detailed procedure for fabricating such thermocouples is given in Appendix (B). In order to minimize the conduction effects and increase the

mechanical strength, each of the fine wires were made only about 1.5 cm. long and was welded in turn to a support lead of the same material, 0.046 cm. in diameter. The assembly was 'V' shaped with the heavier wires bent to hold the fine wires under tension.

A second junction of the same materials was made by gas-welding wires of .046 cm. diameter and served as reference junction of the thermocouple. It was kept at 0°C by immersing it in a thermos flask packed with distilled water and ice. The thermal e.m.f. was measured by a potentiometer. The electrical connections of the circuit are shown in Fig. 4.2. The null method of measuring e.m.f. was preferred; its advantages include the elimination of any errors due to differences between the resistances of the thermocouple leads and its greater accuracy and rapidity of measurement. The first is inherent in the use of a potentiometer; the second was possibly due to the use of a multi-range instrument (a Pye Junior Potentiometer). This could be read to ± 0.0025 millivolts over a range of 0 to 30 millivolts. A rapid measurement of the e.m.f.'s was possible because their values did not differ greatly from one reading to the next over the area probed by the thermocouple.

4.7 Thermocouple holder.

Figure 4.3 shows the thermocouple holder. It consisted

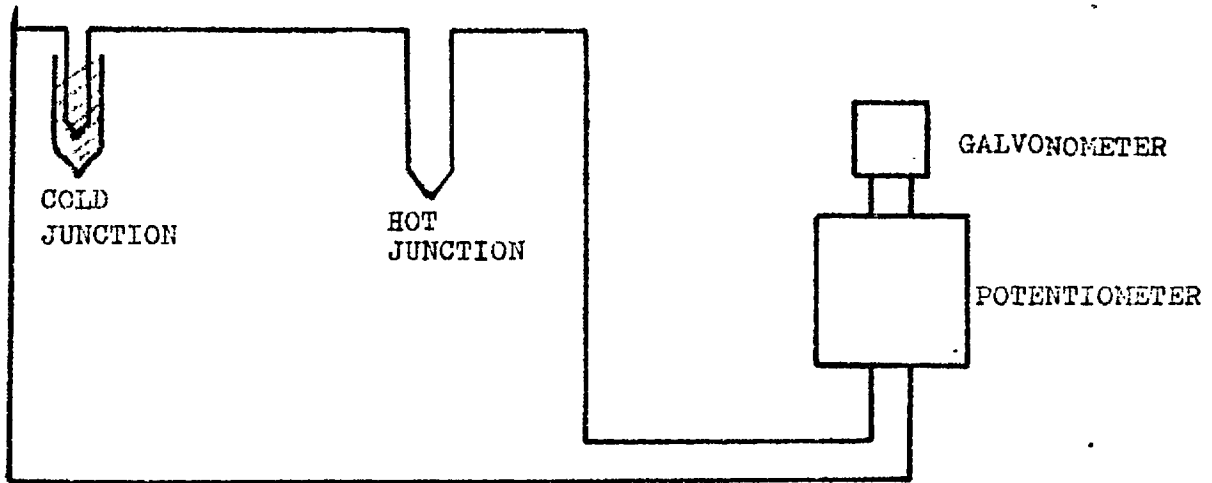


FIGURE 4.2

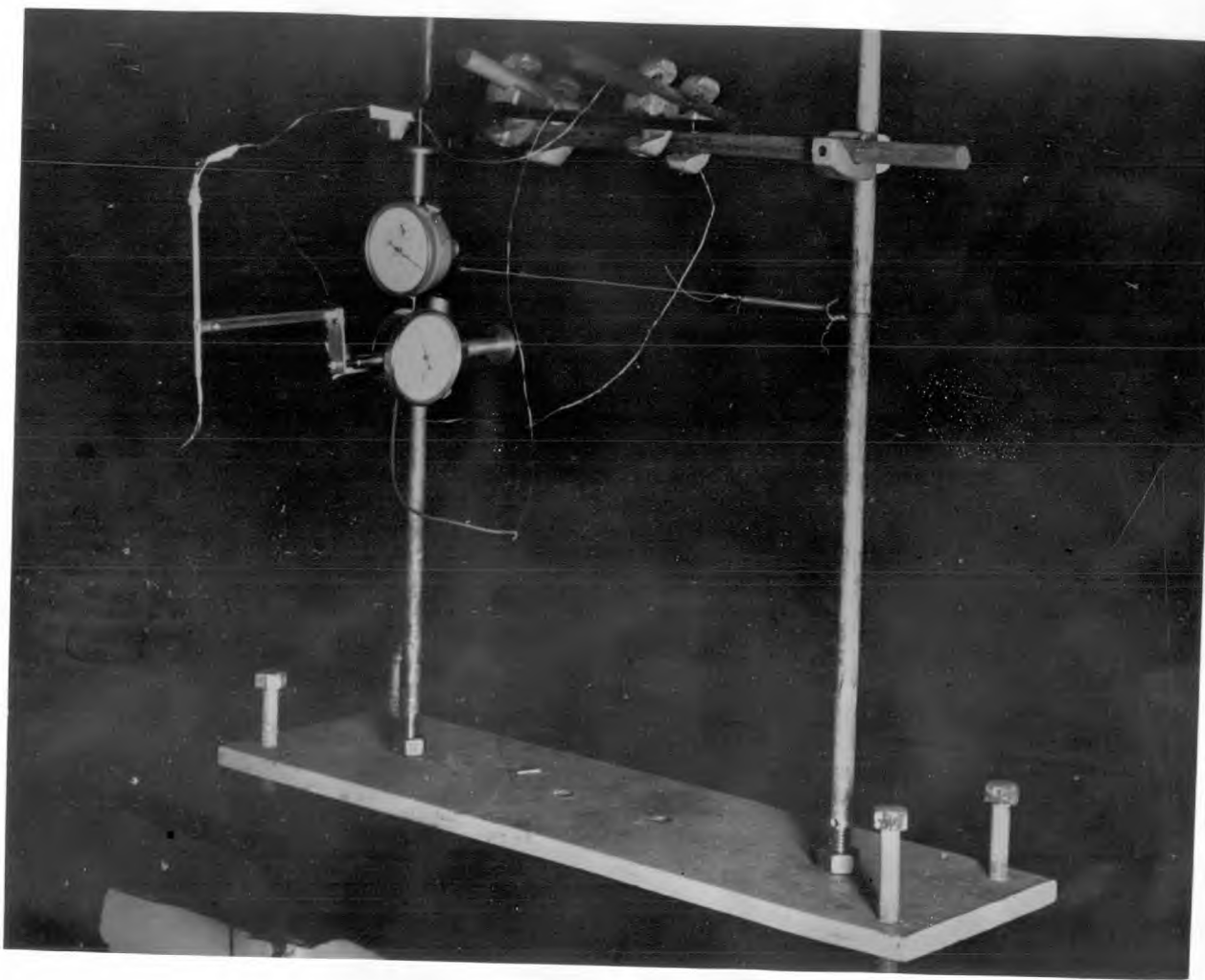


FIGURE 4.3 - Thermocouple Holder.

of two dial gauges with a linear drive of 2.5 cm. travel. The dial gauges were mounted in such a way that they could be moved along two perpendicular directions. A smooth and fine movement was improvised by means of nut and sleeve fitted on the other side of the drive shaft. Thus, forward and backward movements could easily be made. A brass rod which carried a ceramic heat resisting tube was mounted on the free drive shaft of one dial gauge. The overall diameter of the ceramic tube was 2 mm. and it was provided with twin channels to take the thermocouple wires. In order to prevent any slip of the wires they were cemented inside the channels with the help of a high temperature insulating cement.

4.8 Thermocouple traverses.

The thermocouple was introduced into the system from the downstream side of the flame. For this, a slit about 2.5 mm. wide was cut along a radial section through the stabilizer (serving as the roof of the chimney) and the ceramic tube carrying the thermocouple junction was lowered through it. In order to avoid any aerodynamic disturbance of the flame the length of the slit was kept open at the minimum necessary for obtaining a temperature measurement in the region of interest. It was nevertheless ascertained that this opening in the stabilizer had no noticeable effect on the shape of the flame near the heat sink; the flame remained symmetrical in every respect.

The thermocouple holder was so adjusted that with the help of dial gauges the hot junction could be linearly displaced parallel and perpendicular to the heat sink. Its movement was strictly confined to a radial plane of the burner system. This was ensured with the help of a long focus travelling microscope mounted on a sturdy camera stand. After carefully levelling it, the microscope was focused on the bead of the thermocouple. The hot junction was then displaced horizontally using one of the dial gauges through a distance of approximately 2.0 cms. The microscope was also moved along the same direction till the thermocouple junction appeared in its field; the hot junction however was out of focus. The microscope was left untouched and the thermocouple holder was adjusted to bring the bead in focus again. After some trial and error the bead was arranged to be in focus at all points along its horizontal traverse. The process was then repeated for a vertical movement of the hot junction. The motion of the thermocouple junction was thus confined to a radial plane which was defined by the plane of focus of the travelling microscope. A double check - to ascertain that the two motions of the bead were linear and free from back-lash was made by comparing the readings for the displacements as indicated by the dial gauges with those given by the microscope scales. It was found that the agreement was very good and the corresponding

readings differed only by .0025 cm. or less, over a distance of 1.5 cms. in the two directions. Thus over distances of interest in the present study, the hot junction could be located with an accuracy of .0025 cms.

Before making any quantitative runs it was made sure (see Appendix B) that the coating on the thermocouple would stay on long enough to render negligible the contribution of any catalytic recombination of radicals on the surface

4.9 Method of measurement.

In order to obtain a meaningful correlation between the burning velocity and temperature distribution near the heat sink, it was vital that the two properties should be measured in identical flames. The method for reproducing flames of a given mixture strength has already been discussed (Section 3.i.) The salient points are that reproducing a flame for the present study implies, obtaining it at the same location with respect to the burner matrix with the flame having the same mixture composition, shape and giving the same temperature distribution on the matrix surface each time it is stabilized.

Although the flame used to remain steady for about an hour, it was thought advisable to guard against any sudden changes in atmospheric conditions. The help of a colleague was therefore sought to take the thermocouple readings as rapidly as possible. The procedure therefore was as follows:

Having stabilized a flame of the required mixture strength, shape and position, the hot junction was located as near the heat sink as possible without actually touching it. It was then moved up and down until the position of maximum e.m.f. was located. The hot junction was then slightly displaced downstream of this position and a radial scan of thermal e.m.f. was started. The bead was moved away from the heat sink in intervals of 0.051 cms. and, for each position, the e.m.f. was determined by the colleague. The radial scan was continued until the thermal e.m.f. showed no further change. As soon as two identical readings were obtained consecutively, the junction had reached unquenched regions of the flame in which the temperature was expected to remain unaltered. The hot junction was then moved upstream and subsequent radial scans obtained at vertical intervals of 0.102 cms. in exactly the same fashion until all the region of interest near the heat sink was covered. The total time taken for the complete scan was less than seven minutes. For calculating the necessary corrections to thermocouple readings and checking that the flame had not moved during this time, each position of the thermocouple was photographed. Such thermocouple traverses were made for two flames, one without and the other with flow inducted through the slot in the heat sink. These flames were identical with those for which burning velocities has already been determined (Chapter 3).

4.10 Calculation of the true temperature of flame gases.

The local values of the e.m.f. obtained by thermocouple probes were translated into temperatures with the help of standard tables (Kay and Laby, 1958). These temperatures were then corrected for the radiation losses from the hot junction by using the equation:

$$\Delta T_{\text{rad}} = 1.25 \frac{\epsilon \sigma T^4 D^{0.75}}{k} \left(\frac{\eta}{\rho v} \right)^{0.25} \quad (4.7)$$

For calculating the necessary corrections the transport properties η and k of the gas stream were taken to be that of air because the initial mixture was predominantly air. No measurements of the emissivity of the thermocouple employed were made. Kaskan (1957) has reported the values of ϵ for coated (in the manner here employed) and uncoated thermocouple wires. His value for ϵ ($= 0.22$) for the coated wires was used in this investigation.

The velocity 'v' of the gas stream required for evaluating ΔT_{rad} could be obtained from the particle track photographs used for burning velocity measurements. These photographs along with those giving the locations of the thermocouple junction were printed at the same magnification (18.3 x) on Kodak document paper. The prints were processed under standard conditions so that any photographic build up may remain constant for each enlargement. The points were then matched by choosing

the surface of the heat sink and the lower visible edge of the flame as the reference axes. From a knowledge of the time interval between each track and the length of the tracks, the velocity, v , of the gas stream could thus be determined at each location of the thermocouple junction.

The corrections, ΔT_{rad} for each position of the hot junction could thus be evaluated and were never found to exceed 45°C for the flames under study. Nevertheless, there remained some uncertainty regarding the values of ϵ , η and k used for these calculations. It was therefore thought advisable to have an independent check on the reliability of the corrected temperatures. Accordingly the adiabatic flame temperature for the mixture under study was calculated (see Appendix C). The theoretical value of 1430°K was found to be in good agreement with the maximum measured (and corrected as above) temperature of 1412°K (bearing in mind that some radiation losses must occur due to the H_2O and CO_2 molecules present) far away from the heat sink. It was therefore thought safe to infer that values of ϵ , η and k used in these calculations do not lead to any significant error.

4.11 Temperature profiles.

The experimentally determined and corrected temperatures were plotted on a graph. The axes chosen for this purpose were the surface of the heat sink (the ordinate) and an arbitrary

line normal to it as abscissae. This line ($y = 0$) was taken at a small distance beyond the lowest radial scan of the thermocouple in the upstream region of the flame. Two profiles respectively giving the variation of temperature with x and y were constructed (Fig. 4.4, a and b). The isotherms in the test region could then be constructed on matching these profiles. These have been shown in Fig. 4.5.

4.12 The heat loss distribution

For determining the heat loss pattern, the temperature profiles shown in Fig. 4.5 were matched and plotted on an 18.3 x print of the particle track photograph of the flame in question. From the two superimposed distribution patterns the maximum temperature attained by the flame gases flowing along each stream tube could be easily determined. But since, the temperature measurements had been made along a diametral plane of the burner, care had to be exercised to follow only the stream tubes lying in this plane. Only sharply focussed streamlines were therefore considered; heavier tracks caused by bentonite particles of diameter greater than the average were also neglected.

The local heat losses in the region of interest were obtained by a graphical integration of Equation (4.1). The value of specific heat (C_p) of the products of complete combustion of ethylene according to the equation

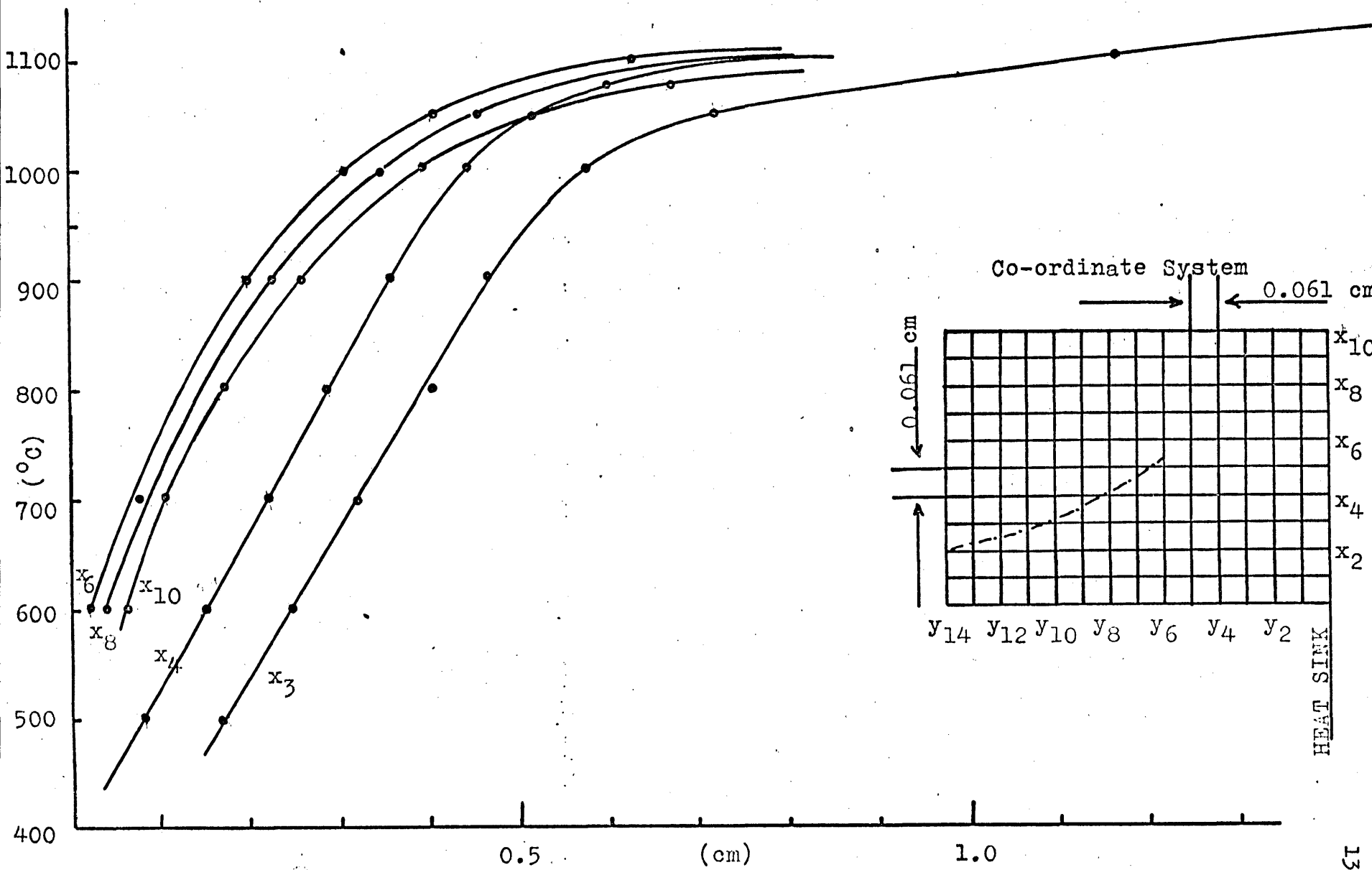


FIGURE 4.4a - SOME TYPICAL PROFILES GIVING THE VARIATION OF TEMPERATURE WITH x CO-ORDINATE

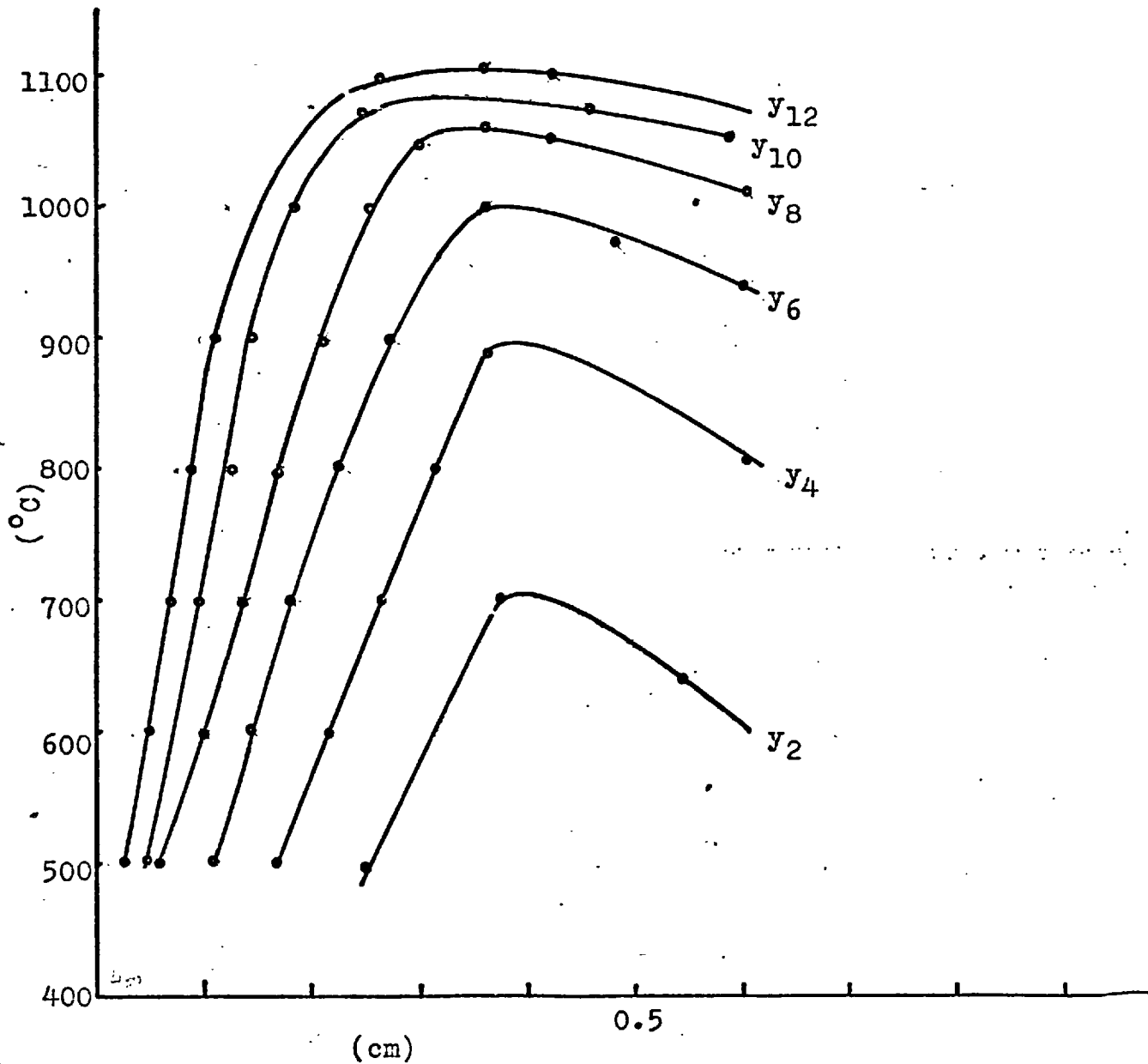
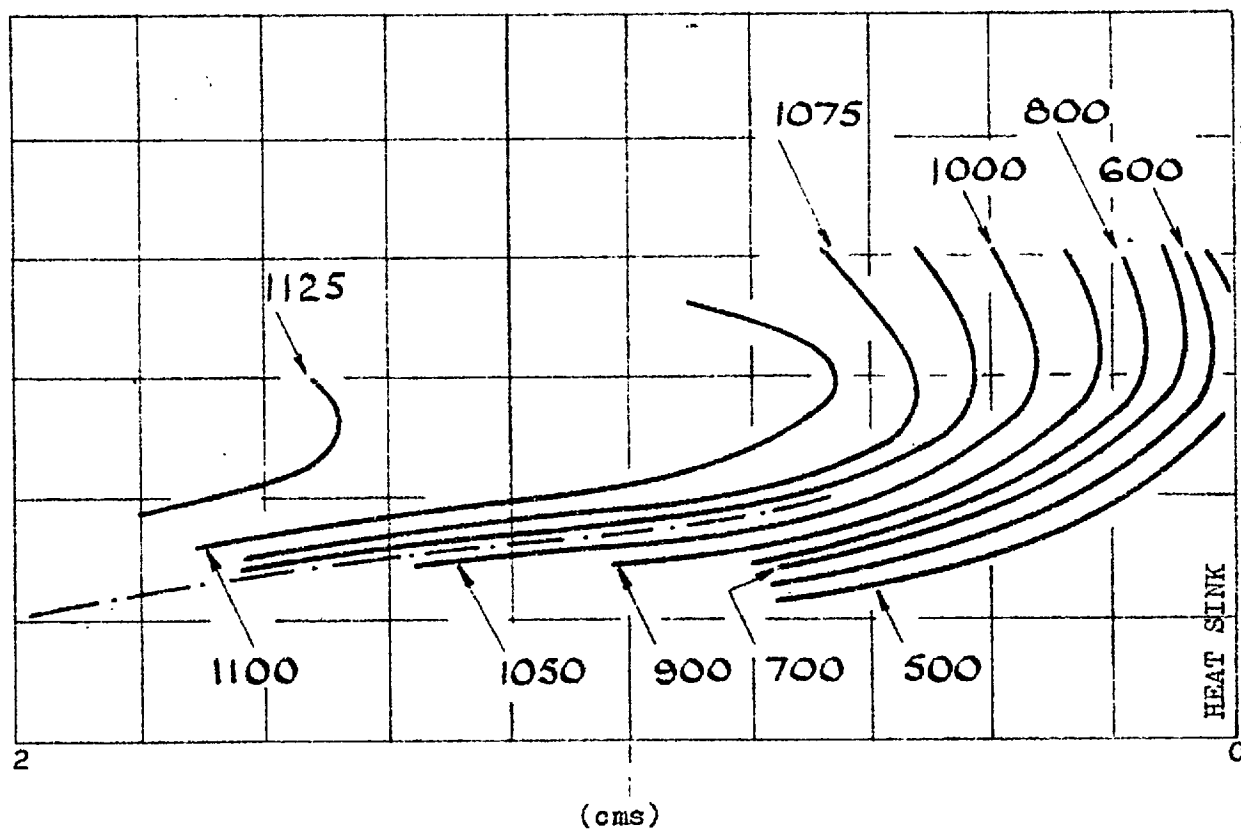
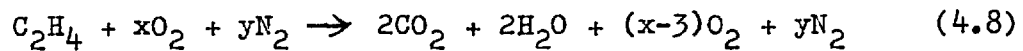


FIGURE 4.4b - SOME TYPICAL PROFILES GIVING THE VARIATION OF TEMPERATURE WITH y CO-ORDINATE.

FIGURE 4.5 - DISTRIBUTION OF TEMPERATURE ($^{\circ}\text{C}$)



were calculated at temperatures ranging from 400°K to the adiabatic flame temperature. The specific heats of the individual product gases were taken from Rossini (1953). From a graph of C_p of the products against temperature, the value of the integral $\int C_p dT$ could be read off as the area bounded by the curve and the x-axis between the ordinates in question. One of these was always the adiabatic flame temperature for the mixture under study while the other was the maximum temperature attained by flame gases along different stream tubes. Thus the heat loss at different distances from the heat sink could be easily determined. It was found that the heat loss fell accurately to zero as the distance from the heat sink increased.

4.13 Conclusions

For representing burning velocity on a heat loss scale, the heat loss along each stream tube was plotted against the burning velocity determined at the point of intersection of the flame and the mean stream line bounded by the two trajectories in question. These values were determined for the flame geometries produced in the presence and absence of suction through the slit and are shown in Fig. 4.6. It will be noticed that in both cases the heat loss falls to zero at the

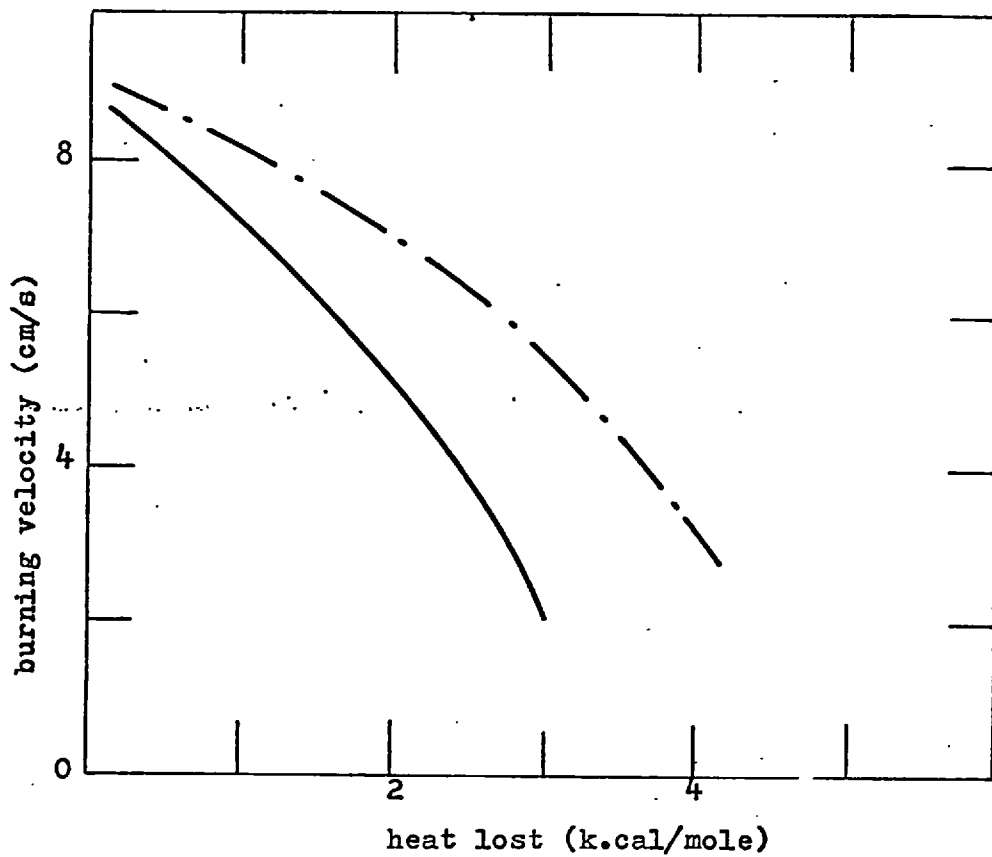


FIGURE 4.6 - VARIATION OF BURNING VELOCITY WITH HEAT LOSS.

—, Unperturbed flow; —·—·—, induced flow.

position where burning velocity assumes its normal value. But the two curves do not coincide in the crucial region. It is therefore apparent that the decrease in burning velocity depends on the orientation of the flame front to the heat sink in a manner which cannot be accounted for by variations in heat loss alone. If it were possible to express reaction rate in a temperature explicit form, equal heat losses up to any particular stage would produce equal temperatures in the reaction zone and hence equal reaction rates. In that event, the differences in burning velocity of the magnitude shown in Fig. 4.6 would not be expected. This was the first experimental evidence that the diffusion of active species might possibly be playing an active part in the system under study because in that case, not only would the temperature be affected by the resultant energy transport and alter the heat release rate, but the chemistry of the phenomenon itself would undergo a change.

CHAPTER 5.THE HEAT RELEASE PATTERN

As discussed in the previous chapter, the variation of burning velocity with heat loss was significant and indicative of a non-thermal mechanism, but the concept of burning velocity, near the heat sink itself deserved closer scrutiny. Although it has been experimentally determined with considerable accuracy the method of determination does not ensure that there is, in fact a propagating flame. Suppose, for example, that at the rate of heat extraction by the sink, the flame does not exist as a propagating reaction zone there. Apparent values of burning velocities will nevertheless be obtained because the reactant mixture will continue to flow through the annulus between the heat sink and the flame and $2/3 \rho_u$ isotherm will still extend to the vicinity of the heat sink. The possibility could not be discounted altogether because near limit mixtures were being employed and at least one theory (e.g. Spalding, 1957) lays down that under these conditions any further heat extraction from the flame leads to complete extinction. Since all the thermal and aerodynamic data was available it was therefore thought desirable to deduce the distribution of the heat release rate within the flame zones affected by the heat sink. Such a determination would throw

light on what happens to the reaction and hence on the doubts expressed above.

5.1 Heat Continuity Equation

The steady-state conservation equation for any property of the gas mass, heat or momentum is obtained by equating its rate of consumption to that of generation. If F is the flow rate per unit area and $q^{'''}$ is the rate of creation per unit volume of some such property the conservation equation in three dimensions can be written as

$$\text{div } F - q^{'''} = 0 \quad (5.1)$$

For the purpose of conservation of heat,

$$F = -k \nabla T + \rho C V T + R \quad (5.2)$$

where k is the thermal conductivity, C the temperature-mean specific heat and V the local velocity of the gas mixture of density ρ at temperature T . The radiation flux R can usually be neglected for transparent gases. Equation (5.1) can therefore be written as

$$\nabla(-k \nabla T + \rho C V T) - q^{'''} = 0 \quad (5.3)$$

For a radial system in cylindrical co-ordinates (x,y) equation (5.3) becomes

$$\begin{aligned}
 - \frac{\partial}{\partial y} \left(k \frac{\partial T}{\partial y} \right) - \frac{1}{x} \frac{\partial}{\partial x} \left(x k \frac{\partial T}{\partial x} \right) + \frac{\partial}{\partial y} \left(\rho V_y C T \right) + \\
 \frac{1}{x} \frac{\partial}{\partial x} \left(x \rho V_x C T \right) - q''' = 0
 \end{aligned} \tag{5.4}$$

where x and y are respectively measured along the radius and axis.

For systems where the value of x is not very small, the equation reduces to that for a two-dimensional system, i.e.,

$$\frac{1}{x} \frac{\partial}{\partial x} \left(x F_x \right) = \frac{\partial F_x}{\partial x} \tag{5.5}$$

The assumption in equation (5.5) implies that the effect of curvature of iso-F surfaces is negligible. It can be justified here since only a slice through a thin annulus of minimum radius greater than that of the heat sink is being considered. Equation (5.4) can therefore be reduced to:

$$- \frac{\partial}{\partial x} \left(k \frac{\partial T}{\partial x} \right) - \frac{\partial}{\partial y} \left(k \frac{\partial T}{\partial y} \right) + \frac{\partial}{\partial x} \left(\rho V_x C T \right) + \frac{\partial}{\partial y} \left(\rho V_y C T \right) - q''' = 0 \tag{5.6}$$

If the flame gases can be assumed to obey perfect gas laws, the product ρT can be taken as constant and hence

$$- \left[\frac{\partial}{\partial x} \left(k \frac{\partial T}{\partial x} \right) + \frac{\partial}{\partial y} \left(k \frac{\partial T}{\partial y} \right) \right] + \rho T \left[\frac{\partial}{\partial x} (V_x C) + \frac{\partial}{\partial y} (V_y C) \right] - q''' = 0 \tag{5.7}$$

Writing thermal conductivity in a temperature explicit form, equation (5.7) gives

$$\begin{aligned}
 - \frac{\partial k}{\partial T} \left[\left(\frac{\partial T}{\partial x} \right)^2 + \left(\frac{\partial T}{\partial y} \right)^2 \right] - k \frac{\partial^2 T}{\partial x^2} - k \frac{\partial^2 T}{\partial y^2} + \rho T \frac{\partial (C_p V_x)}{\partial x} + \\
 \rho T \frac{\partial (C_p V_x)}{\partial y} = q''' \quad (5.8)
 \end{aligned}$$

Thus, for an evaluation of the rate of heat release a knowledge of temperature, velocity and thermal conductivity of the mixture along with their relevant gradients in the region of interest are sufficient. The temperature distribution was known from thermo-couple traverses (see Section 4.8) and the particle track photographs (see Section 3.4) could be used for determining the local velocities.

5.2 Determination of gradients of temperature and velocity.

The spatial gradients of temperature were determined from profiles shown in Fig. (4.4). For greater accuracy these profiles were plotted on a greatly magnified scale (18.3 x) and the derivatives determined graphically at a number of pre-determined points in the form of a grid all over the region of interest. (Fig. 5.1)

This grid was also used for the determination of the derivatives of $C_p V_x$ and $C_p V_y$. It was superimposed on a particle track enlargement of the same magnification (18.3 x) along the same reference axes as used in the determination of temperature derivatives. The local values of the gas stream velocity

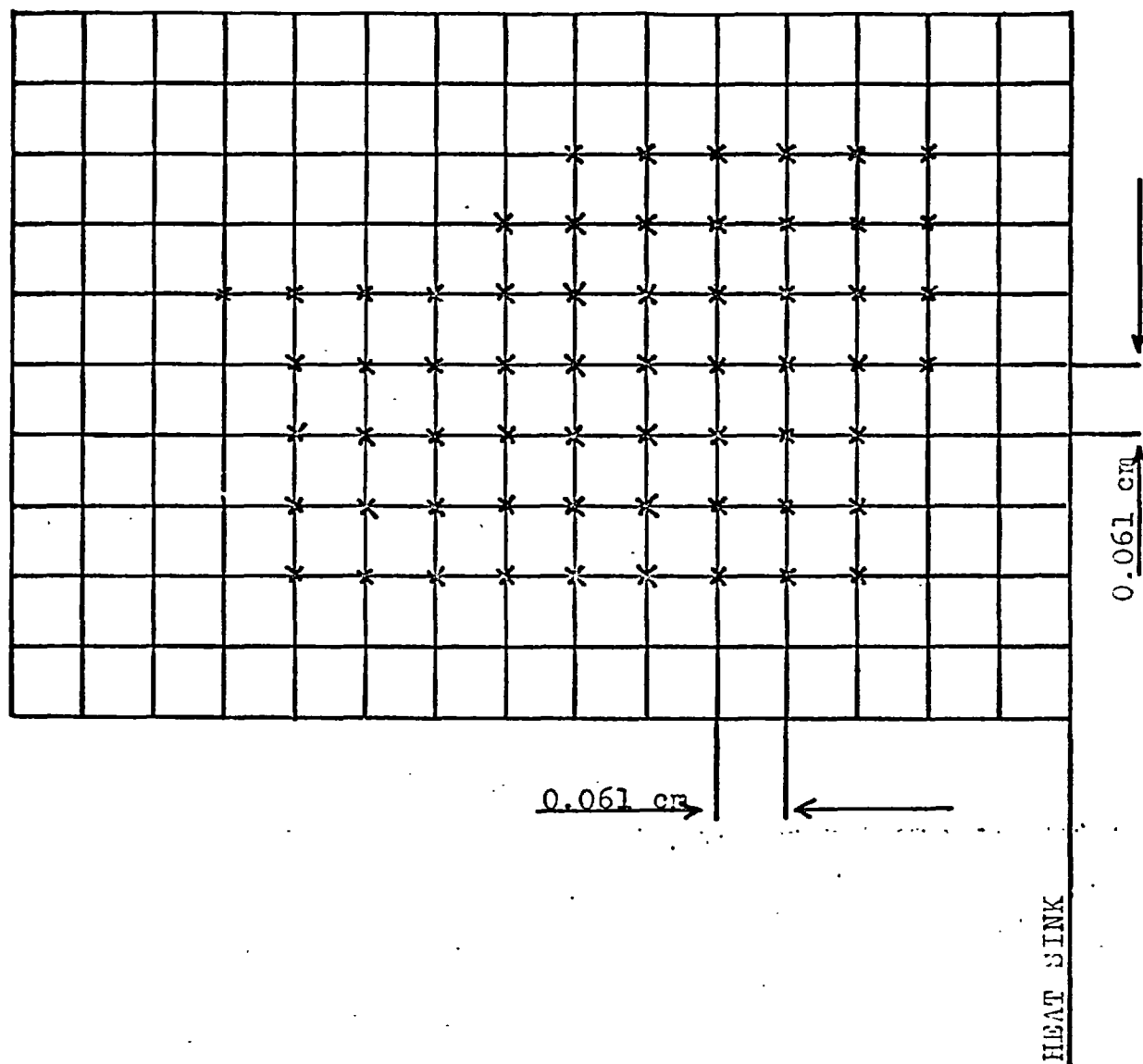


FIGURE 5.1 - POINTS WHERE HEAT RELEASE RATE WAS DETERMINED.

along with its orientation to the y-axis were then measured off (from the enlargements) at the points mentioned above. The horizontal and vertical components of the local velocity were thus evaluated. The components were then multiplied by the local values of the specific heat of the flame gases and plotted against the relevant coordinate axis. The spatial derivative of $C_p V_x$ and $C_p V_y$ were then obtained graphically from these curves.

5.3 Calculation of thermodynamic and transport properties of flame gases.

As regards local values of thermal conductivity and specific heat of the flame gases, which are required for evaluating q''' , one difficulty which arises is that the composition of the mixture throughout the reaction in the vicinity of the heat sink is not known. Even for known gas compositions, experimental data for thermal conductivity are very scarce. Although the thermal conductivity of a few binary mixtures is known, almost no information is available for the case of ternary mixtures. Some methods (e.g., Burgoyne and Weinberg, 1953, and Hirschfelder, 1957) have been proposed for the calculation of conductivities of gaseous mixtures but in view of the lean composition of the reactant mixture it was thought justifiable to treat it as air for the purposes of obtaining the values of C_p and k . The assumption

implied by equation (5.8), that the flame gases behave as a perfect gas (ρT constant) is, of course, perfectly reasonable. The thermal conductivity and specific heat of air were therefore plotted against temperature using the data of F.D. Rossini et al. (1953) and the graphs used for determining the local values at points of interest. The gradients of thermal conductivity needed in eqn.(5.8) were again determined graphically.

5.4 Rate of heat release

The volumetric heat release rate thus calculated is shown in Fig. 5.2(b). These are the local values in a one dimensional plane of the burner. Some of these are not very accurate because the steep thermal gradients prevailing in certain regions render an accurate determination of $\partial^2 T / \partial x^2$ and $\partial^2 T / \partial y^2$ rather difficult there. It was however not considered that this mattered very much because the aim was to see the general pattern of the heat release rather than to deduce accurate absolute values in the vicinity of the heat sink.

The pattern as such reveals some curious features. One is that the zone of maximum reaction rate extends all the way to the heat sink, and that the value of this maximum does not fall off appreciably as the heat sink is approached, in spite of the great reduction in temperature. Another is that the

flame thickness alters in an unexpected manner as the sink is approached. This can be seen if one defines the flame thickness as the zone over which the rate of heat release is greater than some specific threshold value. The dotted curve in Fig. 5.2 is the locus of all the points at which heat release rate is approximately $5.0 \text{ cal.cm}^{-3} \text{ s}^{-1}$ and it will be seen that the flame gets thinner towards the heat sink.

5.5 Discussion.

The second observation, at first sight appears to contradict the expectation that a decrease in burning velocity should lead to an increase in flame thickness. On the contrary, it seems that as the flame loses heat to the sink and the net heat available for its own propagation decreases, it tends to compensate for this by becoming narrow, thereby increasing its gradients for the transport of energy and radicals upstream. This description would apply only if the flame chemistry remains the same. However, it is known that the process of oxidation of CO to CO_2 in hydrocarbon flames is much slower than the oxidation of the hydrocarbons to carbon monoxide and water. This was first mentioned by Friedman and Burke (1954), in connection with their study of low pressure propane-air flames, and by Burgoyne and Hirsch (1954) at atmospheric pressures. In the former investigation it was found that the fraction of heat release occurring by the end of

the luminous zone was only sixty per cent of the total observed heat release. The rest seemed to extend over a region much wider than the luminous zone which was an "afterburning zone". It was in this region that the carbon monoxide was thought to burn to CO_2 . This conjecture was subsequently confirmed (c.f. Westenberg and Fristrom, 1961). If in the present study, part or the whole of this step is quenched by the heat sink, the combustion of ethylene will not proceed to completion, some fraction of CO will remain unburnt and a narrowing of the flame zone can be expected.

The failure of the maximum heat release rate to fall in spite of the considerable fall in temperature is an even more remarkable feature of the system under study. Once again the observation seems to contradict the normally expected situation. For, if the rate of heat generation obeys an Arrhenius type law, a reduction in T, caused by the extraction of heat from the flame, would bring about a steep fall in its value because of its exponential ($\exp(-\frac{E}{RT})$) dependence on temperature. This can be illustrated by an order of magnitude calculation. The effective activation energy E for flame zones deduced in an earlier study (Levy & Weinberg, 1959)² using almost identical ethylene/air flames is 39.6 k.cal/mole. With this value of E, the rate of heat generation at 1100°C would be about two orders of magnitude greater than

that at 800°C . A quick check on Fig. 5.2, however, reveals that the maximum heat release rate observed at 1100°C in the unquenched zone of the flame is not appreciably diminished down to temperatures as low as 800°C at the very least. Thus the expected decrease is being somehow compensated for. Any moderate change in concentration of one of the reactants would not be sufficient to account for the hundred-fold difference in actual and expected values; it would have to be a much more active change of the process. The most probable process potentially capable of greatly increasing the reaction rate would be the diffusion of some active species into the zones in the vicinity of the heat sink. It is, of course, known that chain reactions such as oxidation of hydrocarbons involve active particles as chain carriers. These particles are atoms or free radicals which are chemically very active. In many flame structure studies (e.g. Gaydon & Wolfhard, 1949) it has been deduced that molecules such as O_2 and H_2 dissociate and participate in chain branching reactions, giving rise to high concentrations of free atoms and radicals such as O , H and OH . Because these particles are small, they diffuse rapidly into colder layers of the flame. Here they may react readily, because free radical reactions often have low energies of activation. The spectroscopic examination of flames (Gaydon, 1948) has also confirmed that such free radicals

do exist. It was therefore thought that some such species diffusing into the colder regions of the flame is likely to be responsible for keeping up the heat release rate to a value comparable with that in the hottest parts of the flame.

All these effects; the partial combustion and the differential diffusion of some species towards the heat sink would be expected to show up in the composition pattern. Sampling at various stations followed by analysis for the stable species was therefore undertaken. The procedure adopted is discussed in the next chapter.

CHAPTER 6THE COMPOSITION PATTERN

6.1 Microprobe sampling has been found to be extremely helpful for detailed studies of the chemical structure of flame fronts. The method, in principle, aims at rapidly withdrawing local samples of the gases, freezing their chemical composition and analysing them. In practice, it raises a number of practical problems which have to be dealt with before the technique can be successfully employed. They are connected not only with the thermal and chemical history of the sample following its withdrawal from the flame front, but also with the effect such withdrawal produces on the system under study. But since the technique is a most important way of extracting detailed information from a flame front, considerable efforts have been made to study these problems and minimise their effects as far as possible.

6.2 External effects.

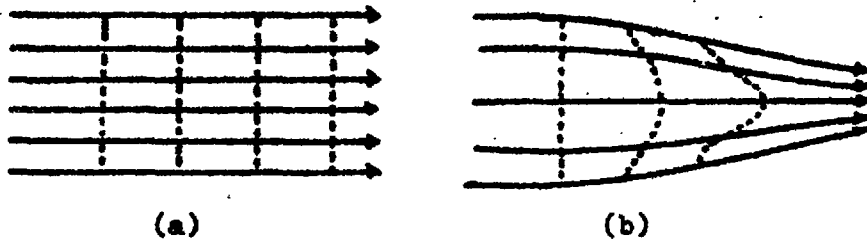
The introduction of any foreign body produces many changes in a flame front. It can alter not only the aerodynamic structure of the system under study but also its thermal structure and composition profiles which in turn may give rise to samples leading to erroneous conclusions regarding the unperturbed conditions prevailing locally. The situation is

no doubt complex and it is only by considering these effects individually that a workable compromise can be achieved.

6.2.1 Aerodynamic effects:

These effects may involve changes in the shapes of streamlines and stream tubes and hence in iso-concentration surfaces in the flame front. In the simplest case of one-dimensional flow (Fig. 6.1a) the surfaces of equal concentration are planes parallel to each other and normal to the streamlines. Sampling by a probe will produce local changes in velocity and the shape of streamlines will generally be distorted as in Fig. 6.1 b. Assuming that the diffusional velocities of the species do not alter initially, this will bring about a change in the shape of concentration contours as shown by broken curves in Fig. 6.1 b. As a result of this, new diffusional velocities will come into play and consequently alter the local chemical composition. In two- and three- dimensional systems the situation will be more complicated.

The extent^{to} which such aerodynamic effects spread depends on the characteristics of the probe and the system under observation. As stated by Fristrom (1965) it has been studied theoretically by Rosen and later both theoretically and experimentally by Westenberg and co-workers (1957). Thus on the basis of certain simplifying assumptions an estimate was made of the extent to which sampling by probes could cause a certain



PRESUMED DISTORTION OF UNIDIMENSIONAL CONCENTRATION
DISTRIBUTION BECAUSE OF FLOW DISTORTION.

FIGURE 6.1

level of velocity distortion. A probe entrance of finite dimensions was considered and the inlet area was assumed to be a sink of radius r and strength (volume flow rate), Q . The distortion of flow, expressed as a fraction of the unperturbed stream velocity v_{∞} , was calculated as a function of the distance from the sink and also of the sampling rate ratio α ($= \frac{Q}{\lambda r^2 v_{\infty}}$). For probes of inlet diameters in the range 10-100 μ and sampling rate ratios lying between 10 and 100, a 5 % distortion was found to exist at a distance of five to ten probe radii upstream. Thus for a probe of radius 25 μ the flow distortion was expected to fall below 5 % at a distance less than 0.2 mm upstream of the probe. These results have been found to be in reasonable agreement with experimental studies (Fristrom, et al, 1957).

The order of magnitude of the associated changes in concentration gradients has been determined by Westenberg and co-workers (1957).

The probe was approximated to a point sink located in a one-dimensional concentration gradient of a binary mixture. Assuming constant temperature and pressure and the absence of any chemical reaction, it was found that the concentration gradient was affected by a very insignificant amount. The theoretical computations were confirmed by an experimental study in a known gradient of acetone in helium. Samples drawn

from such a system were found to have a composition only slightly different from that in the unperturbed case. Although the gradients in these studies were much less than those obtaining in flames, the extrapolation of these results to the latter case is probably justified.

6.2.2. Thermal effects:

The sampling probe can be expected to alter the local heat transfer processes in the flame and thus affect the diffusional transfer of reactive species into the sampling region. Because of the low thermal conductivity of quartz, of which the probes are generally made, the temperature of the probe tip will approximate to that of the gas throughout the flame front, although it will lag behind somewhat in the hottest regions of the flames, where radiation cooling becomes significant. This lag has been found (Fristrom, et al, 1957) to be only a few hundred degrees at the highest temperatures. The change in diffusional transfer of species into the sampling region is therefore expected to be a second order effect.

6.2.3 Composition changes:

Apart from the secondary composition changes due to thermal and aerodynamic effects of a probe, the most serious change can be brought about by any catalytic action. The probe, being a solid body in otherwise gaseous surroundings, may accelerate or inhibit flame reactions. But if the probe is

properly cleaned, the catalytic effect, and especially the acceleration of reactions on the hot quartz surface, can be significantly reduced. The second type of catalysis inhibition of reactions would be expected to be present only in the case of metallic probes at lower temperatures.

6.3 Internal Effects.

It appears that if constructed and used with care, quartz microprobes can be employed for sampling studies in following the course of a chemical reaction. But the probe design should ensure rapid quenching of the reactions, after the sample has been withdrawn. If reliable results are to be obtained, the time needed for freezing the reactions must be small as compared to the reaction half life. If the sampling method involves a rapid adiabatic expansion accompanied by cooling, quenching lags as low as 5 μ sec have been claimed (Fristrom, et al, 1957). Once the reactions have been frozen, further recombinations can take place only along the boundary layers inside the probe which constitute a negligible fraction of the main flow.

An estimate of the effect of probe dimensions and pumping rates on quenching efficiency has been made by Fristrom et al (1957). It was found that if conditions are chosen such that the sample enters the colder regions of the probe in a fraction of a millisecond, the sampling process has a negligible

effect on reactions whose half life is 500 μ sec. or more.

The considerations that emerge as being important from earlier probe sampling studies are concerned with:

- (i) the choice of a suitable probe
- (ii) the control of the sampling rate
- (iii) the rapidity with which reactions are quenched in the sample.

6.4.1 Choice of the probe:

In the present work, the probes were made of quartz, which is capable of withstanding temperatures of the order of 2000°K. Although the inlet diameter of the probes, if between 5 and 100 μ , has not been found critical, the tapering profile does seem to be important. It has been found (Fristrom, et al, 1957) that in very slender probes, pyrolysis can occur. However, Friedman (1955) has shown that tapers of slope lying between 15 and 45 degrees can be safely used to obtain reproducible results unaffected by pyrolysis. Tubing of 1 mm bore and quarter millimeter wall thickness was therefore employed to fabricate the micro-probes. The procedure consisted of heating a central length in an oxygen flame while holding a six inch piece of tubing at its ends. As soon as it became soft, the two ends were quickly drawn apart to give a fine taper in the middle. Such tapers were cut at a place where their outside diameters were about half a millimeter. The inlet holes were

then examined under a microscope. Generally they turned out too large, but by heating the tip uniformly on a small flame their bore could be reduced to the appropriate size. This was achieved by trial and error since any overheating resulted in complete blockage of the probe. With some patience a suitable probe could be fabricated in about an hour.

6.4.2. Sampling

(i) Sampling Bottles:

Since the samples were expected to be gaseous mixtures of non-condensable components, with the exception of water vapour, the sampling bottles were made of glass. These had a capacity of 250 cc. and carried two-way glass taps, one at each end. It was, however, found difficult to maintain a low pressure inside these bottles. On keeping them under vacuum, some of them were observed to de-gas. The ordinary glass taps were therefore replaced with spring loaded high vacuum taps. All the bottles were thoroughly cleaned with chromic acid and baked in an oven at 500°C . The taps were then greased with a thin layer of vacuum grease and the bottles tested for leaks by evacuating them and keeping them under vacuum for several days. This ensured that all the bottles used for storing samples were leak proof and the tests were repeated each time a set of samples was taken from the flame.

(ii) Method of taking samples.

The bottles were connected to the probe, manometer and a vacuum pump, as shown in Fig. 6.2a. via a three-way tap. Since rubber tubing has been known to adsorb certain flame gases, the connections were made with polythene tubing.

For withdrawing the sample, the probe was located at the desired place and the whole line including the bottle was evacuated to a pressure of a fraction of a millimeter. The pump was then isolated and the bottle and the manometer were put in communication with the probe. As the flame gases entered the bottle, the pressure difference indicated by the manometer registered a fall. This was allowed to continue for about five minutes. The bottle was then again evacuated by connecting it to the pump and the process repeated. In this way the system and the sampling bottles were gradually flushed with flame gases. The bottles were then again evacuated until the tap was turned suddenly to disconnect the pump and connect the bottle and the manometer to the probe. The gases were aspirated until the pressure in the bottle showed a rise of 10 cms. of Hg. At this moment the taps of the bottles were closed. The whole process took about a half an hour.

Samples were taken in this manner at twelve points which comprised of four sets at three locations - two on either side of the flame and the third on the luminous zone

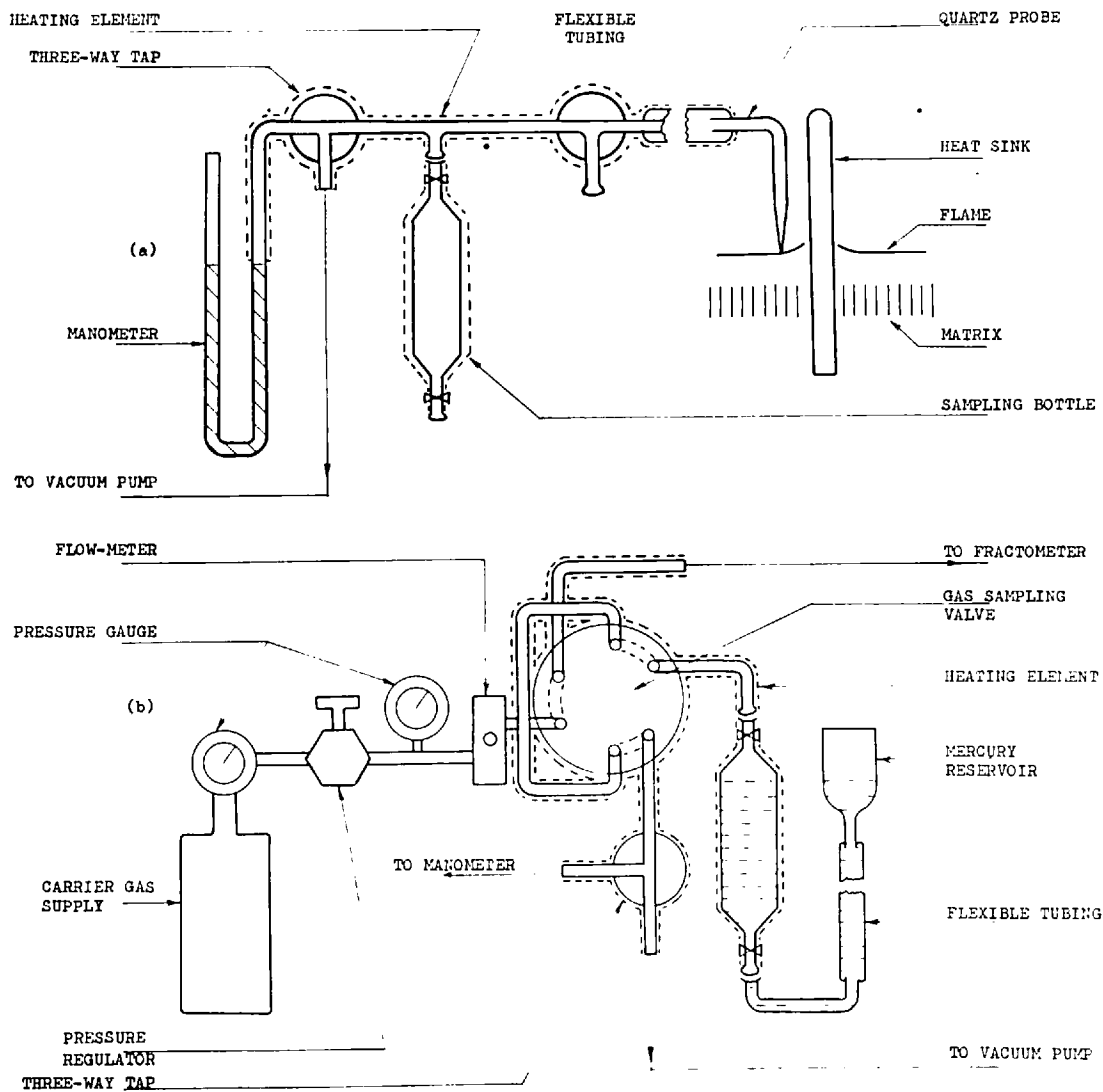


FIGURE 6-2 - ANALYTICAL APPARATUS. (a) THE PROBE SYSTEM. (b) THE GAS CHROMATOGRAPHY SYSTEM.

itself. The position of the probe was adjusted visually, using the micromanipulator discussed in the context of temperature measurements. Each probe position was however photographed both at the beginning and at the end of the sample withdrawal. A constant vigil was kept for any movement of the flame front. The slightest change could be noticed by reference to the cross line provided in the field of view of the camera used for taking the photographs of the probe locations. If the flame was found to move during the above process, all the samples were rejected.

6.5 Outline of gas chromatography system.

The essentials of the gas chromatography system are shown in Fig. 6.2.b. It was basically a Perkins Elmer "Fractometer". The carrier gas, which was helium in the present study, was supplied from cylinders fitted with regulating valves. Its rate of flow could be controlled by a fine pressure regulator coupled with a 0-30 p.s.i. gauge. With the help of a gas sampling valve, the carrier gas could be made either to by-pass the sample or to entrain it. The gas sampling valve was so designed that accurately known sample sizes (of either 1/2 ml., 1 ml, 5 ml or 25 ml) could be introduced into the carrier gas stream. The sample thus entered into the columns where its components were separated. After separation, the gases flowed through the detector and on

to the exit system.

The detector was made of two thermal conductivity cells with matched hot wire elements. One of these, carrying the pure carrier gas served for reference, while the other, carrying the carrier with the separated components, served as the sensing element. The filaments were heated by a constant current which could be adjusted to any desired value by suitable regulators. The presence of the sample in the carrier changes the thermal conductivity of the mixture and hence the temperature and resistance of the sensing element. The resulting change in potential difference can be measured and compared with that across the element in the reference cell. The two hot wires actually formed the adjacent arms of a sensitive bridge circuit. The changes could be directly recorded by a Honeywell one second potentiometric recorder of 0 - 1 mV range.

The unit was also provided with signal attenuator control, polarity switch and a precise control for the temperature of the oven in which the detector unit was housed.

6.6 Choice of columns

In the present case, three columns packed with (i) silica gel, (ii) molecular sieve and (iii) carbowax 1500 on Teflon, were used. The first column was made of copper tube of 0.25" outside diameter and a meter in length. It was uniformly packed with silica gel of 80-100 mesh size. The

second column was 3 meters long and was packed with molecular sieve 13 x. The third column, bought from Perkin and Elmer, was made up of a one meter stainless steel tube packed with carbowax 1500 on Teflon. The working conditions and the gases for which each of these was used is given in table I.

6.7 Determination of water

It was thought that in all likelihood, the species responsible for the increased heat release rate observed in the vicinity of the heat sink either directly or on reaction with some other molecule, could be a hydrogen atom or possibly some small radical involving hydrogen. Since only stable species could be analysed with the chromatograph, the distribution of water vapour near the heat sink was considered important, as most of the hydrogen could be expected to end up as water vapour.

But the determination of water vapour involved several problems. To begin with, it was found that for certain samples, the room temperature was below the dew point and condensation of water vapour had therefore to be avoided. Moreover, water, being a polar molecule, its adsorption on the surfaces of the chromatograph components could lead to large errors. While the condensation of water could be avoided by raising the temperature of these surfaces, adsorption had to be reduced to a minimum by minimizing the surface area as far as practicable.

In view of these uncertainties, it seemed worthwhile to

TABLE 1.

Gases to be separated	Column Material	Column length, m	Column Temperature	Carrier gas cc/min.
Ar+ O ₂ , N ₂ CO, CH ₄	Molecular Sieve 13 x	3	Room Temperature	He 60
CO ₂ , C ₂ H ₆ C ₂ H ₄	Silica gel 80-100 mesh	1	50°C	He 60
H ₂ O	Carbowax 1500 on Teflon	1	100°C	He 60

explore methods other than chromatographic, for the purpose of estimating H_2O . Many ideas were tried, but mention will be made of only two, which seemed the most promising. The first aimed at determining the quantity of water vapour by the dew point method. The sample was lead through an oblong glass vessel (Fig. 6.3) carrying mercury in a small bulb. A copper-constantan thermocouple was kept touching the pool of mercury which was cooled from outside. It was hoped that the dew point could thus be determined with the aid of the thermocouple, by observing the mercury surface. However, once the dew appeared, water in the vicinity of the mercury pool seemed to be retained. This was revealed by a gradual elevation of the dew point. The method, in this form did not yield reproducible results and was therefore discarded.

The second method aimed at directly determining the amount of water in a known volume of the sample. The apparatus used is shown in Fig. 6.4. Two U-tubes, A and B, both open to the atmosphere were filled with dibutylphthalate to the same height. They were then connected to two calcium chloride towers through stop-cocks, C and D. The manometer, A, carried a three-way valve for introducing the sample. With stop-cocks C and D closed the sample was introduced and the difference in the two levels of A noted. The sample was then transferred from A to B by opening the stop-cocks and

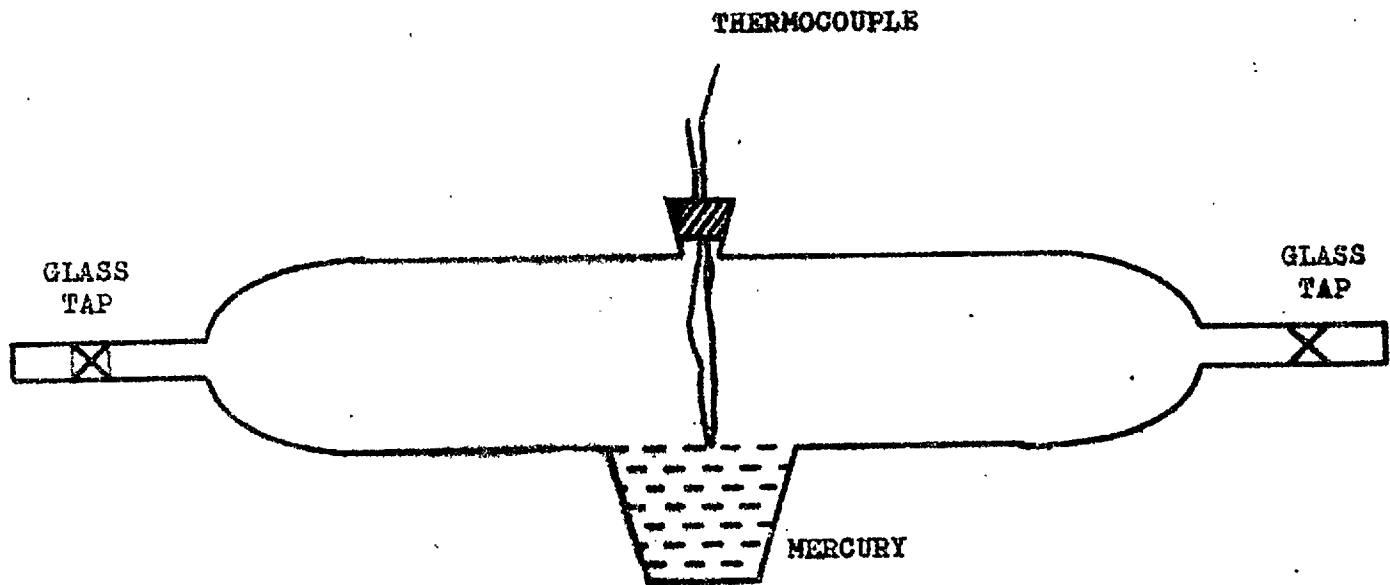


FIGURE 6.3.

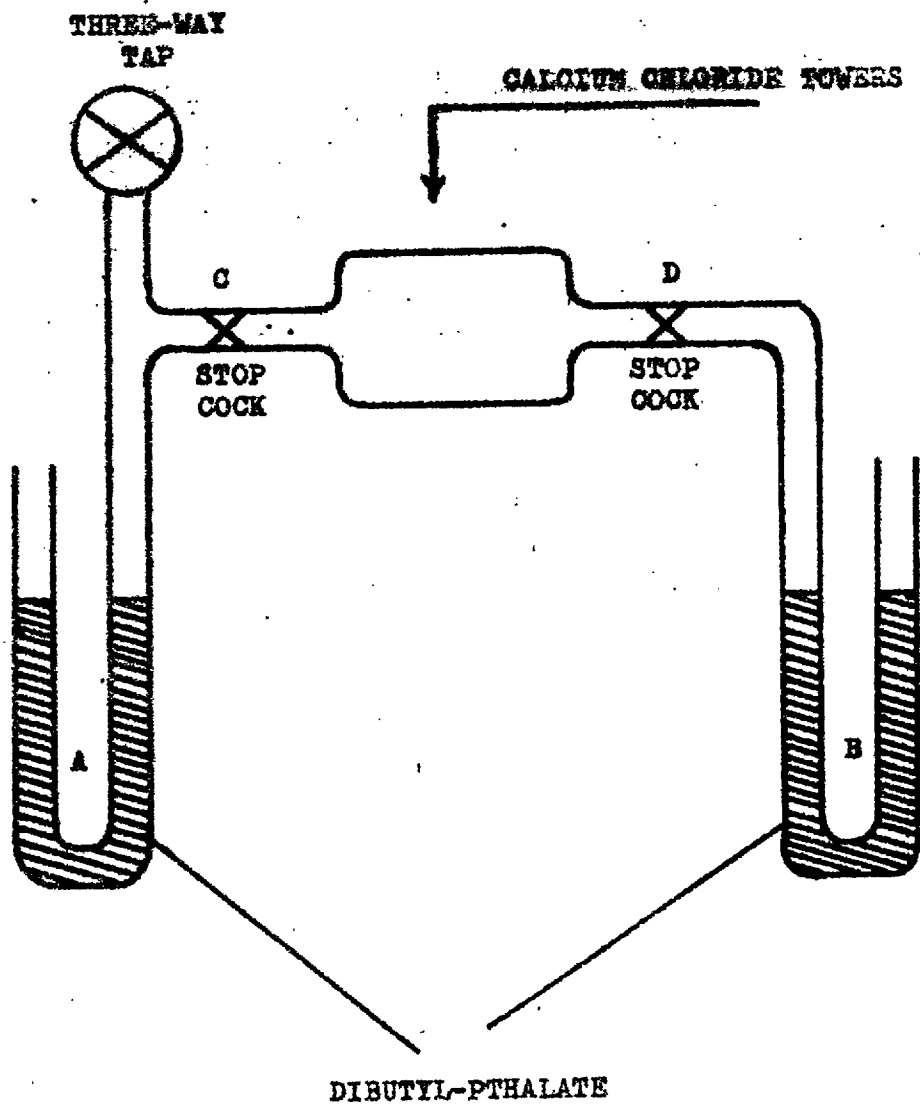


FIGURE 6.4.

manipulating the free arms of the two manometers. After passing the sample a few times through the calcium chloride towers, the difference of the levels in B was kept at its initial value. Under this condition the difference in levels of A gives a measure of the remaining volume. However, the moisture content in the sample deduced in this way did not give reproducible results. This may again be due to retention of water by parts of the apparatus other than the drying towers.

Since neither of the above methods gave useful results, recourse was made to chromatography. The apparatus (Fig. 6.2 a and b) was therefore modified for this purpose. The connecting lines were replaced by glass capillaries and their temperature, as well as that of the sampling bottles, sampling loop and valve, was raised by means of a heating element. The heating current was controlled and kept steady with the help of a variac and an ammeter. The temperature of the connecting lines on the sampling system was kept at 60°C whereas the sampling loop was maintained at 51°C . It was found that this temperature was sufficient to give reproducible results when used with a loop pressure of half an atmosphere.

In order to obtain reliable results, in the case of H_2O , the non-linearity of the distribution isotherm (see e.g. Markstein, 1958) had also to be avoided as far as possible. The phenomenon, frequently called "tailing", leads to

asymmetric chromatogram peaks in the case of polar substances. Since low concentrations move slower through the column than higher ones, some water vapour is retained by the column for appreciable times. Successive samples having the same vapour concentrations tend to give peaks of increasing heights and area. But after this initial variation they attain a steady value and it is these values which yield reliable estimates of water vapour concentration.

6.8 Preparation of standard mixture.

In order to obtain accurate quantitative data from gas chromatography it is advisable to calibrate against a standard mixture of composition nearly the same as expected in the samples. A few representative samples of the flame gases were therefore sent away for analysis. On the basis of this analysis a synthetic standard mixture of all the constituent species in the appropriate proportions, except water vapour, was prepared as follows. A three litre glass flask was evacuated to a pressure of a fraction of a millimeter, as indicated by a manometer. The different gases detected in the analysis were then introduced from their cylinders. Since the desired composition was known, each gas could be let in to the required partial pressure as read off the manometer. The mixture thus prepared was again sent for analysis and its composition obtained to within an accuracy of $\pm 1\%$ and this served as the standard for

quantitative analysis of the flame gases.

In order to obtain a calibrating standard for water vapour detected in the flame gas samples, the apparatus shown in Fig. 6.5. was used. The suction produced by the pump causes an air stream to bubble through boiling water. This steam-laden air then passes through water at room temperature where it sheds the water vapour in excess of that necessary to saturate it. The saturated air passes through the sampling loop to the pump and then to the exhaust. After the apparatus had been flushed with vapour saturated air, the sample was collected in the loop until the pressure inside became approximately half an atmosphere. A thermocouple helped in ascertaining the temperature of the air stream entering the sampling loop. The sample thus introduced in the loop provided a standard for quantitative estimation of water vapour in the flame gases.

6.9 Analysis of the samples.

For determining the exact amount of the different gases present in the samples, the appropriate columns were set up in the fractometer. The samples were then introduced in a one millilitre sampling loop. The sampling loop, Fig. 6.2b. was evacuated by a rotary pump backed by a diffusion pump. The taps of the sampling bottle were then opened and the loop flushed with the sample by displacement of mercury. The taps were closed and the loop evacuated. After the desired vacuum

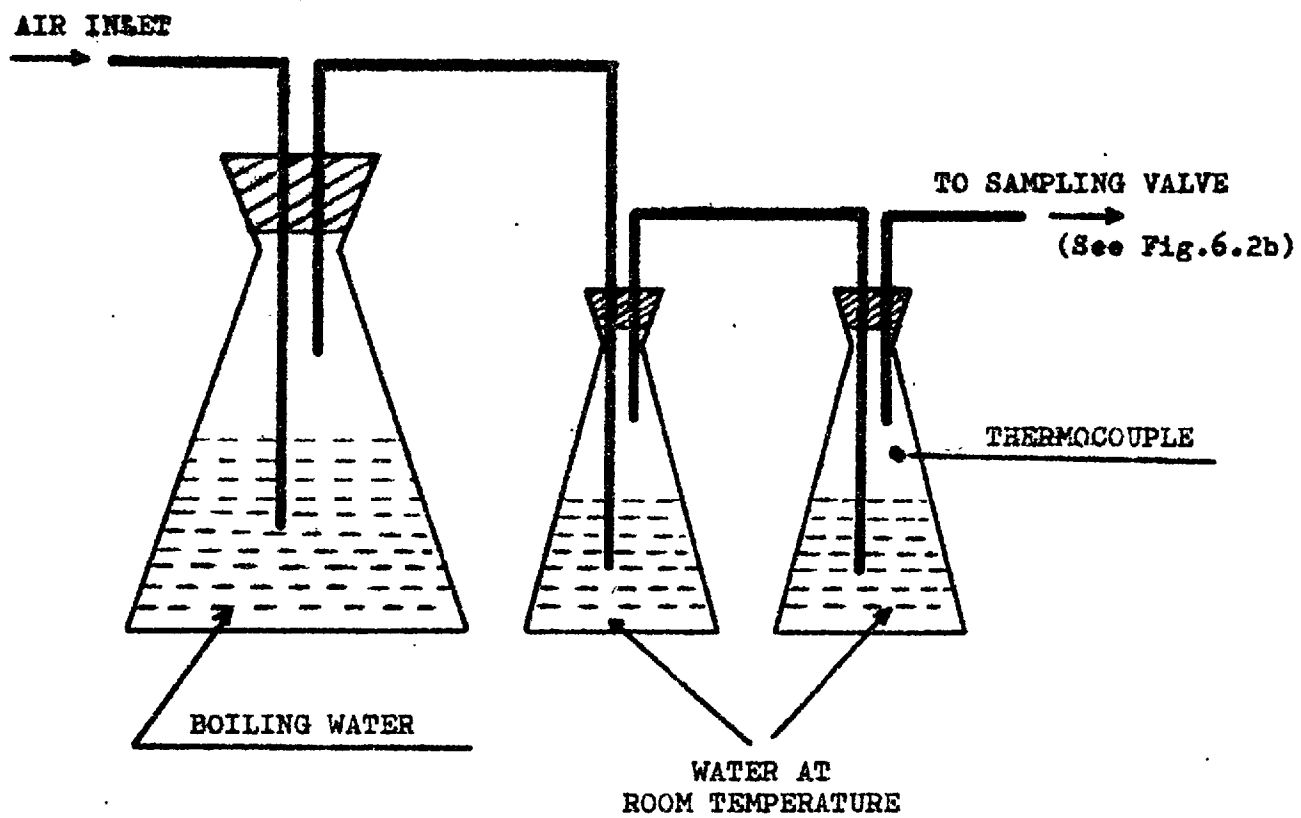


FIGURE 6.5.

was reached the sample was again introduced as before until the manometer attached to the loop indicated an appreciable rise of pressure. The system was allowed to attain a steady state and the loop was cut off from the bottle. The temperature of the sample inside the loop was determined by a copper-constantan thermocouple and its pressure was carefully noted on the manometer. In all cases, except in the estimation of water vapour, the samples were introduced at room temperature and atmospheric pressure. For the case of H_2O , the samples were roughly at half the atmospheric pressure and $51^{\circ}C$ temperature. They were first analysed using the carbowax on Teflon column, then on molecular sieve and finally on the silica gel column. For this the sampling valve was turned so that the sample was swept away by the carrier gas. For detecting the components the attenuation control was manipulated in such a way as to give the maximum deflection on the recorder. The process was repeated with each of the three columns in turn and the peaks for all the species present in the sample were obtained.

The peaks obtained by such analysis were immediately calibrated with the help of the standard mixture. A sample of this mixture was analysed under conditions identical to those used for analysing the flame gas samples. Thus knowing the area of the peaks of known concentrations of the corresponding species, the peaks observed during an analysis of the samples

could be directly translated into actual amounts of each species present in the sample by simply comparing their areas.

6.10 Results.

The percentage composition of these samples was determined at atmospheric pressure (76.0 cm) and room temperature, (23°C). The stable species as found at various positions in the flame in the case of two of the best sets of results are given in Table II. The significance of these results will be discussed in the next chapter.

TABLE II ANALYSIS OF GASES AT VARIOUS POSITIONS IN THE FLAME

%	set	0 mm from heat sink			2 mm from heat sink			4 mm from heat sink			6 mm from heat sink		
		A	O	B	A	O	B	A	O	B	A	O	B
N ₂	<i>a</i>	76.44	74.19	74.35	77.6	74.5	75.7	77.9	75.51	75.13	77.71	74.61	72.30
	<i>b</i>	76.9	75.91	75.11	78.32	77.40	75.72	78.64	75.8	75.3	80.2	77.7	—
O ₂	<i>a</i>	14.4	19.8	20.87	13.89	19.45	22.6	14.3	20.26	21.97	11.57	17.30	21.85
	<i>b</i>	14.84	18.97	21.5	14.65	19.04	21.5	14.80	20.13	22.5	14.8	20.4	—
CO	<i>a</i>	0.46	0.24	0.02	0.37	0.33	0.01	0.08	0.39	0.00	trace	1.06	0.06
	<i>b</i>	0.49	0.52	0.02	0.47	0.53	0.02	0.27	0.49	0.00	0.02	0.53	—
CO ₂	<i>a</i>	4.91	0.67	0.07	5.05	0.86	0.09	5.24	0.89	0.07	5.57	2.38	0.14
	<i>b</i>	4.82	1.57	0.13	4.82	1.56	0.14	5.34	1.26	0.09	5.57	1.12	—
C ₂ H ₄	<i>a</i>	0.13	2.20	2.52	0.065	2.14	2.58	0.00	2.05	2.54	0.00	0.91	2.43
	<i>b</i>	0.18	1.72	2.53	0.11	1.72	2.56	0.00	1.85	2.59	0.00	1.88	—
H ₂ O	<i>a</i>	5.06	1.17	0.69	5.17	1.28	1.22	5.16	2.30	0.99	4.56	3.41	0.97
	<i>b</i>	6.23	3.81	0.62	5.51	1.90	0.68	5.20	2.89	0.79	4.92	2.47	—
C ₂ H ₆ CH ₄ H ₂	below detectable limit in all analyses												
total	<i>a</i>	101.40	98.27	98.52	102.15	98.56	102.2	102.68	101.4	100.70	102.4	99.7	97.75
	<i>b</i>	103.0	102.5	99.90	103.88	102.0	100.6	104.3	102.4	101.3	105.5	104.1	—

A = above flame, O = on flame, B = below flame.

(*a*) and (*b*) are two independent sets of analyses.

CHAPTER 7CHEMICAL EFFECTS

7.1 As mentioned in Section 5.5 , the results of the gas chromatographic analysis summarised in Table II were expected to throw further light on the possible reasons for the experimental observations regarding burning velocity, heat release rate and flame thickness in the vicinity of the heat sink. In addition to giving directly the percentage volume concentration of stable species in the regions of interest, the results in Table II could also be used to extract information regarding the distribution of the "concentration of elements" involved in the combustion processes taking place near and away from the heat sink. This was the principal method used in the analysis, any deviation from conservation of the elements along a stream tube being used to deduce deviation across its boundaries. The stable species whose distribution appeared most relevant to the overall reaction were ethylene, and the two oxides of carbon. An examination of the distribution of the former was expected to provide evidence of any fuel escaping unburnt near the heat sink. The occurrence of the two oxides of carbon and their relative concentrations in the relevant regions was used as a measure of the extent of completeness of combustion of the

hydrocarbon. Bringing the information together it could then be ascertained whether the reaction extends right up to the heat sink and if so, whether it goes to completion or whether the quenching of the slower stages of combustion is responsible for the narrowing of the reaction zone near the heat sink.

The reasons for the chemical patterns so observed were sought in the diffusion of active species as revealed by the balance of elements. In the past, less analytical studies have revealed the importance of diffusive transport of H and OH radicals in flame processes. Thus Tanford and Pease (1947) found a remarkable correlation between the burning velocity of moist carbon monoxide flame and the hydrogen atom concentration; also no correlation with oxygen atom concentration and a very slight one with hydroxyl radical concentration. Gaydon and Wolfhard (1949) found that in many hydrocarbon flames the beginning of marked exothermic reactions appeared to correspond with the limit of diffusion of hydrogen atoms against the gas stream. Simon (1953) reviewed the studies in which the diffusion of light, chemically active particles seems to play an important part in the flame processes. In view of this it was considered even more desirable to analyse the gas chromatographic data to see if such species were in some way contributing to the

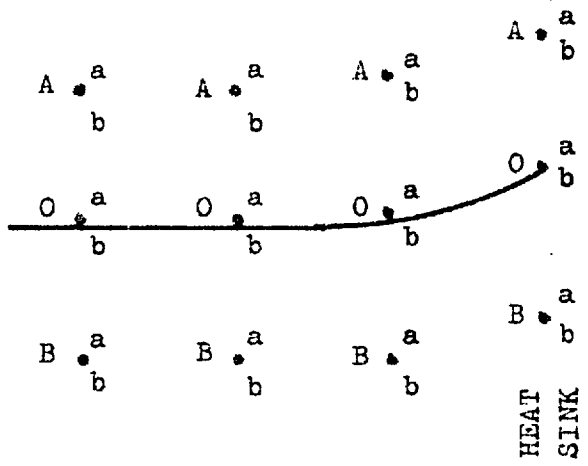
observed properties of the systems under study.

In order to obtain a graphic distribution of the species, their concentrations (see Table II) were shown on a plot of their locations. The scheme of such plots is shown in Fig. 7.1a.

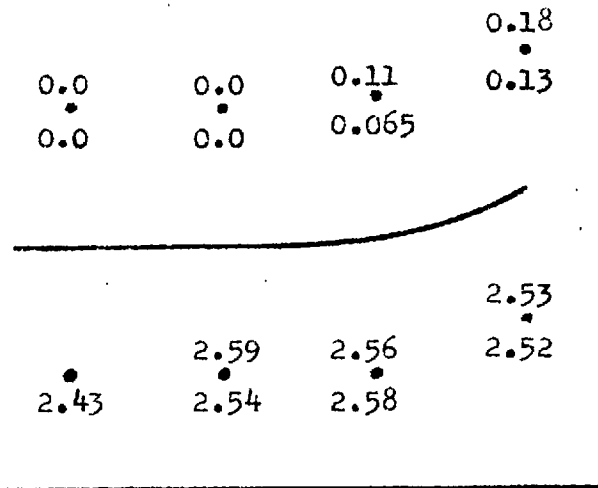
7.2 Concentration of C_2H_4 .

Fig. 7.1 b, shows the amount of fuel detected above and below the flame in various locations. It will be seen that the concentration of ethylene below the flame was nearly the same as in the reactant mixture (2.61 %); in fact a setting in of the combustion processes can just be detected in the colder regions of the flame. Above the flame the ethylene concentration is non-detectable in the unquenched region but rises to a small but measurable amount near the heat sink. However, the amount of fuel escaping unburnt is still only 6% of the original ethylene concentration. This is in perfect agreement with the large values of heat release rate extending very close to the heat sink. Any annulus around the cooled sink in which reaction is non-existent, or so slow that fuel can pass through unchanged, must be vanishingly small.

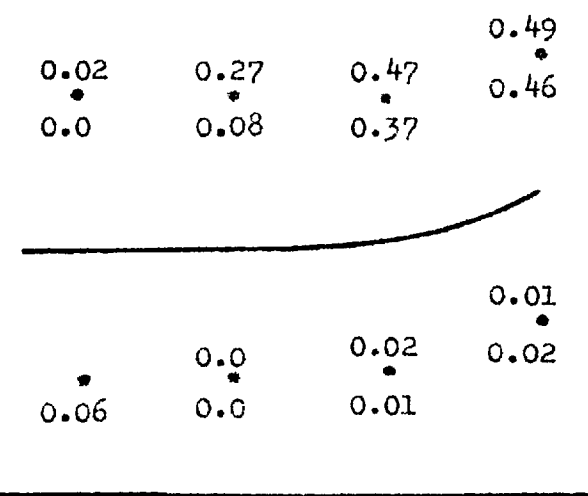
(a) Scheme of sampling points - correlation with table 2.



(b) C_2H_4 above and below the flame



(c) CO above and below the flame



(d) CO_2 expected minus CO_2 found above flame

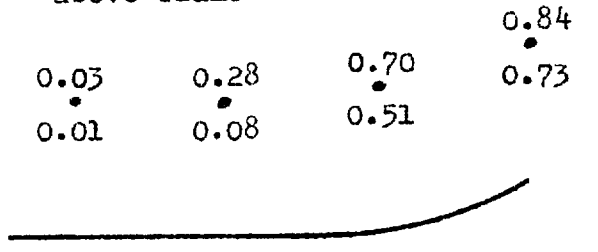


FIGURE 7.1 - CONCENTRATION PATTERN

7.3 Concentration of oxides of carbon.

Although hardly any fuel passes through unchanged, an appreciable amount of CO remains unoxidised to CO₂ close to the heat sink (Fig. 7.1 c). It will be seen that no significant amount of CO occurs either in the burnt products far from the heat sink or in the reactants anywhere. Very close to the heat sink, however, up to 1/2 % of CO is found in the products. This is still only about 10% of the amount that would be formed if all the C in the fuel was converted to CO. However, since its distribution in the products is likely to be very much spread out by diffusion, close to the heat sink, an appreciable amount appears to be formed. This again is in agreement with the heat release rate results, in particular with the narrowing of the zone of heat release. As mentioned earlier, it would be reasonable to expect that the disappearance of the slower second stage - the CO oxidation step - would greatly narrow the zone of appreciable heat release. The manner in which CO is formed at the expense of the CO₂, characteristic of the unquenched zones is shown in Fig. 7.1 d, which in fact shows values of CO₂ expected on complete conversion of all the fuel minus the CO₂ actually formed.

7.4 Distribution of elements.

The derived profiles of H and O are shown in Fig. 7.2 a and d. They were obtained by summing the hypothetical "partial pressures of elements" (e.g. the oxygen atom concentration was obtained by summing the atom concentration in the species H_2O , CO and CO_2 or total $O = H_2O + CO + 2CO_2$, similarly, total $H = 2H_2O + 4C_2H_4$). These would remain constant along each streamline in the absence of differential diffusion across the stream tube boundaries. Any departure from such constancy would be evidence of the diffusion of the corresponding species in the regions of interest. In order to bring this out more explicitly, the difference between the species (H + O) actually found and expected was determined at the various locations mentioned before. Thus, Fig. 7.2 b shows the difference between H found and H expected. In this instance, individual results of the two analyses are given rather than their averaged values, because of the inaccuracy in determining water, mentioned earlier; H_2O being the major hydrogen-containing species. Since it is possible that some water may have been lost to individual analyses, it seems better not to lose data by averaging. The results indeed give the appearance of water having been lost in two of the analyses close to the heat sink. Nevertheless the general

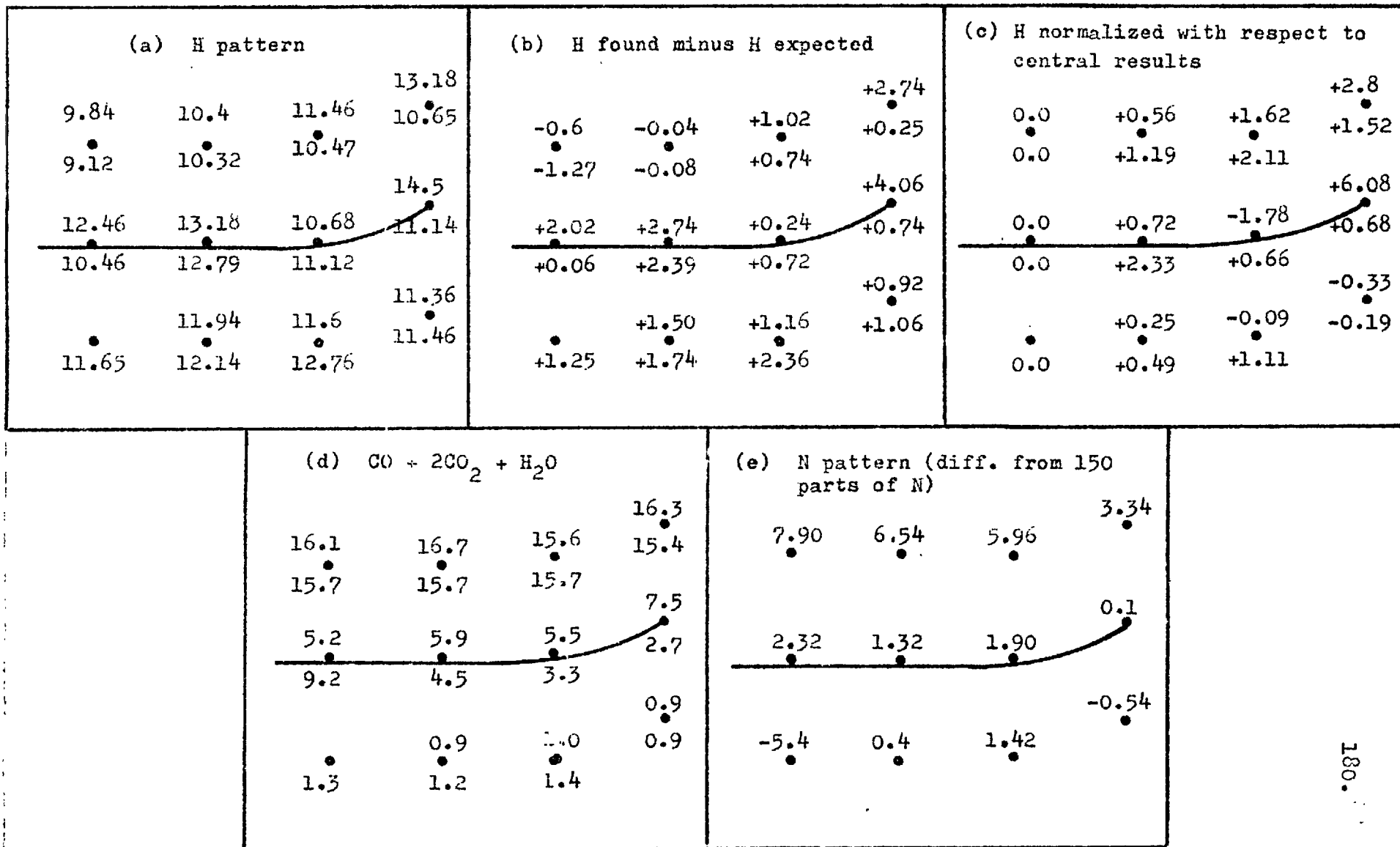


FIGURE 7.2 - CONCENTRATION PATTERN

pattern is clear: hydrogen, or one of its compounds diffuses against the gas stream in the unidimensional system away from the heat sink. The water found in the reactants immediately below the flame must, in fact, be formed from the diffusing species since the reactants are sensibly dry. In addition to this diffusion upstream, hydrogen also diffuses towards the heat sink in the regions where reaction is rapid and where the temperature is high. In order to separate the back-diffusion from the effect near the heat sink, the results were 'normalized' with respect to the central unperturbed regions. This was done by subtracting from the readings along each contour the value along that contour farthest from the heat sink (Fig. 7.2 c). There is again evidence of some inaccuracy, but the general conclusion is that when back diffusion has been subtracted, the remaining diffusive flows are towards the heat sink on and above the flame and back towards the centre below it. It must be noted, that the normalized set represents the components along the flame contour of a two-dimensional pattern - a clearer picture will emerge below.

The upstream diffusion of hydrogen is, of course, expected and well known; indeed before the advent of comprehensive theories of flame propagation, attempts at accounting for burning velocities in terms of this effect were

made (Tanford and Pease, 1947). The normalized pattern suggests that hydrogen atoms or a small hydrogen-containing radical diffuses towards the wall which acts as a sink for it. Moreover, it seems that, as a result of this flow, the reaction rate in the vicinity of the heat sink is increased or rather does not fall steeply as would be expected.

Apart from hydrogen atoms, the only other small hydrogen-containing radical which suggests itself is OH. If such large scale diffusion of OH were taking place, it should be revealed by an imbalance in the distribution of O as much as of H. Accordingly, as shown in Fig. 7.2 d, $\text{CO} + 2\text{CO}_2 + \text{H}_2\text{O}$ values were analysed.

It will be seen that there is absolutely no trend above and below the flame, the fluctuation in the middle being due to small variations in the position of the sampling probe with respect to the reaction zone. It therefore appears that the species responsible for the large diffusion flow is not OH.

If the diffusion of hydrogen atoms is at all important it is likely to dominate the scene, because its diffusion coefficient is so very much greater than that of any other species present. Because of the constant pressure requirements, other gases must diffuse in the opposite direction to

compensate for this diffusive flow. Nitrogen makes up about 76 % of the gas. It can be used as an inert indication since it does not participate in the reaction and, unlike H_2O , its concentration is determined with great accuracy by the method of analysis. It therefore seemed desirable to record the distribution of N_2 and use it as index of hydrogen diffusion in the opposite direction. More rigorously, the distribution of N_2 is an index of the algebraic sum of the diffusive flows of all the species in the opposite direction, but because of the vastly greater diffusion coefficient of H the use of N_2 as an index of the diffusion of H alone is a reasonable approximation. Fig. 7.2 e shows local values of nitrogen concentration. The standard deviation of the two sets is only 0.77%. These results are accurate enough to allow one to draw continuous smooth contour lines through them and these are shown in Fig. 7.3 . Lines of nitrogen flux must be orthogonal to these contours and they have been sketched out in Fig. 7.3, with the arrows reversed in order to indicate the deduced diffusion pattern of H. In this form it will be seen to be the same as that indicated by the distribution of hydrogen in Fig. 7. 2 b and c, allowing for the occasional errors due to inaccuracies in the water determination.

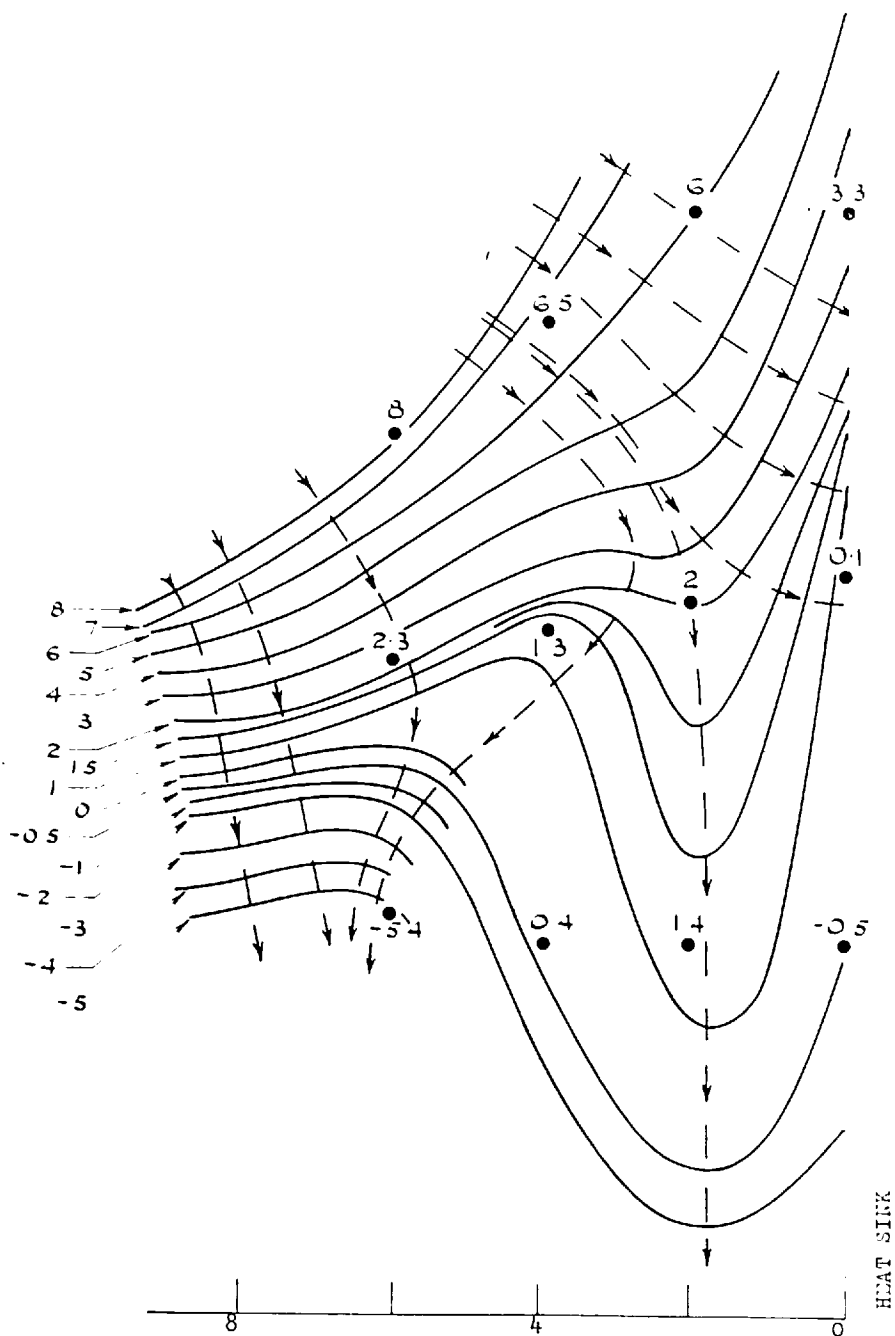


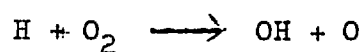
FIGURE 7-3- LOCI OF NITROGEN CONCENTRATION.

(The orthogonals indicate the diffusional flow directions).

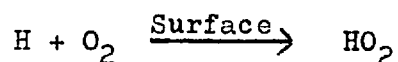
7.5. Discussion

Bringing all the evidence together it appears that hydrogen, most probably in the form of its atoms, diffuses towards the heat sink in the vicinity of the reaction zone. The solid surface, or the gases in contact with it, must act as a sink for this species and in this process the hydrogen itself, or something resulting from its interaction with the heat sink greatly promotes reaction rate.

There may possibly be more than one reaction mechanism which would account for these observations, but there is one which appears particularly plausible. Normally, the most important reaction in hydrogen flames appears to be



(see, for example Fenimore and Jones, 1959). This has a relatively large activation energy and would therefore be rendered ineffective at low temperatures near the heat sink. The reaction which seems likely to take its place is



This is a reaction which has been considered in somewhat different contexts by Dixon-Lewis and Williams (1963); and Clyne and Thrush (1963) and is one which would be favoured

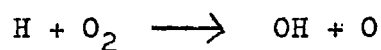
by the presence of an extended surface. It has also been considered in explosion limit investigations (Baldwin, Corney, Doran, Mayor and Walker, 1963; Voevodskii and Kondratiev, 1961) and it is thought to become important at lower temperatures and higher pressures than are characteristic of low-pressure flame structure studies on which much of this kinetic information is based (see e.g. Fristrom and Westenberg, 1965). It could take over from the first reaction mentioned above by forming OH and H and/or a hydrocarbon radical and oxygen. Another piece of evidence which is particularly relevant to the present study and favours this mechanism is the investigation of chilled ethylene flames by Gaydon (1942). Among other results, hydrocarbon bands and associated peroxide formation were observed near the heat sink.

CHAPTER 8.CONCLUSIONS AND RECOMMENDATIONS FOR FUTURE WORK

The variation of burning velocity of lean ethylene/air flames with distance from a heat sink has been analysed and found not to be exclusively a function of heat loss. The distribution of heat release rate near the heat sink shows some surprising features; notably a narrowing of the flame zone towards the heat sink and no decrease in reaction rate, in spite of a considerable fall in temperature. Analysis of the composition pattern suggests that the former is due to lack of completion of the CO oxidation and the latter to a large diffusive flux of hydrogen atoms towards the heat sink. A plausible mechanism which accounts for all the observations and is in accord with previous work is that the reaction



proceeds on the surface and replaces the



reaction which cannot fulfil its normal key role at the reduced temperatures near the heat sink.

As regards future development in this field, two important conclusions emerge. The first is that the theory

of this phenomenon is likely to prove even more intractable than has hitherto been supposed. It will be noted that a comprehensive theory would not only have to take into account the effect on reaction rate of small concentrations of species rapidly diffusing from the flame; the active species, if the above hypothesis concerning the mechanism is correct, originates not in the flame, but on the wall, following reaction there of a flame species. The subject of flame kinetics and the mathematics which allows it to be incorporated in the flame equations will have to advance considerably further before predictions become possible under these conditions. Secondly the results obtained in the present investigation at atmospheric pressure and with very inelaborate equipment (particularly on the analytical side) suggest that the use of flames in the vicinity of cold surfaces could considerably extend the usefulness of flame structure studies for kinetic and mechanistic studies, if the arsenal of low pressure flames and radical sampling probes (see, for example, Fristrom and Westenberg, 1965) were brought to bear on this problem.

APPENDIX (A)

The most direct method of calibrating capillary and other flowmeters measuring gaseous flow is that using a bubble meter. In principle this consists of measuring the rate of advance of the gaseous interface in quiescent atmosphere inside a vessel of a known constant or variable cross-section. This interface can be visualized by entraining a soap film in the flow under observation.

The apparatus (Fig. A.1) consists of a glass bulb carrying a side tube for introducing the gaseous flow. The top open end of this bulb is hermetically sealed to the observation tube again made of glass. This tube carries two or more marks at pre-determined intervals of volume. The length and diameter of this tube are determined by the flow rate to be measured. The lower end of the bulb is joined to a rubber bulb.

The bulb is filled with soap or detergent solution so that its level is just below the lower end of the observation tube. The strength and quality of this solution is largely a matter of trial and error, but a 1% solution of teepol or any detergent has been found to give satisfactory results. The gas is led through the side tube and is made to entrain a soap film during its upward passage through the tube. This

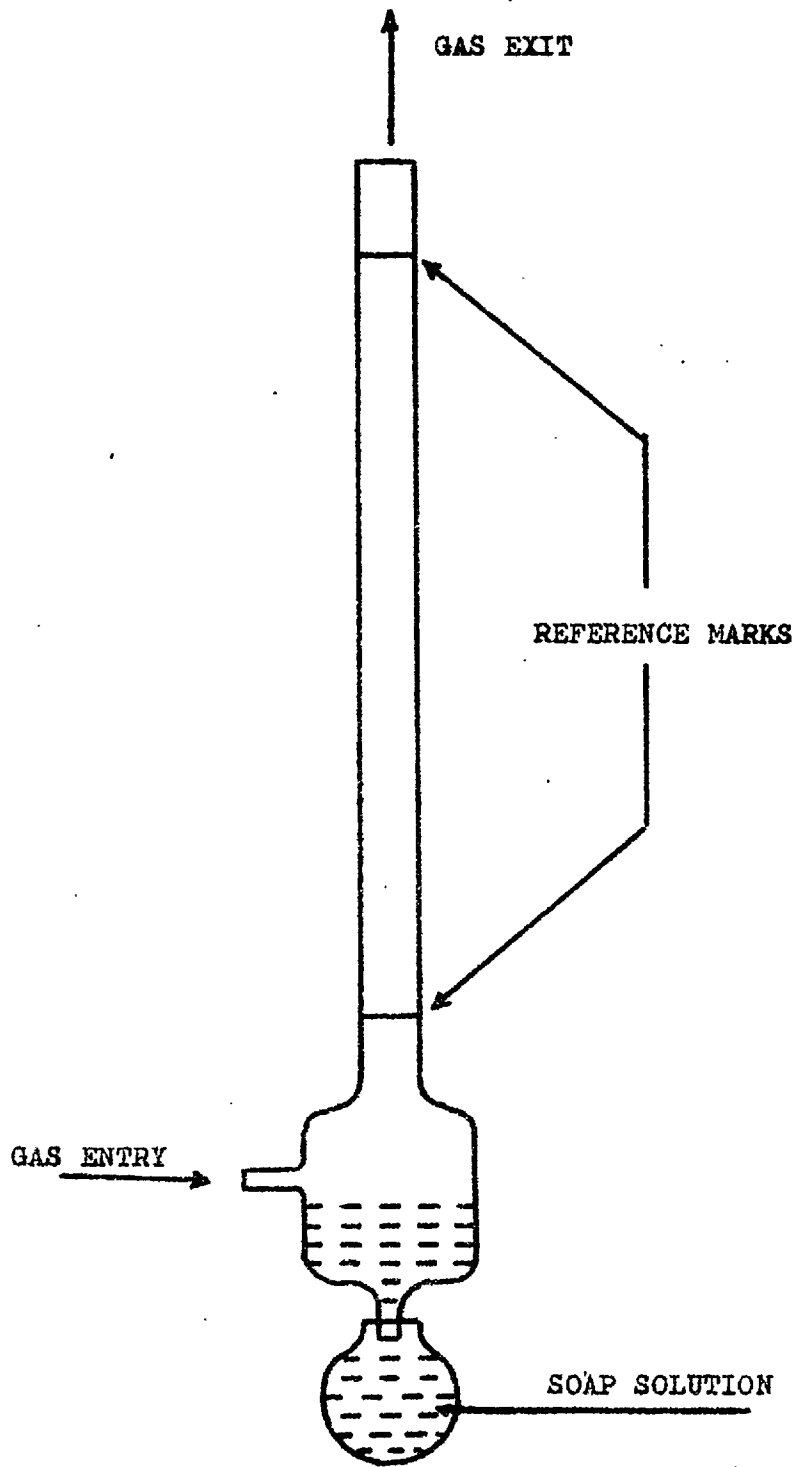


FIGURE A.1.

is done by gently squeezing the bulb so that the soap solution momentarily forms a film at the inlet of the observation tube. The film then moves downstream in the tube, thereby giving an airtight interface between the gas flow and the outside air. If accurate results are required, the gas flow is first saturated with water vapour, by passing it through a water bath at a known constant temperature. It is then led into the bulb, where it sheds the excess water vapour and continues into the observation tube.

If under known conditions of room temperature, $T^{\circ}\text{K}$, and line pressure, P , the soap film sweeps a volume, V , (through the tube) in t secs., the flow rate of the gas at S.T.P. is given by

$$\frac{P - p}{T} \cdot \frac{273.2}{760} \cdot V \text{ cm}^3 \text{sec}^{-1} \quad (1)$$

where p is the saturated vapour pressure of water at room temperature T .

Thus the only observations needed are the time intervals, t , for sweeping a known volume, V , at different flow rates. The flow rates thus calculated (from eqn. 1.) can be plotted against, say, the corresponding pressure drops in a capillary flowmeter and an absolute calibration curve obtained for the gas in question.

APPENDIX B.

Butt-welded and coated thermocouples are one of the important parts of the apparatus used in the present investigation. In order to calculate the radiation losses from the wire the butt weld must be of known shape. The reliability of the results depends upon the complete stoppage of the catalytic effect of Pt and Pt-Rhodium wires on the reactions going on in the flame. Such catalytic effects have been observed in the case of mixtures like hydrogen-air, carbon monoxide-air and hydrocarbon-air and it was therefore essential to prevent them. The methods employed in the present study for fabricating the thermocouple junction and coating the wires with silica for suppressing the catalytic reactions on their surface are described below.

The method of butt-welding usually followed consists of placing the wires end on and discharging a small condenser across the narrow gap. One difficulty with this technique is that the shape and the diameter of the junction cannot be controlled. Also, the chances of placing two wires of 0.0025 cm. diameter end on seemed quite remote even with the help of a microscope.

In the present investigation, the wires were placed in contact by crossing them at any position. A small D.C. was

then passed. Due to the magnetic field of the current, a slight tug to bring them end on would not result in pulling them apart. When the desired position of the wires was reached, the applied voltage was increased so that a fusion could take place. The diameter of the junction thus formed can be controlled to a certain extent by suitably adjusting the voltage. After a few trials and errors, the technique was perfected to obtain a junction which was approximately cylindrical. Under favourable conditions the diameter of the junction was found to be nearly the same as that of the wires.

These thermocouples were very fragile and difficult to handle and this rapid method for their fabrication therefore proved to be of great help in quickly replacing those damaged beyond repair.

Bare platinum wires when immersed in reacting gaseous mixtures exhibit catalytic effects. Due to this an uncoated thermocouple may not be expected to give reliable temperatures. It was in fact observed by Friedman (1953) that the values of temperatures determined in propane-air flames by an uncoated thermocouple were significantly different from those obtained by coated thermocouples. Although such catalytic effects cannot be altogether eliminated (see e.g. Cookson, et al, 1964) a suitable coating of silica is very effective in reducing them to a minimum (Kaskan, 1957). The method used by Kaskan consists

of immersing the butt-welded thermocouples in a flame stabilized on a Meker burner, a spray of hexamethyl-disiloxane being introduced. This was achieved in the present work by bubbling a small amount of coal gas through the solution and recombining the stream with the main gas flow being fed to the burner. The flame temperature must be controlled according to the wire diameter. It was found that a temperature of about 1800°K gave satisfactory results for 0.0025 cm. wires. At higher temperatures the coat showed a tendency to agglomerate into little beads; below 1700°K it was powdery. The thickness of the coat could be adjusted by varying the time for which the wires were immersed in the flame.

It was also found that the coating was more successful with wires of smaller diameter (about 0.0025 cm.). The reason probably was that with larger diameter (about 0.01 cm) the flame temperature had to be increased to compensate for loss of heat by radiation. This diminished the efficiency of silica wetting of the wire surface. After successfully coating a few thermocouples tests were made to ascertain that the readings obtained with them were reproducible and the coat would last for several hours. A trial ethylene-air flame was stabilized and the hot junction was moved upstream starting from a position above the flame. The thermal e.m.f. was noted at six positions of the thermocouple. The junction was then taken

back through the same distance and again the e.m.f.'s were determined at those positions. The difference between corresponding readings was never found to exceed 0.3% . This was done over extended periods of time and the coating examined under a microscope. It was found that they were undamaged even after two to three hours of continuous use.

APPENDIX (C)

The final flame temperature attained by a combustible mixture can be calculated from thermochemical data. If the heat released during combustion is retained by the flame gases, all of it should be available in the form of increased enthalpy of the products at the final flame temperature. The calculation of the adiabatic flame temperature is then straight forward at temperatures low enough for dissociation to be unimportant. But in the presence of dissociation of products, or such processes ^{as} /heat transfer to a sink or any appreciable gain in kinetic energy of the flame gases, some of the heat of reaction will be used up. In such cases the heat available for raising the temperature of the products is less by the amount used up by these competing processes and the calculation of final flame temperature becomes more involved.

The adiabatic flame temperature can be calculated by equating the energy fluxes entering and leaving the flame. The energy transport is entirely by convection because the mass flow rate is constant and no temperature and concentration gradients exist in the initial and final states. The calculation therefore reduces to equating the heat of combustion per unit mass of the mixture to its rise in enthalpy.

The heat of combustion per mole of the fuel is usually

tabulated under standard temperature and pressure. If the initial mixture is at temperatures other than this, the heat of combustion at this temperature can be found from Kirchoff's equation

$$W_{T_2} = W_{T_1} + \int_{T_1}^{T_2} (C_p' - C_p'') dT$$

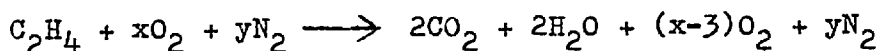
where W_{T_1} and W_{T_2} are the heats of reaction at temperatures T_1 and T_2 and C_p' and C_p'' are the specific heats of the unburnt and burnt mixtures at constant pressure.

The mole numbers of the products of combustion are determined by writing down the relevant chemical equation and expressing the actually used quantities of all gases as fractions of the amount of fuel present in the mixture. On the assumption of no external heat losses, the available heat of combustion W_{T_2} will be spent in raising the enthalpy of the products - including any excess or unused reactants. The final flame temperature which is the upper limit of the integral giving the enthalpy of the products $\int_{T_u}^{T_f} C_p dT$ can then be calculated by equating the two quantities.

In practice the equation is easy to solve graphically. An alternative method consists of trying suitable arbitrary values of T_f , deducing the corresponding value of the integral and comparing it with W_{T_2} until the value of T_f

which gives agreement is obtained as the adiabatic flame temperature.

For the flames studied in the present work, the relevant chemical equation was



and W_{T_2} at the temperature of the downstream face of the matrix was 61°C . In the absence of heat losses to the sink, the sum of the excess enthalpies of the products at 1430°K was found to be very nearly the same as W_{T_2} .

REFERENCES

- Anagnostou, E. and Potter, A.E., 1959, Combustion and Flame, 3, 453.
- Anderson, J.W. and Fein, R.S., 1949, J. Chem. Phys., 17, 1268.
- Baldwin, R.R., Corney, N.S., Doran, P., Mayor, L. and Walker, R.W. 1963, 9th Symposium (International) on Combustion, p.184.
- Blank, M.V., Guest, P.G., von Elbe, G. and Lewis, B., 1949, 3rd Symposium (International) on Combustion, p.363.
- Belles, F.E., Simon, D.M. and Weast, R.C., 1954, Industr. Engng. Chem., 46, 1010.
- Belles, F.E. and Berlad, A.L., 1956, N.A.C.A., T.N.3409.
- Berlad, A.L., 1954, J. Phys. Chem., 58, 1023.
- Berlad, A.L., and Potter, A.E., 1955, 5th Symposium (International) on Combustion, p.728.
- Berlad, A.L. and Yang, C.H., 1960, Combustion and Flame, 4, 325.
- Burgoyne, J.H. and Weinberg, F.J., 1953, 4th Symposium (International) on Combustion, p.294.
- Burgoyne, J.H. and Weinberg, F.J., 1954, Proc. Roy. Soc., A.224, 284.
- Burgoyne, J.H. and Hirsch, H., 1954, Proc. Roy. Soc., A.227, 73.
- Botha, J.P., 1956, Ph.D. Thesis, Cambridge University.
- Botha, J.P. and Spalding, D.B., 1954, Proc. Roy. Soc., A.225, 71.
- Chen, T.N. and Toong, T.Y., 1960, Combustion and Flame, 4, 313.
- Clyne, M.A.A. and Thrush, B.A., 1963, Proc. Roy. Soc., A.275, 559.

- Cookson, R.A., Dunham, P.G. and Kilham, J.K., 1964, Combustion and Flame, 8, 168.
- Cullen, R.E., 1953, Trans. Amer. Soc. Mech. Engrs. 75, 43.
- Daniell, P.J., 1930, Proc. Roy. Soc., A.126, 393.
- Daniell, W., 1956, 6th Symposium (International) on Combustion, 886.
- Dixon-Lewis, G. and Isles, G.L., 1962, 8th Symposium (International) on Combustion, p.448.
- Dixon-Lewis, G. and Williams, A., 1963, 9th Symposium (International) on Combustion, p.576.
- Egerton, A.C. and Thabet, S.K., 1952, Proc. Roy. Soc., A.211, 445.
- Egerton, A.C., Everett, A.J. and Moore, N.P.W., 1953, 4th Symposium (International) on Combustion, p.689.
- El-Mawla, A. Gad and Mirsky, W., 1965, Prog. Report No. 4, Dept. Mech. Engrg., University of Michigan, (U.S.A.).
- Friedman, R., 1949, 3rd Symposium (International) on Combustion, p.110.
- Friedman, R., 1953, 4th Symposium (International) on Combustion, p.259.
- Friedman, R. and Johnston, W.C., 1950, J. Appl. Phys., 21, 791.
- Friedman, R. and Burke, E., 1954, J. Chem. Phys., 22, 824.
- Friedman, R. and Cyphers, J.A., 1955, J. Chem. Phys., 23, 1875.
- Fristrom, R.M., 1965, Phys. Fluids, 8, 273.
- Fristrom, R.M., Prescot, R., Neuman, R.K., and Avery, W.H., 1953, 4th Symposium (International) on Combustion, p.267.
- Fristrom, R.M., Avery, W.H., Prescot, R., and MaHuck, A., 1954, J. Chem. Phys., 22, 106.

- Fristrom, R.M., Prescott, R., Grunfelder, C., 1957, Combustion and Flame, 1, 102.
- Fristrom, R.M. and Westenberg, A.A., 1961, J. Phys. Chem., 65, 591.
- Fristrom, R.M. and Westenberg, A.A., 1965, "Flame Structure", McGraw-Hill, New York, Chap. IX; *ibid* p.53; Chap. VII, p.126.
- Gaydon, A.G., 1942, Proc. Roy. Soc., A.979, 439.
- Gaydon, A.G., 1948, "Spectroscopy and Combustion Theory", Chapman and Hall, London.
- Gaydon, A.G. and Wolfhard, H.G., 1949, Proc. Roy. Soc., A.196, 105.
- Gaydon, A.G. and Wolfhard, H.G., 1953 "Flames", Chapman and Hall, London.
- Garner, W.E. and Pugh, A., 1939, Trans. Faraday Soc., 35, 283.
- Gerstein, M. and Potter, A.E., 1958, Heat Transfer and Fluid Mechns. Institute, p.68.
- Hirschfelder, J.O., 1957, J. Chem. Phys. 26, 282.
- Holm, J.M., 1932, Phil. Mag., 14, 18.
ibid, 1933, 15, 329.
- Kaskan, W.E., 1957, 6th Symposium (International) on Combustion, p.134.
- Kaskan, E.W., 1960, Combustion and Flame, 4, 285.
- Klaukens, H., Wolfhard, H.G., 1948, Proc. Roy. Soc., A.193, 512.
- Kay, G.W.C. and Laby, T.H., 1958, "Tables of Physical and Chemical Constants", 12th Edn. Longmans, London.

- Kydd, P.H. and Foss, W.I., 1964 (a), Report No. 64-RL-3590C,
Gen. Elec. Res. Lab., Schenectady, N.York.
- Kydd, P.H. and Foss, W.I., 1964 (b), Combustion and Flame, 6, 267.
- Lewis, B. and von Elbe, G., 1943, J. Chem. Phys., 11, 75.
- Lewis, B. and von Elbe, G., 1961, "Combustion, Flames and
Exposions of Gases", Academic Press, London, p.213-227,
and p.323.
- Levy, A., 1958, Ph.D. Thesis, London Uuiversity.
- Levy, A. and Weinberg, F.J., 1959¹, 7th Symposium (International)
on Combustion, p.296.
- Levy, A. and Weinberg, F.J., 1959², Combustion and Flame, 3, 229.
- Linnet, J.W., 1953, 4th Symposium (International) on Combustion,
p.20.
- MacAdams, W.H., 1954, "Heat Transmission" 3rd Ed., p.259-61.
- Markstein, G.H., 1958, 7th Symposium (International) on
Combustion, p.289.
- Mayer, E., 1957, Combustion and Flame, 1, 438.
- Miler, J., Inami, H., Rosser, W.H. and Wise, H., 1958, Quart.
Prog. Rept., No. 3, Stanford Research Institute.
- Palmer, K.N., 1956, J. Inst. Fuel., 29, 305.
- Palmer, K.N., 1957, 7th Symposium (International) on Combustion,
p.497.
- Palmer, K.N., 1963, Combustion and Flame, 7, 121.
- Potter, A.E. and Berlad, A.L., 1956, N.A.C.A. Tech. Rep. 1264.

- Potter, A.E., 1960, "Progress in Combustion Science and Technology"
Vol. I, Pergamon Press, London, p.176.
- Putnam, A.A. and Jensen, R.A., 1949, 3rd Symposium (International)
on Combustion, p.89.
- Powling, J.A., 1949, Fuel (London), 28, 25.
- Rossini, F.D. et al, 1953, "Selected Values of Physical and
Thermodynamic Properties of Hydrocarbons and Related
Compounds", Carnegie Press.
- Silverman, S., 1952, Amer. Phys. Soc. Meeting, Washington D.C.
- Simon, D.M., Belles, F.E. and Spakowski, A.E., 1953, 4th
Symposium (International) on Combustion, p.126.
- Simon, D.M., 1954, "Selected Combustion Problems", Butterworths,
London, p.59-91.
- Singer, J.M. and von Elbe, G., 1957, 6th Symposium (International)
on Combustion, p.127.
- Smith, F.A., 1937, Chem. Rev., 21, 389.
- Spalding, D.B., 1957, Proc. Roy. Soc., A.240, 83.
- Spalding, D.B., and Yumlu, V.S., 1959, Combustion & Flame, 3, 513.
- Statham, I.C.F. and Wheeler, R.V., 1930, S.M.R.B. Paper No. 60.
- Tanford, C. and Pease, R.N., 1947, J. Chem. Phys., 15, 861.
- Tanford, C. and Pease, R.N., 1947, J. Chem. Phys., 15, 431.
- Van Tiggelen, A., 1946, Bull. Soc. Chim. Belg., 55, 202.
- Van Tiggelen, A., 1949, Bull. Soc. Chim. Belg. 58, 259.
- Voevodskii, V.B. and Kondratiev, V.N., 1961, "Progress in
Reaction Kinetics," Vol.I, Pergamon Press, New York, p.41.
- von Elbe, G. and Mentser, M., 1945, J. Chem. Phys., 13, 89.

- von Elbe, G., Lewis, G.B. and co-workers, 1949, 3rd Symposium,
(International) on Combustion, p.363.
Ibid. p.80.
- von Karman, T. and Millan, G., 1953, 4th Symposium (International)
on Combustion, p.173.
- Waldman, L., 1961, "Rarefied Gas Dynamics" (edited by L. Talbot)
Academic Press, p.323.
- Weinberg, F.J., 1953, Ph.D. Thesis, London University.
- Weinberg, F.J., 1955, Proc. Roy. Soc., A.230, 331.
- Weinberg, F.J., 1955, Fuel, London, 34, S.84 (Supplement).
- Weinberg, F.J., 1956, Fuel, London, 35, 161.
- Weinberg, F.J., 1956, Proc. Roy. Soc., A.235, 510.
- Weinberg, F.J., 1963, "Optics of Flames", Butterworths, London,
Chaps. IV, VI and VIII.
- Westenberg, A.A., Raezer, S.D. and Fristrom, R.M., 1957,
Combustion and Flame, 1, 467.
- Wohl, K., Kapp, N.M. and Gazley, C., 1949, 3rd Symposium
(International) on Combustion, p.3.
- Wohl, K., 1953, 4th Symposium (International) on Combustion,
p.68.
- Yumlu, V.S., 1966, Combustion and Flame, 10, 147.

Ph.D. Thesis by G. P. Tewari - October, 1967.

"A STUDY OF THE INTERACTION OF FLAMES AND SURFACES"

ERRATA

- p.24 line 16 For 'experical' read 'empirical'
- p.32 line 3 For ' $\frac{d\tau}{dz} = \left(\frac{\partial\tau}{\partial z}\right)_1$ ' read ' $\frac{d\tau}{dz} = \left(\frac{d\tau}{dz}\right)_1$ '
- p.78 line 2 For (Axial) read (Peripheral)
- p.117 Eqn. 4.3 For (θ) read ($\theta =$)
- p.180 Fig. 7.2c For 2.8 read 3.34
- " " For 6.8 read 2.04